

CLEARED  
FOR PUBLIC RELEASE  
PL/PA 16 DEC 96

Sensor and Simulation Notes

Note 166

January 1973

The Effective Radii Approximation for the Capacitance of a  
Body Within an Enclosure

R. W. Latham  
Northrop Corporate Laboratories  
Pasadena, California

Abstract

A study is made of the effective radii approximation of the electrostatic capacitance between a metallic body and a metallic enclosure within which the body is contained. The study includes derivations of the order of magnitude of the error of the approximation as the size of the body approaches zero, and tables of the effective radii of enclosures whose shapes are either right circular cylinders or rectangular parallelepipeds are given. Some upper and lower bounds on the effective radius of an enclosure are also discussed.

PL 91-0971

Sensor and Simulation Notes

Note 166

January 1973

The Effective Radii Approximation for the Capacitance of a  
Body Within an Enclosure

R. W. Latham  
Northrop Corporate Laboratories  
Pasadena, California

Abstract

A study is made of the effective radii approximation of the electrostatic capacitance between a metallic body and a metallic enclosure within which the body is contained. The study includes derivations of the order of magnitude of the error of the approximation as the size of the body approaches zero, and tables of the effective radii of enclosures whose shapes are either right circular cylinders or rectangular parallelepipeds are given. Some upper and lower bounds on the effective radius of an enclosure are also discussed.

Key words: electromagnetic pulses, magnetic fields, electric fields



## Contents

I.	Introduction	4
II.	The Problem and its Approximate Solution	8
III.	Accuracy of the Approximation -- Analytical Study	13
	A. General Case	13
	B. One Conductor is Really a Sphere	18
IV.	Accuracy of the Approximation -- Examples	25
	A. Sphere in an Infinite Cylinder	26
	B. Sphere Between Two Infinite Plates	33
	C. Disk in an Infinite Cylinder	39
	D. Disk in a Circular Aperture	50
V.	Enclosure Radius Calculations -- Available Methods	58
	A. Integral Equation Methods	58
	B. Method of Nets	62
	C. Method of Inversion	64
	D. Separation of Variables Method	70
VI.	Enclosure Radius Calculations -- Two Simple Shapes	71
	A. Finite Circular Cylinders	71
	B. Rectangular Parallelepipeds	77
VII.	Enclosure Radius Calculations -- Bounds	85
	A. Upper Bounds	85
	B. Lower Bounds	91
VIII.	Conclusions and Possible Extensions	96
IX.	References and Other Relevant Publications	99

## Acknowledgement

I talked to Dr. M. I. Sancer several times about some of the topics discussed in this note. He will write a separate note that will include a careful discussion of bounds on the capacitance. Mr. R. W. Sassman did most of the numerical calculations and Mrs. Georgene Peralta did the typing and drawing. Dr. C. E. Baum instigated the work.

## Figures

1.	A body inside a general enclosure - - - - -	9
2.	A body inside a spherical enclosure - - - - -	19
3.	A sphere in an infinite cylinder- - - - -	27
4.	Error of the approximation for the case of a sphere in an infinite cylinder- - - - -	36
5.	A sphere between parallel plates- - - - -	37
6.	Error of the approximation for the case of a sphere between parallel plates- - - - -	42
7.	A disk in an infinite cylinder- - - - -	43
8.	Error of the approximation for the case of a disk in an infinite cylinder- - - - -	52
9.	A disk in a circular aperture (cross-section) - - - - -	53
10.	Error of the approximation for the case of a disk in a circular aperture- - - - -	57
11.	A general enclosure shape - - - - -	59
12.	A spherical enclosure with a circular hole- - - - -	66
13.	A right circular cylindrical enclosure- - - - -	72
14.	Effective radii of right circular cylindrical enclosures- - - - -	76
15.	A rectangular parallelepiped enclosure- - - - -	78
16.	Effective radii of rectangular parallelepipeds -- (c/b) a parameter - - -	83
17.	Effective radii of rectangular parallelepipeds -- (b/a) a parameter - - -	84
18.	Accuracy of the volume upper bound for right circular cylinders - - - - -	88
19.	A hemispherically-capped circular cylinder- - - - -	89

## Tables

1.	Capacitance of a sphere in an infinite cylinder - - - - -	34
2.	Capacitance of a sphere between parallel plates - - - - -	40
3.	Capacitance of a disk in an infinite cylinder - - - - -	51
4.	Capacitance of a disk in a circular aperture- - - - -	56
5.	Effective radius of a spherical enclosure with a hole - - - - -	69
6.	Effective radii of right circular cylindrical enclosures- - - - -	75
7.	Effective radii of rectangular parallelepipeds- - - - -	82

## I. Introduction

The calculation of electrostatic capacitance is an old subject. People have been calculating the capacitances of wierd-shaped objects for well over a hundred years. Examples of capacitance calculations are given in even the most elementary texts on electromagnetism, so why should one bother to read or write a note on this supposedly closed subject? Well, there are at least three reasons. The first reason is that capacitance calculations are of considerable importance in the design of high quality satellite simulators, and the time for such designs has come. A few of the following paragraphs of this introduction will elaborate on that statement. The second reason is that the satellite simulator application has provoked the development of an approximate capacitance formula that is particularly applicable to a body within an enclosure. This approximation has received little attention in the literature. The two primary purposes of the present note are to demonstrate its accuracy and to facilitate its application. The third reason for the study of capacitance is less pragmatic than the first two, but for the author, at least, it is more forceful: calculating capacitance is fun.

Returning to the more practical justifications of this note, let us take a few paragraphs now to say what a satellite simulator is supposed to simulate and why it is necessary to calculate capacitances in order to design one properly. A satellite simulator is intended to recreate the environment of an orbiting satellite exposed to the direct  $\gamma$ -rays and X-rays of a high altitude nuclear detonation [1], [2]. The incident photons eject electrons from the satellite materials, and the ejected electrons are the source of what has been called the system generated EMP. A satellite simulator, as it is currently thought of, would simulate the required environment by means of a large metallic vacuum chamber within which the satellite under test would be situated. A collimated photon beam would be incident through one wall of the vacuum chamber, and would eject electrons from the test object.

The ejection of electrons from a satellite in orbit leaves the satellite with a positive charge. The positive charge gives the satellite a positive potential with respect to infinity. The magnitude of this positive potential, which is directly proportional to the positive charge and inversely proportional to the electrostatic capacitance of the satellite, determines what fraction of

the ejected electrons escapes completely from the system and goes off to infinity. Similarly, the ejection of electrons from a satellite in a simulator gives the satellite a positive potential with respect to the simulator enclosure, and this positive potential is one of the major factors determining what fraction of the electrons ejected from the satellite end up on the walls of the enclosure. Thus we see that the potential of the satellite with respect to the enclosure immediately after the pulse of photons, this potential being directly proportional to the initial charge left on the satellite by the ejected electrons and inversely proportional to the capacitance between the satellite and its enclosure, is an important quantity to consider when designing a satellite simulator. This potential should be about the same as the potential with respect to infinity of the satellite in orbit. Since the ejected charges in the two cases will be made to be roughly the same, equality of potential means that the capacitance between the satellite and its enclosure should be close to the capacitance of the satellite with respect to infinity. This will be true in the limit of very large enclosures, but construction limitations restrict one to the consideration of enclosures that are only moderately large compared to the size of the satellite. With this restriction to enclosures of moderate size in mind, it is clear that it is important to be able to calculate the capacitance between a test object and its enclosure in order to determine if a proposed simulator would be large enough to make a realistic test on a particular satellite. Of course, this capacitance criterion is only one of several criteria that must be used in judging the quality of a proposed satellite simulator design, but it is an important one.

There is a second use to which satellite-enclosure capacitance calculations can be put. If one is satisfied with matching the net charge left on the satellite in the simulator, after the low energy electrons have returned, with the net charge left in the actual case (the initial charge knocked off is assumed to be about the same in both cases), it might be possible to get away with a fairly small enclosure by giving the satellite a negative charge before exposing it to the pulse of photons. This initial charge should be enough to make the potential of the satellite with respect to the enclosure, immediately after the electron ejection, approximately equal to the potential of the satellite in orbit, immediately after the electron ejection. The magnitude

of the required initial charge can be calculated in a trivial manner when the relevant capacitances are known.

A precise calculation of capacitance should take into account the space charge created by the initial ejection of electrons. We will not consider the effect of space charge in this note, in the belief that it will have only a secondary effect on the value of capacitance but a very large effect on the difficulty of its calculation. Another effect that we will not take into account is the detailed construction of the walls of the enclosure. The real enclosure will probably have wall linings made up of resistive materials for mode damping and have wire grids close to the walls for the control of secondary electrons. We will idealize the enclosure by assuming it to have smooth walls at a constant potential.

Thus we arrive at the classical electrostatic problem of calculating the capacitance between an object and a smooth metallic enclosure within which it is contained.

But there is a special way in which we would like to look at this problem. In order to evaluate the usefulness of various proposed simulators for testing one of the myriad of existing satellites, it would be very convenient if the capacitance between a satellite and a simulator could be calculated from two characteristic numbers. One of these numbers would characterize the satellite, without regard to the particular simulator it is in. The other number would characterize the simulator, without regard to the particular satellite it contains. Such a separation is impossible in general. But, if the satellite is not too large compared to the size of its enclosure, such a separation is possible as a fairly accurate approximation. One approximation that accomplishes this separation is the effective radii approximation ([2], Section V); a precise statement of this approximation will be given in the next section. One primary purpose of the present note is to examine the accuracy of this approximation. The other primary purpose is to facilitate the use of the effective radii approximation by making it easy to estimate the effective radius of any given enclosure. The calculation of the effective radius of test objects has been discussed elsewhere [3].

Following the initial description of the effective radii approximation in the next section, Section III presents a study of the accuracy of the

approximation from a fairly general point of view and a determination of the order of magnitude of its error when the test object is small compared to the size of the enclosure. The four examples of Section IV demonstrate the results of Section III and build further confidence in the overall accuracy of the approximation.

Sections V through VII are concerned with the calculation of the effective radii of enclosures. Section V presents an outline of the most important available methods. Section VI gives two specific examples of effective radius calculation; in one case the enclosure is a circular cylinder with flat end caps and in the other case the enclosure is a rectangular parallelepiped. Section VII is a discussion of certain bounds that can be put on the effective radii of enclosures. The numerical results of Section VI can be quite useful in conjunction with the bounds discussed in Section VII; this is demonstrated by an example.

In Section VIII, we review the most significant results of the note and suggest several possible extensions of the work.

There are a large number of interesting and useful papers in the literature that discuss the calculation of electrostatic capacitance. Indeed at one time, a very long time ago of course, this subject held a great deal of fascination for physicists of a mathematical bent. But in the last fifty years or so, the flow of capacitance papers has trickled off to a torrent. It was therefore decided that it was possible to survey the work of this period, at least, and come up with a reasonably useful list of publications. Section IX contains this list. We have managed to make a specific reference to most of the works in the list at least once in this note. There has been a good deal of selection in making the list. Publications were only included if they were interesting, or if they contained useful results, or if they contained extensive further bibliographies, and there are undoubtedly some papers satisfying one or more of these criteria that have been neglected out of ignorance. The list must therefore be considered as suggestive and somewhat subjective, rather than exhaustive. It is offered in the hope that it will reduce the pain of the literature search for other workers who become interested in the subject of capacitance calculation.

## II. The Problem and its Approximate Solution

Figure 1 is a representation of the problem to be studied. We will keep as uniform a notation as possible throughout this note. We will denote the body representing the satellite under test by  $B$ , its surface by  $S_b$ , and the outward normal from its surface by  $\underline{n}_b$ . We will denote the idealized simulator enclosure by  $E$ , its surface by  $S_e$ , and the inward normal from its surface by  $\underline{n}_e$ . The volume between  $S_e$  and  $S_b$  will be denoted by  $V$ . We will denote the capacitance between  $B$  and  $E$  by  $C$ , and we will denote the capacitance of  $B$ , when it is isolated in free space, by  $C_b$ . The electrostatic potential within  $V$  will be denoted by  $\phi(\underline{r})$ , while the electrostatic potential outside  $B$  when  $E$  is absent will be denoted by  $\chi(\underline{r})$ . Rationalized MKS units will be used throughout.

The capacitance between  $B$  and  $E$  can be defined through the solution of Laplace's equation for the electrostatic potential,

$$\nabla^2 \phi(\underline{r}) = 0 \quad \underline{r} \text{ in } V, \quad (2.1)$$

subject to the boundary conditions

$$\phi(\underline{r}) = 1 \quad \underline{r} \text{ on } S_b \quad (2.2)$$

$$\phi(\underline{r}) = 0 \quad \underline{r} \text{ on } S_e, \quad (2.3)$$

and a subsequent computation of the total charge on  $B$  (identically equal to  $C$  because of the one volt difference in potential between  $B$  and  $E$ ) through

$$C \equiv Q = -\epsilon_0 \int_{S_b} \frac{\partial \phi}{\partial n_b} dS. \quad (2.4)$$

The capacitance of  $B$  with respect to infinity can be similarly defined through the solution of Laplace's equation throughout the whole infinite region exterior to  $B$

$$\nabla^2 \chi(\underline{r}) = 0 \quad \underline{r} \text{ outside } B, \quad (2.5)$$

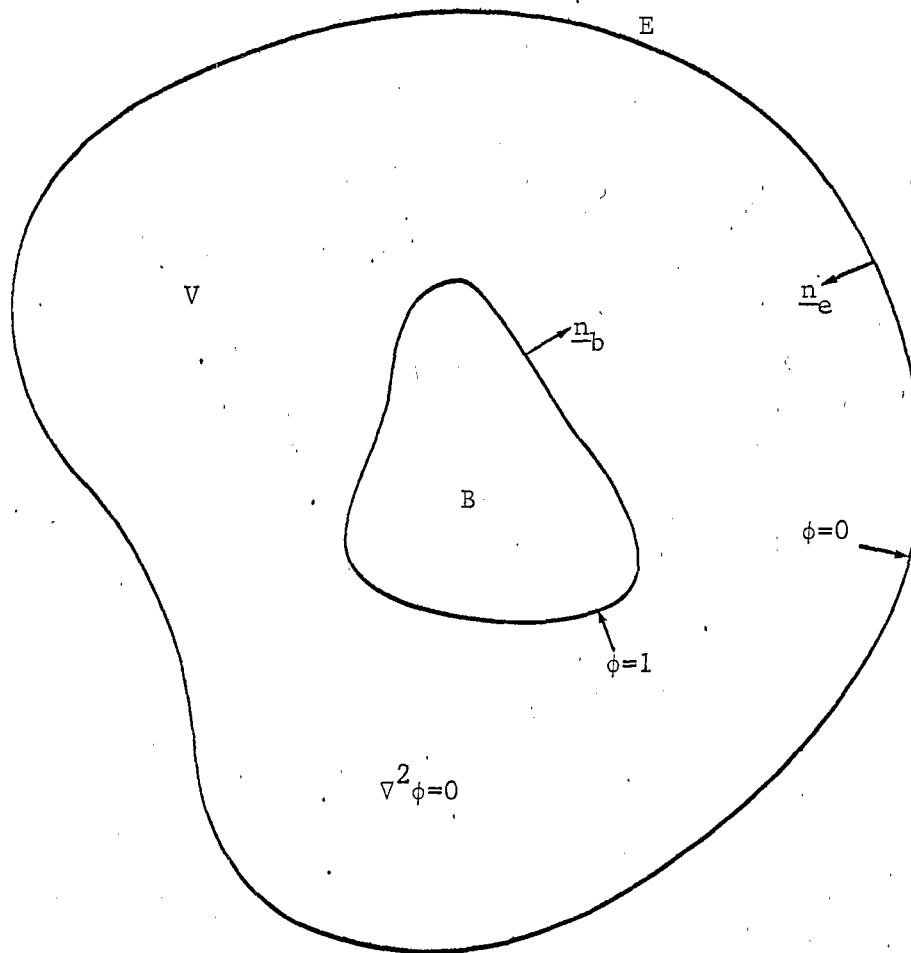


Figure 1. A body inside a general enclosure.

subject to the boundary conditions

$$\chi(\underline{r}) = 1 \quad \underline{r} \text{ on } S_b \quad (2.6)$$

$$\chi(\underline{r}) \rightarrow 0 \quad \underline{r} \rightarrow \infty, \quad (2.7)$$

and a subsequent computation of  $C_b$  through an evaluation of the integral

$$C_b \equiv Q_b = -\epsilon_0 \int_{S_b} \frac{\partial \chi}{\partial n_b} dS \quad (2.8)$$

The value of  $C$  will vary as  $B$  is rotated and translated within  $E$ , but, with our satellite simulator application in mind, we need to consider only certain special positions of  $B$ .  $B$  must still be allowed to have an arbitrary angular orientation, since a satellite must be subjected to photon pulses coming from several angles of incidence while the simulator's photon source will be fixed. However, for a given angular orientation, we want to consider only that position of  $B$  within  $E$  where  $C$  is a minimum. This is in keeping with the desire to make  $C$  as close as possible to  $C_b$ , since  $C$  will always be greater than  $C_b$ . We will denote the minimum value of  $C$  by  $\bar{C}$ .

Sometimes the position of  $B$  that makes  $C$  a minimum will be obvious by inspection. For example, if both  $B$  and  $E$  have a center of symmetry, a likely candidate for the minimum  $C$  position is the position where the centers of symmetry coincide. This position is clearly the wrong one in some cases, for example if  $E$  has the shape of a dumbbell, but it is probably the right one if  $E$  is convex. It would seem that  $E$  will be convex in any practical simulator design. We will assume that the coincidence of the centers of symmetry defines  $\bar{C}$  for the four examples of Section IV.

An accurate calculation of  $\bar{C}$  is quite difficult in general, but for the case where  $B$  and  $E$  are both spheres it is easy. Clearly, for two spheres,  $C$  is a minimum when  $B$  and  $E$  are concentric, and, from standard texts ([4], §2.03),  $\bar{C}$  is given by

$$\frac{\bar{C}}{C_b} = \frac{1}{1 - (r_1/r_2)}, \quad (2.9)$$

where  $r_1$  is the radius of the inner sphere and  $r_2$  is the radius of the outer sphere.

It would be nice if an equation like (2.9) held for a general B and E, where  $r_1$  would be some number characterizing B, regardless of the shape of E, and  $r_2$  would be some number characterizing E, regardless of the shape of B. The effective radii approximation is based on this wish.

The effective radius of a general B,  $r_1$ , is defined as the radius of the sphere that has the same capacitance with respect to infinity as B has with respect to infinity [2], i.e.,

$$r_1 \equiv \frac{C_b}{4\pi\epsilon_0} \quad (2.10)$$

This parameter has been called the "outer radius" of B by Szegö [5] and others. In the electrostatic system of units the capacitance of a body is equal to its  $r_1$  in centimeters.

The effective radius of a general E,  $r_2$ , is defined as the radius of the spherical enclosure that has the same  $\bar{C}$  with respect to an infinitesimal test sphere as E has with respect to the same infinitesimal test sphere [2]. By juggling equation (2.9), it thus follows that  $r_2$  is given by

$$\frac{1}{r_2} \equiv \lim_{r_1 \rightarrow 0} \left[ \frac{1}{r_1} - \frac{4\pi\epsilon_0}{\bar{C}_1} \right] \quad (2.11)$$

where  $\bar{C}_1$  is equal to the  $\bar{C}$  between E and a spherical B of radius  $r_1$ . The parameter  $r_2$  has been called the "inner radius" of E by Szegö [5]. An equivalent, more easily applied definition of  $r_2$  will be given in the next section. Numerical methods for computing the  $r_2$  of enclosures of arbitrary shape are discussed in Section V.

Once  $r_1$  and  $r_2$ , the effective radii of B and E, have been determined, the effective radii approximation to  $\bar{C}$  can be calculated. This approximation consists in the assumption that equation (2.9) is nearly correct in general, i.e., denoting the effective radii approximation to  $\bar{C}$  by  $\tilde{C}$ , we have

$$\frac{\bar{C}}{C_b} \approx \frac{\tilde{C}}{C_b} \equiv \frac{1}{1-(r_1/r_2)} \quad (2.12)$$

A general discussion of the accuracy of this approximation is given in the next section. A further examination of its validity, through the study of four particular examples whose  $\bar{C}$  can be calculated quite accurately, is presented in Section IV.

We can note in passing that, according to equation (2.12), the relative difference between  $\bar{C}$  and  $C_b$ , which should be small if an accurate simulation is to be assured, is given approximately by

$$\frac{\bar{C}-C_b}{C_b} \approx \frac{(r_1/r_2)}{1-(r_1/r_2)} \quad (2.13)$$

There are a couple of further points about equation (2.12) that should be brought up before we close this section.

The first point is that (2.12) is just the kind of equation one wants for satellite simulator applications. It separates the effect of B and E quite nicely. It is trivial to apply when  $r_1$  and  $r_2$  are known (no tables or curves are necessary). And the concept of the two spheres equivalent to B and E somehow appeals to one's intuition.

The other point is that the dependence of  $\bar{C}$  on the angular orientation of B does not appear in approximation (2.12). This is necessary if one is to reduce the characterization of B to a single number. Nevertheless, it is an indication that one should not expect excessive accuracy from the approximation in general. But for small  $(r_1/r_2)$ , which is the case of greatest practical interest, the accuracy of equation (2.12) could be quite high. If, in addition, the angular orientation of B is truly irrelevant, i.e., if either B or E is spherical, one can see that there is a chance of an even higher degree of accuracy. This is more than just wishful thinking, as we shall see in the next section.

### III. Accuracy of the Approximation -- Analytical Study

In this section, we will derive estimates of  $\Delta$ , the difference between  $(\bar{C}/C_b)$  and  $(\tilde{C}/C_b)$ . This is a difficult task if B is almost as large as E. But if B is not very large compared to E or, equivalently, if  $(r_1/r_2)$  is not very close to unity, we can make a good deal of progress by studying the order of magnitude of  $\Delta$  as  $(r_1/r_2)$  approaches zero. Since, for accurate simulation,  $(r_1/r_2)$  should be made as small as possible within cost and constructional limitations, our small  $(r_1/r_2)$  estimates of  $\Delta$  should be sufficient for the present purposes.

We will first study the case where both B and E are of arbitrary shape (Subsection A). We will show that, in that case,  $\Delta$  is of order  $(r_1/r_2)^3$  as  $(r_1/r_2)$  approaches zero.

We will then study the special case where E is a sphere (Subsection B) and show, after a rather long argument, that then  $\Delta$  is of order  $(r_1/r_2)^5$  as  $(r_1/r_2)$  approaches zero. By invoking a special form of the inversion theorem it will then follow rather simply that if B is a sphere then  $\Delta$  is of order  $(r_1/r_2)^6$  as  $(r_1/r_2)$  approaches zero. These two special cases that have a higher order of accuracy for  $\tilde{C}$  are of more than academic interest. There is a good possibility that the E of a satellite simulator will be approximately spherical. We will not examine here the effect on  $\Delta$  of small perturbations from the spherical shape of E, but our results could be useful as estimates of the kind of  $\Delta$ 's one can expect if E is almost a sphere.

For completeness, it might be well to recall that, for the trivial special case where both B and E are spheres,  $\Delta \equiv 0$ .

Thus we see, in all cases, that  $\tilde{C}$  is a compact representation of an approximation to  $\bar{C}$  that is accurate to a higher order in  $(r_1/r_2)$  than one might expect. Sometimes this accuracy can be very striking indeed, as we shall see in a couple of the examples in Section IV.

#### III.A. General Case

Let us first set some notation and restate the definition of  $r_2$  in a form that is more useful for calculation.

The position of B will be denoted by the position vector of its free

space center of charge,  $\underline{r}_b$ . This position vector is defined by removing E, calculating  $\sigma_b(\underline{r})$ , the surface charge density on  $S_b$ , possibly by solving the integral equation

$$1 = \frac{1}{4\pi\epsilon_0} \int_{S_b} \frac{\sigma_b(\underline{r}')}{|\underline{r}-\underline{r}'|} dS' \quad \underline{r} \text{ on } S_b, \quad (3.1)$$

and then computing

$$\underline{r}_b = \left[ \int_{S_b} \sigma(\underline{r}) dS \right]^{-1} \int_{S_b} \sigma(\underline{r}) \underline{r} dS. \quad (3.2)$$

The value of  $\underline{r}_b$  where C attains its minimum will be denoted by  $\underline{r}_{bm}$  in general. The value of  $\underline{r}_b$  where C attains its minimum when B is an infinitesimal test sphere will be denoted by  $\underline{r}_e$ . If B and E have a center of symmetry, and E is convex, it seems clear, on physical grounds, that  $\underline{r}_{bm} = \underline{r}_e$ . But in any case, since the center of charge must be within the smallest sphere bounding B, we know from the definition of  $\underline{r}_e$  that

$$|\underline{r}_{bm} - \underline{r}_e| \rightarrow 0 \text{ as the size of } B \rightarrow 0,$$

and, since  $r_1$  is a measure of the size of B, it is safe to assume that

$$\frac{|\underline{r}_{bm} - \underline{r}_e|}{r_2} = o(r_1/r_2), \quad (3.3)$$

although the left hand side may be actually of higher order in  $(r_1/r_2)$ .

Let us denote the Green's function for the interior of E by  $G_e(\underline{r}, \underline{r}')$ . This function is defined through

$$\nabla^2 G_e(\underline{r}, \underline{r}') = -\delta(\underline{r} - \underline{r}')$$

$$G_e(\underline{r}, \underline{r}') = 0 \quad \text{if } \underline{r} \text{ is on } S_e$$

$G_e(\underline{r}, \underline{r}')$  has a singularity at  $\underline{r} = \underline{r}'$ , but it can be written as

$$G_e(\underline{r}, \underline{r}') = \frac{1}{4\pi|\underline{r}-\underline{r}'|} - \psi(\underline{r}, \underline{r}') \quad (3.4)$$

where  $\psi(\underline{r}, \underline{r}')$  is regular at  $\underline{r} = \underline{r}'$ , symmetric in  $\underline{r}$  and  $\underline{r}'$ , and positive within E ([6], Chap. IX, §3). The potential on a small sphere of radius  $r_1$ , carrying a charge Q and having its center at  $\underline{r}_b$ , is given, if  $\phi = 0$  on  $S_e$ , by

$$\phi(\underline{r} \text{ on } S_b) = \frac{Q}{4\pi\epsilon_0 r_1} - \frac{Q}{\epsilon_0} \{ \psi(\underline{r}_b, \underline{r}_b) + o(r_1) \}$$

Thus the capacitance between the small sphere and E is given by

$$C = 4\pi\epsilon_0 \left[ \frac{1}{r_1} - 4\pi[\psi(\underline{r}_b, \underline{r}_b) + o(r_1)] \right]^{-1},$$

and thus, according to our previous, basic definition of  $r_2$  in equation (2.11)

$$\frac{1}{r_2} \equiv \lim_{r_1 \rightarrow 0} 4\pi[\bar{\psi}(\underline{r}_b, \underline{r}_b) + o(r_1)]$$

i.e.

$$\frac{1}{r_2} \equiv 4\pi\bar{\psi}(\underline{r}_b, \underline{r}_b) \quad (3.5)$$

where  $\bar{\psi}(\underline{r}_b, \underline{r}_b)$  is the minimum value of  $\psi(\underline{r}_b, \underline{r}_b)$ . From our definition of  $\underline{r}_e$  in the paragraph following equation (3.2) we can thus write

$$\frac{1}{r_2} \equiv 4\pi\psi(\underline{r}_e, \underline{r}_e) \quad (3.6)$$

Equation (3.6) is the alternative definition of  $r_2$  that we have been working toward. We will use it in the calculations of Sections IV and VI and also in this subsection.

Now let us study the behavior of  $\psi(\underline{r}, \underline{r}')$  when both  $\underline{r}$  and  $\underline{r}'$  are in a  $\delta$ -neighborhood of  $\underline{r}_e$ . Employing a Taylor's series expansion, and using the fact that the characteristic length over which  $\psi$  can be expected to vary significantly is of order  $r_2$ , we can write

$$\begin{aligned} \psi(\underline{r}, \underline{r}') &= \psi(\underline{r}_e, \underline{r}_e) + (\underline{r} - \underline{r}_e) \cdot \nabla_1 \psi(\underline{r}_e, \underline{r}_e) + (\underline{r}' - \underline{r}_e) \cdot \nabla_2 \psi(\underline{r}_e, \underline{r}_e) \\ &+ \psi(\underline{r}_e, \underline{r}_e) o[(\delta/r_2)^2] \end{aligned} \quad (3.7)$$

where the subscript on the gradient operators denote the position of the argument on which they have worked. From the symmetry of  $\psi$ , we know that

$$\nabla\psi(\underline{r},\underline{r}') = \nabla\psi(\underline{r}',\underline{r})$$

i.e.

$$\nabla_1\psi(\underline{r},\underline{r}') = \nabla_2\psi(\underline{r},\underline{r}'), \quad (3.8)$$

and, by definition,

$$\nabla\psi(\underline{r},\underline{r}) = 0 \quad \text{when } \underline{r} = \underline{r}_e$$

i.e.

$$\nabla_1\psi(\underline{r}_e,\underline{r}_e) + \nabla_2\psi(\underline{r}_e,\underline{r}_e) = 0 \quad (3.9)$$

Thus, from equations (3.8) and (3.9)

$$\nabla_1\psi(\underline{r}_e,\underline{r}_e) = \nabla_2\psi(\underline{r}_e,\underline{r}_e) = 0, \quad (3.10)$$

and so, when  $\underline{r}$  and  $\underline{r}'$  are close to  $\underline{r}_e$ , we can combine equations (3.7) and (3.10) and write

$$\psi(\underline{r},\underline{r}') = \psi(\underline{r}_e,\underline{r}_e)\{1 + O[(\delta/r_2)^2]\} \quad (3.11)$$

Now let us try to calculate  $\bar{C}$ . By a standard application of Green's theorem, we can write the integral equation for the surface charge on B in the form

$$1 = \frac{1}{4\pi\epsilon_0} \int_{S_b} \frac{\sigma(\underline{r}')}{|\underline{r}-\underline{r}'|} dS' - \frac{1}{\epsilon_0} \int_{S_b} \psi(\underline{r},\underline{r}')\sigma(\underline{r}')dS', \quad (3.12)$$

or, if B is small and  $\underline{r}_b - \underline{r}_e = \underline{d}$

$$1 = \frac{1}{4\pi\epsilon_0} \int_{S_b} \frac{\sigma(\underline{r}')}{|\underline{r}-\underline{r}'|} dS' - \frac{\psi(\underline{r}_e, \underline{r}_e)}{\epsilon_0} \{1 + o[(\delta/r_2)^2]\} \int_{S_b} \sigma(\underline{r}') dS' \quad (3.13)$$

where

$$\begin{aligned} \delta &= |\underline{r} - \underline{r}_e| \\ &= |\underline{r} - \underline{r}_b + \underline{r}_b - \underline{r}_e| \\ &\leq |\underline{r} - \underline{r}_b| + |\underline{r}_b - \underline{r}_e| \\ &= O(r_1 + d). \end{aligned} \quad (3.14)$$

But, recalling equation (3.3), we see from equation (3.14) that, when  $\underline{r}_b = \underline{r}_{bm}$ ,  $(\delta/r_2)$  is of order  $(r_1/r_2)$ . Thus, invoking the new form of the definition of  $r_2$  and rearranging, we see that the charge density we desire is given by the solution of the equation

$$1 + \frac{Q}{4\pi\epsilon_0 r_2} \{1 + o[(r_1/r_2)^2]\} = \frac{1}{4\pi\epsilon_0} \int_{S_b} \frac{\sigma(\underline{r}')}{|\underline{r}-\underline{r}'|} dS' \quad (3.15)$$

where

$$Q = \int_{S_b} \sigma(\underline{r}) dS. \quad (3.16)$$

Now, by comparing (3.1) and (3.15) it is evident that

$$\frac{Q}{Q_b} = 1 + \frac{Q}{4\pi\epsilon_0 r_2} \{1 + o[(r_1/r_2)^2]\}.$$

Rearranging this equation, and using the fact that  $r_1 \equiv Q_b/4\pi\epsilon_0$ , we find that

$$\frac{Q}{Q_b} = \frac{\bar{C}}{C_b} = \left[1 - \frac{r_1}{r_2} \{1 + o[(r_1/r_2)^2]\}\right]^{-1}$$

i.e.

$$\begin{aligned} \frac{\bar{C}}{C_b} &= \frac{1}{1-(r_1/r_2)} + o[(r_1/r_2)^3] \\ &= \frac{\tilde{C}}{C_b} + o[(r_1/r_2)^3] \end{aligned} \quad (3.17)$$

Thus we have the general estimate of  $\Delta$  that was mentioned in the introduction to this section

$$\Delta \propto (r_1/r_2)^3 \quad \text{as } (r_1/r_2) \rightarrow 0.$$

Numerical examples C and D of Section IV exhibit this type of  $\Delta$  behavior. Thus one cannot prove a higher order dependence of  $\Delta$  on  $(r_1/r_2)$  than cubic, in general (an improvement in the result would be a bound on the proportionality constant, but we will not attempt to derive such a bound here). Nevertheless, as we shall see in the following subsection, if one restricts either B or E to be a sphere, one can establish a higher order dependence of  $\Delta$  on  $(r_1/r_2)$ .

### III.B. One Conductor is Really a Sphere

The situation to be studied is shown in figure 2, where B is of some arbitrary shape and is enclosed in a spherical E. The results for a spherical B inside an E of arbitrary shape will follow from an application of the inversion theorem. Let us first obtain the form of the inversion theorem that will be most useful for this purpose.

In its most general form, the inversion theorem states that, if  $\phi(r, \underline{\Omega})$  is a solution of Laplace's equation, then so is  $(R/r)\phi(R^2/r, \underline{\Omega})$ , where  $r$  is the distance from some point and  $\underline{\Omega}$  denotes the angular orientation of  $\underline{r}$  with respect to that point ([6], Chap. IX, §2). Let  $\phi_1(r, \underline{\Omega})$  be the solution of Laplace's equation in  $V$  that is equal to unity on the  $S_e$  of figure 2 and equal to zero on the  $S_b$  of figure 2. If  $e$  denotes the radius of the E sphere, the capacitance between B and E is clearly given by

$$C = \epsilon_0 e^2 \int_{S_e} \frac{\partial \phi_1(r, \underline{\Omega})}{\partial r} d\Omega \quad (3.18)$$

Now let us invert the whole geometry, using an inversion sphere of radius  $R$  whose center is at the center of E (note that, although the figure is drawn for the case where the inversion sphere is between  $S_b$  and  $S_e$ ,  $R$  can really be any radius we choose). The potential in the inverted region that is equal to unity on  $S'_e$ , the inversion of  $S_e$ , and equal to zero on  $S'_b$ , the inversion of  $S_b$ , is just

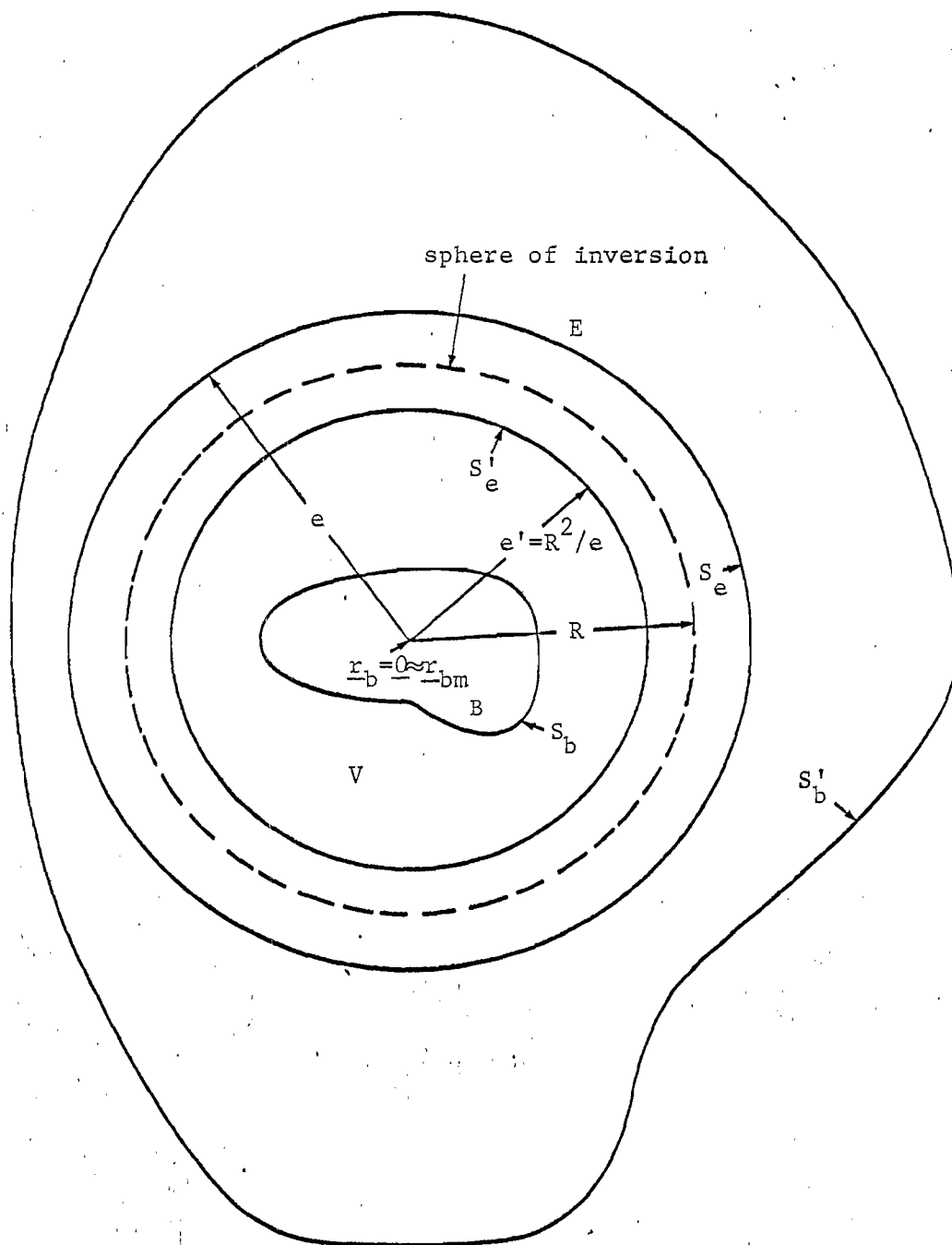


Figure 2. A body inside a spherical enclosure.

$$\Phi'(r, \underline{\Omega}) = (e'/r) \Phi_1(R^2/r, \underline{\Omega}) \quad (3.19)$$

where  $e' (=R^2/e)$  is the radius of the inverted  $S_e$  sphere. The capacitance between  $S'_b$  and  $S'_e$  is thus given by

$$\begin{aligned} C' &= \epsilon_0 e'^2 \int_{S'_e} \left[ \frac{e'}{r^2} + \frac{e'R^2}{r^3} \frac{\partial \Phi_1(e, \underline{\Omega})}{\partial r} \right] d\Omega \\ &= 4\pi\epsilon_0 e' + (e'/R)^2 C \end{aligned} \quad (3.20)$$

Equation (3.20) is a form of the inversion theorem that is quite suited to our needs. In particular, there are two special cases of it that are of immediate importance. These are:

Case 1:

Fix  $R$  and let  $e$  become large. Then  $e'$  becomes small, and the inverted problem is the one defining  $r'_2$ , the  $r_2$  of the inverted  $S_b$  surface. From the basic definition of  $r_2$ , equation (2.11), we have

$$\frac{1}{r'_2} = \lim_{e' \rightarrow 0} \left[ \frac{1}{e'} - \frac{4\pi\epsilon_0}{C'} \right]$$

which, by a substitution from equation (3.20), is just

$$\frac{1}{r'_2} = \frac{C}{4\pi\epsilon_0 R^2}$$

But, since  $e$  is large,  $(C/4\pi\epsilon_0)$  is just the  $r_1$  of  $B$ , and so we can write

$$r_1 r'_2 = R^2 \quad (3.21)$$

Thus the  $r_2$  of any  $B$  is proportional to the inverse of the  $r_1$  of any surface obtained from  $S_e$  by spherical inversion about  $\underline{r}_e$ , the proportionality constant being equal to the square of the radius of inversion. This fact was originally proved by Szegö [5] and later by Boukamp [7], who was apparently unaware of Szegö's work. It was mentioned by Baum [2] as a way of calculating  $r_2$ 's.

Other people seem to have been mainly interested in it as a way of calculating  $r_1$ 's [7], [8].

Case 2:

From equation (3.20), we have

$$\frac{C'}{C_b} = 1 + \frac{C}{4\pi\epsilon_0 e} = 1 + \frac{C}{C_b} \cdot \frac{r_1}{e}.$$

By using the equivalent radii approximation for  $(\bar{C}/C_b)$ , and recalling that  $e = r_2$ , it follows that

$$\frac{\bar{C}'}{C_b} = 1 + \frac{r_1/r_2}{1-r_1/r_2} + \frac{r_1}{r_2} O[(r_1/r_2)^n]$$

where  $n$  is the order of  $\Delta$  for small  $(r_1/r_2)$  when  $E$  is a sphere. But, from equation (3.21),  $r_1/r_2 = r_1'/r_2'$ , and so

$$\frac{\bar{C}'}{C_b} = \frac{1}{1-(r_1'/r_2')} + O[(r_1'/r_2')^{n+1}] \quad (3.22)$$

Therefore, if  $n$  is the order of  $\Delta$  when  $E$  is a sphere, the order of  $\Delta$  when  $B$  is a sphere is  $n+1$ . The rest of this subsection is devoted to proving that  $n$  is five.

Employing the interior Green's function for a sphere ([6], Chap. IX, §4), we can write the following integral equation for the surface charge density on the  $B$  of figure 2

$$1 = \frac{1}{4\pi\epsilon_0} \int_{S_b} \frac{\sigma(\underline{r}')}{|\underline{r}-\underline{r}'|} dS' - \frac{1}{4\pi\epsilon_0} \int_{S_b} \frac{\sigma(\underline{r}')}{|\underline{r}-\underline{r}'|(e/r')^2} dS' \quad \underline{r} \text{ on } S_b \quad (3.23)$$

where the origin of coordinates is the center of  $S_e$ . Expanding the second integrand in equation (3.23) for small  $(r/e)$  and  $(r'/e)$ , we obtain

$$\begin{aligned} 1 + \frac{Q}{4\pi\epsilon_0 e} + \frac{\underline{r} \cdot \underline{p}}{4\pi\epsilon_0 e^3} - \frac{1}{4\pi\epsilon_0} \int_{S_b} \frac{\sigma(\underline{r}')}{e} \left( \frac{r r'}{e^2} \right)^2 \left( \frac{1 - \cos \gamma(\underline{r}, \underline{r}')}{2} \right) dS' + O[(r_1/e)^6] \\ = \frac{1}{4\pi\epsilon_0} \int_{S_b} \frac{\sigma(\underline{r}')}{|\underline{r}-\underline{r}'|} dS' \end{aligned} \quad (3.24)$$

where

$$Q = \int_{S_b} \sigma(\underline{r}) dS,$$

$$\underline{p} = \int_{S_b} \sigma(\underline{r}) \underline{r} dS,$$

and  $\gamma(\underline{r}, \underline{r}')$  is the angle between  $\underline{r}$  and  $\underline{r}'$ . We will now neglect terms of order  $(r_1/e)^5$  and higher. We will assume that we know the solution for  $\sigma(\underline{r})$  when  $E$  is removed and  $\phi(\underline{r}$  on  $S_b$ ) is either a constant or a linear function of position. That is to say we will assume  $\sigma_b(\underline{r})$  and  $\sigma_1(\underline{r})$  are known, where

$$1 = \frac{1}{4\pi\epsilon_0} \int_{S_b} \frac{\sigma_b(\underline{r}')}{|\underline{r}-\underline{r}'|} dS' \quad \underline{r} \text{ on } S_b \quad (3.25)$$

$$\underline{r} - \underline{r}_b = \frac{e}{4\pi\epsilon_0} \int_{S_b} \frac{\sigma_1(\underline{r}')}{|\underline{r}-\underline{r}'|} dS' \quad \underline{r} \text{ on } S_b \quad (3.26)$$

where  $\underline{r}_b$  is the position of the center of charge of  $B$ . By applying Green's reciprocation theorem ([4], §3.07) to the two problems defined by equations (3.25) and (3.26), it follows that

$$\int_{S_b} \sigma_1(\underline{r}) dS = 0 \quad (3.27)$$

Now, from the definitions of  $\sigma_b(\underline{r})$  and  $\sigma_1(\underline{r})$ , it is easy to show that, correct to fourth order in  $(r_1/e)$ , the solution of equation (3.24) may be written as

$$\sigma(\underline{r}) = \left( 1 + \frac{Q}{4\pi\epsilon_0 e} + \frac{\underline{r}_b \cdot \underline{p}}{4\pi\epsilon_0 e^3} \right) \sigma_b(\underline{r}) + \frac{\underline{p} \cdot \sigma_1(\underline{r})}{4\pi\epsilon_0 e^2} \quad (3.28)$$

If we integrate this equation over  $S_b$ , use equation (3.27), and rearrange the terms, we can quickly establish the following equation for  $(C/C_b)$ .

$$\frac{C}{C_b} = \left[ 1 - \frac{r_1}{e} \left( 1 + \frac{\underline{r}_b \cdot \underline{p}}{Qe^2} \right) \right]^{-1} + O \left[ \left( \frac{r_1+r_2}{e} \right)^5 \right] \quad (3.29)$$

But, from the definition of  $\underline{p}$ , and equations (3.26) and (3.28),

$$\begin{aligned}
 \underline{p} &= \underline{r}_b Q + \int_{S_b} (\underline{r} - \underline{r}_b) \sigma(\underline{r}) dS \\
 &= \underline{r}_b Q + \left\{ \int_{S_b} (\underline{r} - \underline{r}_b) \underline{\sigma}_1(\underline{r}) dS \right\} \cdot \frac{\underline{p}}{4\pi\epsilon_0 e^2} \\
 &= \underline{r}_b Q + \left\{ \frac{e}{4\pi\epsilon_0} \iint_{S_b} \frac{\underline{\sigma}_1(\underline{r}) \underline{\sigma}_1(\underline{r}')}{|\underline{r} - \underline{r}'|} dS dS' \right\} \cdot \frac{\underline{p}}{4\pi\epsilon_0 e^2} \quad (3.30)
 \end{aligned}$$

and it can be shown, using the definition of  $\underline{\sigma}_1(\underline{r})$ , that

$$\frac{1}{(4\pi\epsilon_0)^2 e} \iint_{S_b} \frac{\underline{\sigma}_1(\underline{r}) \underline{\sigma}_1(\underline{r}')}{|\underline{r} - \underline{r}'|} dS dS' = \frac{\underline{p}}{4\pi e^3} \equiv \underline{0} \quad (3.31)$$

where  $\underline{p}$  is the electric polarizability tensor of B (see, for example, [9] for some of the interesting properties of this tensor).  $\underline{p}$  is proportional to  $V_b$ , the volume of B, and has dimension  $V_b$ . It follows from equations (3.29) through (3.31) that, to order  $(r_1/e)^4$ ,

$$\frac{\underline{c}}{\underline{c}_b} = \left[ 1 - \frac{r_1}{e} \left( 1 + (\underline{r}_b/e) \cdot [\underline{I} - \underline{0}]^{-1} \cdot (\underline{r}_b/e) \right) \right]^{-1} \quad (3.32)$$

For small  $(V_b/4\pi e^3)$ , it can be shown that  $[\underline{I} - \underline{0}]^{-1}$  is positive definite and hence, to order  $(r_1/e)^4$ ,  $\underline{r}_{bm} = 0$ . Therefore, to the same order of accuracy,

$$\frac{\overline{c}}{\underline{c}_b} = \frac{1}{1 - (r_1/e)} \quad (3.33)$$

Since  $r_2 = e$ , we have thus shown that, if E is a sphere

$$\Delta \propto (r_1/r_2)^5. \quad (3.34)$$

From this equation, and the second special case of the inversion theorem at the beginning of this subsection, it is clear that if B is a sphere,

$$\Delta \propto (r_1/r_2)^6 \quad (3.35)$$

There is a point about the above arguments that might, at first, be a little disturbing. If B doesn't have a center of symmetry, then we know that the inclusion of terms of higher order than the fourth will probably shift  $\underline{r}_{bm}$  from zero. Will this change, if used in conjunction with equation (3.32), have enough effect to change the order of  $\Delta$ ? The answer is no, because if one includes the next order term (the term involving  $\gamma$  in equation (3.24)) as a perturbation, it turns out that  $\underline{r}_{bm} \propto (r_1/r_2)^3$ . When this type of variation is substituted back in equation (3.32), the extra error term is of higher order than five. Thus equation (3.34) is valid for any small B.

Before concluding this section, it might be well to point out that equation (3.32) can be useful as it stands for studying the variation of C with  $\underline{r}_b$  when  $r_b$  is close to zero. For example, if B is a sphere, it is not difficult to show that

$$\underline{Q} = (r_1/r_2)^3 \underline{I},$$

and thus

$$\frac{C}{C_b} = \left\{ 1 - \frac{r_1}{r_2} \left[ 1 + \frac{(r_b/r_2)^2}{1 - (r_1/r_2)^3} \right] \right\}^{-1} + O \left[ \left( \frac{r_1 + r_b}{r_2} \right)^5 \right] \quad (3.36)$$

It would seem that a useful future project might be to determine the generalization of equation (3.32) when E is an enclosure of arbitrary shape. In other words, what is  $C(\underline{r}_b)$  for small  $|\underline{r}_b - \underline{r}_{bm}|$  in general? We will not pursue this question further in this note.

#### IV. Accuracy of the Approximation -- Examples

In Section III, we found the order of magnitude of the error in  $\tilde{C}$  as  $(r_1/r_2)$  approaches zero. Our results suffice to indicate that  $\tilde{C}$  is a good approximation to  $\bar{C}$  for most satellite simulator applications, i.e., those cases where the satellite is fairly small compared to the size of the simulator enclosure.

But we have not found how large  $(r_1/r_2)$  can become before the equivalent radii approximation is useless. It would be nice to know the answer to this, because some satellite simulator designs will allow  $(r_1/r_2)$  to be a fair-sized fraction (a half, say) and compensate for the fact that  $C \neq C_b$  by precharging. Design calculations for this type of simulator would be greatly simplified if the equivalent radii approximation could still be used.

Establishing the largest value of  $(r_1/r_2)$  such that  $(C_b \Delta / \bar{C}) < \delta$ , for a given  $\delta$ , is a difficult task for a B and E of general shape. It amounts to solving the capacitance problem exactly. In the present section, we hope only to develop some intuition along this line by presenting the numerical solutions of four particular problems. It would seem, from these solutions, that  $(C_b \Delta / \bar{C})$  is of the order of .01, or less, if

$$\max_{\underline{r} \text{ on } S_b} |\underline{r} - \underline{r}_b| < \frac{1}{2} \min_{\underline{r} \text{ on } S_e} |\underline{r} - \underline{r}_e|, \quad (4.0)$$

but this must remain, for the present, a criterion of a rather conjectural nature.

The formulations of the following four problems are not new. The formulations of problems B and D have been given by the present author; the formulations of problems A and C are due to other authors. Appropriate references will be made within each subsection. The analytical treatment of each problem will consequently be kept rather brief; we will summarize the previous treatments. We have made new computer calculations for problems A, B, and C in order to augment the available numerical data. For problem B, there was no previous numerical data available at all; for problems A and C we have increased the number of cases previously treated by an order of magnitude. All results have been tabulated in such a way as to make it easy to evaluate the accuracy of the equivalent radii approximation for these four problems.

It might be well to point out here that in Subsections A and B we actually treat pairs of problems, each pair being related by a spherical inversion. We have not dignified the inverted problems by devoting separate subsections to them, but we have presented numerical results for them since these can be obtained by manipulations on the results for the original problems, and the results for the inverted problem exhibit a different kind of  $\Delta$  behavior (see Section III.B). To the best of the author's knowledge, explicit statements of the inverted problems have not been made before in the literature.

#### IV.A. Sphere in an Infinite Cylinder

The geometry of the problem to be solved is shown in figure 3a. The radius of the sphere is  $b$ ; the radius of the infinite cylinder is  $a$ . From symmetry, it is clear that  $r_{bm} = r_e$ , and this point can be chosen as any point on the axis of the cylinder. We can thus denote the capacitance between B and E, when  $r_e = r_b = 0$ , by  $\bar{C}$ . If this geometry is inverted, using an inversion sphere of radius  $(eb)^{1/2}$ , we obtain the situation shown in figure 3b, where B is the torus generated by rotating a circle of diameter  $b'$  ( $=eb/a$ ) about its tangent along the  $z$ -axis. It is easy to show, using the forms of the inversion theorem given in Section III, that once we have calculated  $\bar{C}/C_b$  we can obtain  $\bar{C}'/C_b'$ , the corresponding quantity for the inverted problem, from

$$\frac{\bar{C}'}{C_b'} = \left( \frac{\bar{C}}{C_b} - 1 \right) \frac{r_2}{r_1}, \quad (4.1)$$

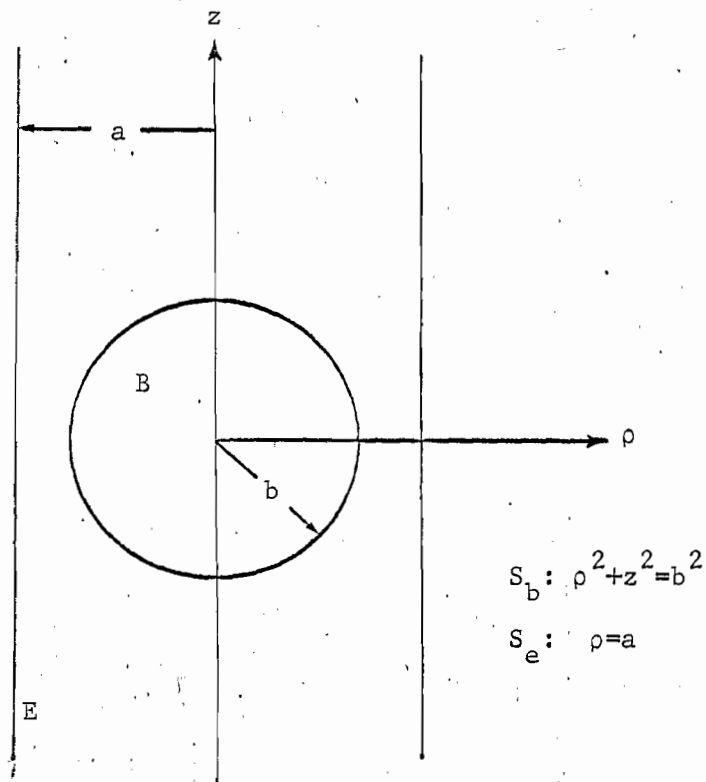
and that

$$\frac{\tilde{C}}{C_b} = \frac{\tilde{C}'}{C_b'} = \frac{1}{1-(r_1/r_2)} = \frac{1}{1-(r_1'/r_2')}, \quad (4.2)$$

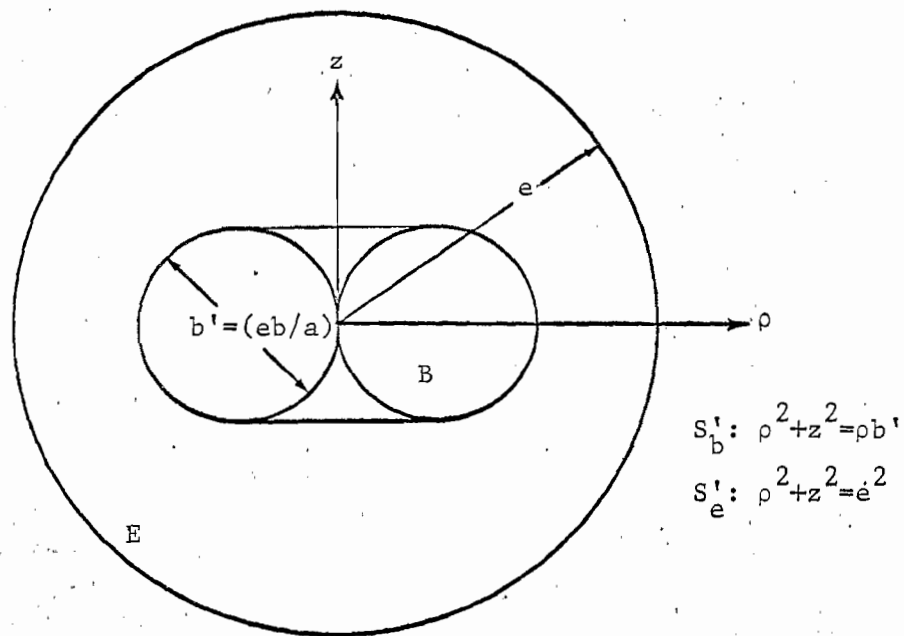
where

$$r_1 = b \qquad r_2 = \alpha a$$

$$r_1' = (eb/\alpha a) = (b'/\alpha) \qquad r_2' = e$$



3a. original geometry.



3b. geometry after inversion.

Figure 3. A sphere in an infinite cylinder.

and, as will be shown,

$$\alpha = \left[ \frac{2}{\pi} \int_0^{\infty} \frac{dx}{I_0^2(x)} \right]^{-1} \quad (4.3)$$

$$= 1.148515$$

In equation (4.3),  $I_0(x)$  is the modified Bessel function of the first kind, of order zero.

With these simple relations in mind, let us now concentrate on calculating the capacitance in the situation shown in figure 3a, and return to the situation shown in figure 3b only to present the results for that case. Thus we want to solve the problem

$$\nabla^2 \phi(\rho, z) = 0 \quad \rho \leq a \quad \text{and} \quad r \geq b \quad (4.4)$$

$$\phi(r=b) = 1; \quad \phi(\rho=a) = 0$$

where

$$r = \sqrt{\rho^2 + z^2},$$

and then compute

$$\frac{\bar{C}}{C_b} = - \frac{1}{4\pi b} \int_{S_b} \frac{\partial \phi(r=b)}{\partial r} dS \quad (4.5)$$

This problem has had a fairly long history. Apparently Knight [10] was the first worker to formulate it in terms of an infinite set of linear algebraic equations for the coefficients of the spherical harmonic expansion of the surface charge density on the sphere. Also, by making what was at that time a large numerical effort, Knight actually computed the capacitance, to four figure accuracy, for  $(b/a)$  values of .1, .2, .3, .4, and .5. His labor would have been reduced had he been aware of some earlier work of Watson [11], in

which the integrals that must be evaluated to determine Knight's matrix elements are elegantly transformed into some rather rapidly converging sums.

A later treatment of the problem was given in 1960 by Smythe [12], who used a slightly different method from Knight's to obtain the same infinite set of equations. Smythe was apparently unaware of Knight's or Watson's work at the time, although by 1963, when he treated the more general problem of a spheroid inside a cylinder (and also corrected some small numerical errors in his 1960 paper) [13], he refers to Knight's work, and also to Watson's. Smythe had a digital computer available (a Burrough Datatron 205), and so he could evaluate the required integrals more accurately than Knight. His corrected values for  $(\bar{C}/C_b)$  [13] are accurate to at least seven figures. He treats  $(b/a)$  values of .1(.1).9 and .95.

A still later treatment is that of Chang and Chang in 1968 [14]. These workers again obtain Knight's equations. They evaluate the necessary integrals to four figure accuracy. The interesting thing about the Chang's work is that a statement is made ([14], eq. 17) that is equivalent to the equation

$$\frac{\bar{C}}{C_b} = \frac{1}{1-(b/\alpha a)} + O[(b/a)^5]. \quad (4.6)$$

Actually, a close examination of the equations from which this is derived ([14], eqs. (13) and (16)) reveals that the order of the error could actually be stated as  $O[(b/a)^6]$ . This type of error has been shown to hold for a sphere inside an E of general shape in Section III.B. Nevertheless, the first part of equation (4.6) is a special case of the equivalent radii approximation, and statements of this kind are few and far between in the literature on electrostatics.

In fact, these statements are so rare that it is worth a digressory paragraph to bring up a later work of Chang and Chang [15]. In [15], the method of matched asymptotic expansions ([16], Chap. 5) is used to show that, for a general axisymmetric B inside an infinite cylindrical E ([15], eq. 22)

$$\frac{\bar{C}}{C_b} = \frac{1}{1-(r_1/\alpha a)} + O[(r_1/a)^2].$$

It is interesting that again Chang and Chang overstate the error by an order

of magnitude. The point where this overstatement comes in is in going from their equation (14) to their equation (15) since, near B,  $\tilde{\rho}$  and  $\tilde{z}$  are small, and an approximate evaluation of the integral in (14) for small  $\tilde{\rho}$  and  $\tilde{z}$  leads to a third order error term in (15). Alternatively, one can recall the third order error derived for a general B and E in Section III.A of this note. The example in reference [15] exhibits the third order error, but the authors overlook this fact.

Now let us derive Knight's equations and calculate  $(\bar{C}/C_b)$  for (b/a) values of .01(.01).99.

By standard techniques, the Green's function for an infinite cylinder, when the source point is at the origin, can be shown to be

$$G_e(\rho, z; 0, 0) = \frac{1}{4\pi r} - \frac{1}{2\pi^2} \int_0^\infty \frac{K_0(\lambda a)}{I_0(\lambda a)} I_0(\lambda \rho) \cos \lambda z d\lambda, \quad (4.7)$$

where  $I_0$  and  $K_0$  are modified Bessel functions. The validity of this representation of  $G_e$  is clear from the facts that it satisfies Laplace's equation for  $r > 0$ , has the correct singularity as  $r \rightarrow 0$ , and is equal to zero on  $\rho = a$  (the last relation follows from the known Fourier transform of  $K_0(\lambda a)$  given, for example, in [17], page 412).

Any z-derivative of  $G_e$  is also a solution of Laplace's equation for  $r > 0$  that is equal to zero on  $\rho = a$ . We may use the identity ([14] Appendix A)

$$I_0(\lambda \rho) \cos \lambda z = \sum_{m=0}^{\infty} \frac{\lambda^{2m} r^{2m}}{(2m)!} (-)^m P_{2m}(z/r), \quad (4.8)$$

to write the even z-derivatives of  $G_e$  as

$$\phi_n \equiv \frac{1}{(2n)!} \frac{\partial^{2n} G_e}{\partial z^{2n}} = \frac{P_{2n}(z/r)}{4\pi r^{2n+1}} - \sum_{m=0}^{\infty} M_{nm} r^{2m} P_{2m}(z/r) \quad (4.9)$$

where

$$M_{nm} = \frac{1}{2\pi^2} \frac{(-)^{n+m}}{z^{2n+2m+1}} \cdot \frac{1}{(2n)!(2m)!} \int_0^\infty \frac{\lambda^{2(n+m)} K_0(\lambda)}{I_0(\lambda)} d\lambda \quad (4.10)$$

By partial integration and the use of the Wronskian relation for modified

Bessel functions

$$\int_0^\infty \frac{\lambda^{2n} K_0(\lambda) d\lambda}{I_0(\lambda)} = \frac{1}{2n+1} \int_0^\infty \frac{\lambda^{2n}}{I_0^2(\lambda)} d\lambda \equiv \frac{I(2n,1)}{2n+1}, \quad (4.11)$$

and thus

$$M_{nm} = \frac{(-1/a^2)^{n+m} I(2n+2m,1)}{2\pi^2 a (2n)! (2m)! (2n+2m+1)}$$

The  $I(2n,1)$  must be evaluated numerically. Smythe has given a table of them [13]. We found it necessary to extend his table in order to obtain accurate  $\bar{C}$  results for  $(b/a)$  close to unity. We will not tabulate these intermediate results here, but we will indicate the method by which they were calculated. The way we calculated the  $I(2n,1)$  was to use Watson's results [11] to write them in the form

$$I(2n,1) \equiv \int_0^\infty \frac{\lambda^{2n} d\lambda}{I_0^2(\lambda)} \quad (4.12)$$

$$= \beta \sum_{m=0}^{\infty} \frac{[(m+\frac{1}{2})\beta]^{2n}}{I_0^2[(m+\frac{1}{2})\beta]} + \pi(-)^n \sum_{m=1}^{\infty} \frac{\mu_m^{2n-1}}{J_1^2(\mu_m)} \left[ \frac{g_m}{\cosh^2 g_m} - \frac{(2n+1)e^{-g_m}}{\cosh g_m} \right] \quad (4.13)$$

where

$$g_m = \pi\mu_m/\beta,$$

the  $\mu_m$ 's are the roots of

$$J_0(\mu_m) = 0,$$

and  $\beta$  may be any value we choose. By choosing  $\beta$  carefully, both series in equation (4.13) can be made to converge rapidly. We note, as a matter of interest, that the first series in equation (4.13) is just the numerical integration of the integral defining  $I(2n,1)$  in (4.12) based on the rectangular integration rule with rectangles of width  $\beta$ . The second series may thus be

looked upon as a correction term to be added to the result of a simple numerical integration.

It is a convenient time to note, from equation (4.7), that the nonsingular part of  $G_e$  at the origin is given by

$$-\frac{1}{2\pi^2} \int_0^\infty \frac{K_0(\lambda a)}{I_0(\lambda a)} d\lambda.$$

Thus, from equations (3.6) and (4.11),

$$r_2 = [(2/\pi)I(0,1)]^{-1} a,$$

This proves equation (4.3).

Now, any combination of the  $\phi_n$ 's is also a solution of Laplace's equation and equal to zero on the cylinder. The combination that is equal to unity over the sphere is clearly given by

$$\phi(\rho, z) = \sum_{n=0}^{\infty} a^{2n+1} x_n \phi_n(r, z/r) \quad (4.14)$$

where

$$\sum_{n=0}^{\infty} \frac{x_n P_{2n}(z/r)}{4\pi(b/a)^{2n+1}} - \sum_{n,m=0}^{\infty} x_n a^{2n+1} b^{2m} M_{nm} P_{2m}(z/r) = 1 \quad (4.15)$$

over the entire sphere. The orthogonality of the  $P_m$ 's over the sphere allows us to write these equations as

$$\left\{ 1 - \frac{2}{\pi} \frac{(b/a)^{4n+1} I(4n,1)}{[(2n)!]^2 (4n+1)} \right\} x_n = 4\pi(b/a) \delta_{n0} + (b/a)^{4n+1} \sum_{m \neq n} \frac{2}{\pi} \frac{2(-)^{n+m} I(2n+2m,1)}{(2n)!(2m)!(2n+2m+1)} x_m. \quad (4.16)$$

These equations may be solved for the  $x_n$ 's by truncating the series and inverting the resulting finite matrix equation. One can keep doubling the number of  $x_n$ 's involved until he is satisfied that the accuracy of the lower  $x_n$ 's is adequate. From equations (4.5), (4.9) and (4.14) it follows that

$$\frac{\bar{C}}{C_b} = \frac{x_0}{4\pi(b/a)}, \quad (4.17)$$

and so an accurate value of  $x_0$  is all we need. Equation (4.17), in conjunction with an iteration solution of equation (4.16), demonstrates the sixth order error of  $(\bar{C}/C_b)$  for this special case.

Accurate values of  $\bar{C}/C_b$  are given in table 1, along with the corresponding values of  $\tilde{C}/C_b$  and the percentage error in  $\tilde{C}/C_b$ . The numerical results exhibit the sixth order error dependence. This data is also presented graphically in figure 4.

We have used equation (4.2) to calculate the data in the last two columns of table 1, which are for a toroid inside a sphere (the geometry of figure 3b), from the data in the second two columns of table 1. Here the error exhibits the expected fifth order dependence on  $(b'/e)$ . This data is also presented graphically in figure 4.

In the table, we have not given all the significant figures for  $\bar{C}/C_b$  and  $\tilde{C}/C_b$  that were necessary to calculate the error to .001%. These figures were available from the computer printout, which is believed to be accurate to eight significant figures, but these extra figures are not very interesting except for the calculation of the percentage error.

#### IV.B. Sphere Between Two Infinite Plates

The geometry of the problem to be solved is shown in figure 5a. The radius of the sphere is  $b$ ; the distance between the parallel plates is  $2a$ . From symmetry, it is clear that  $r_{bm} = r_e$ , and this point can be chosen anywhere on the plane midway between the plates. We can thus denote the capacitance between B and E when  $r_e = r_b = 0$  by  $\bar{C}$ . If this geometry is inverted, using an inversion sphere of radius  $(eb)^{1/2}$ , we obtain the situation shown in figure 5b, where B is made up of two identical spheres, whose diameters are  $b'$  ( $=eb/a$ ), in contact at the origin. With the notation we have chosen, equations (4.1) and (4.2) can be directly applied to the present case, but equation (4.3) must be changed to

$$\begin{aligned} \alpha &= (\ln 2)^{-1} \\ &= 1.442695 \end{aligned} \quad (4.18)$$

Table 1. Capacitance of a sphere in an infinite cylinder

$b/a$ or $b'/e$	$\bar{C}/C_b = \bar{C}'/C'_b$	$\bar{C}/C_b$	$(C_b \Delta \bar{C})\%$	$\bar{C}'/C'_b$	$(C'_b \Delta \bar{C}')\%$
.01	1.00878	1.00878	.000	1.00878	.000
.02	1.01772	1.01772	.000	1.01772	.000
.03	1.02682	1.02682	.000	1.02682	.000
.04	1.03608	1.03608	.000	1.03608	.000
.05	1.04552	1.04552	.000	1.04552	.000
.06	1.05512	1.05512	.000	1.05512	.000
.07	1.06490	1.06490	.000	1.06490	.000
.08	1.07487	1.07487	.000	1.07487	.000
.09	1.08502	1.08502	.000	1.08502	.000
.10	1.09537	1.09537	.000	1.09537	.000
.11	1.10592	1.10592	.000	1.10592	.000
.12	1.11667	1.11667	.000	1.11667	.000
.13	1.12764	1.12764	.000	1.12764	.000
.14	1.13882	1.13882	.000	1.13882	.000
.15	1.15022	1.15022	.000	1.15023	.000
.16	1.16186	1.16186	.000	1.16187	.001
.17	1.17373	1.17373	.000	1.17374	.001
.18	1.18585	1.18585	.000	1.18586	.001
.19	1.19823	1.19823	.000	1.19824	.001
.20	1.21086	1.21086	.000	1.21088	.002
.21	1.22376	1.22376	.000	1.22379	.002
.22	1.23694	1.23694	.000	1.23698	.003
.23	1.25041	1.25041	.001	1.25045	.004
.24	1.26417	1.26418	.001	1.26423	.005
.25	1.27824	1.27825	.001	1.27831	.006
.26	1.29262	1.29265	.002	1.29272	.007
.27	1.30734	1.30736	.002	1.30746	.009
.28	1.32239	1.32242	.003	1.32254	.011
.29	1.33779	1.33784	.003	1.33797	.013
.30	1.35356	1.35362	.004	1.35378	.016
.31	1.36970	1.36977	.005	1.36996	.019
.32	1.38624	1.38632	.006	1.38655	.023
.33	1.40317	1.40328	.008	1.40355	.027
.34	1.42053	1.42066	.009	1.42097	.031
.35	1.43832	1.43848	.011	1.43884	.037
.36	1.45656	1.45675	.013	1.45718	.043
.37	1.47527	1.47550	.016	1.47600	.050
.38	1.49446	1.49475	.019	1.49533	.058
.39	1.51417	1.51451	.022	1.51517	.067
.40	1.53439	1.53480	.027	1.53557	.077
.41	1.55517	1.55566	.031	1.55654	.088
.42	1.57652	1.57710	.037	1.57811	.101
.43	1.59846	1.59915	.043	1.60030	.115
.44	1.62102	1.62183	.050	1.62315	.131
.45	1.64423	1.64519	.058	1.64668	.149
.46	1.66811	1.66923	.067	1.67093	.169
.47	1.69269	1.69401	.078	1.69593	.191
.48	1.71801	1.71956	.090	1.72172	.215
.49	1.74410	1.74591	.103	1.74834	.243
.50	1.77100	1.77310	.119	1.77584	.273

Table 1 (Continued)

b/a or b'/e	$\bar{c}/c_b = \bar{c}'/c'_b$	$\bar{c}/c_b$	$(c_b \Delta / \bar{c})\%$	$\bar{c}'/c'_b$	$(c'_b \Delta' / \bar{c}')\%$
.51	1.79873	1.80119	.136	1.80426	.307
.52	1.82735	1.83020	.156	1.83365	.344
.53	1.85690	1.86020	.178	1.86407	.385
.54	1.88741	1.89124	.202	1.89556	.430
.55	1.91895	1.92338	.230	1.92820	.480
.56	1.95156	1.95667	.261	1.96206	.536
.57	1.98529	1.99119	.297	1.99719	.596
.58	2.02021	2.02702	.336	2.03370	.664
.59	2.05638	2.06422	.380	2.07165	.737
.60	2.09387	2.10289	.429	2.11115	.819
.61	2.13276	2.14313	.484	2.15230	.908
.62	2.17311	2.18503	.546	2.19520	1.007
.63	2.21502	2.22871	.614	2.23999	1.115
.64	2.25858	2.27430	.691	2.28680	1.234
.65	2.30389	2.32193	.777	2.33577	1.366
.66	2.35105	2.37174	.873	2.38707	1.510
.67	2.40018	2.42392	.980	2.44089	1.668
.68	2.45141	2.47865	1.099	2.49742	1.843
.69	2.50487	2.53612	1.232	2.55690	2.035
.70	2.56072	2.59658	1.381	2.61957	2.247
.71	2.61912	2.66028	1.547	2.68571	2.480
.72	2.68024	2.72751	1.733	2.75565	2.737
.73	2.74428	2.79860	1.941	2.82975	3.021
.74	2.81146	2.87392	2.173	2.90841	3.334
.75	2.88201	2.95389	2.434	2.99210	3.680
.76	2.95619	3.03901	2.725	3.08136	4.063
.77	3.03429	3.12983	3.053	3.17681	4.487
.78	3.11663	3.22700	3.420	3.27916	4.957
.79	3.20356	3.33128	3.834	3.38926	5.480
.80	3.29549	3.44355	4.300	3.50807	6.061
.81	3.39284	3.56487	4.826	3.63678	6.709
.82	3.49612	3.69649	5.421	3.77677	7.432
.83	3.60588	3.83991	6.095	3.92973	8.242
.84	3.72276	3.99697	6.860	4.09770	9.151
.85	3.84748	4.16994	7.733	4.28320	10.174
.86	3.98083	4.36162	8.730	4.48939	11.329
.87	4.12377	4.57559	9.875	4.72026	12.638
.88	4.27735	4.81644	11.193	4.98095	14.127
.89	4.44281	5.09019	12.718	5.27826	15.829
.90	4.62158	5.40495	14.493	5.62127	17.785
.91	4.81535	5.77188	16.572	6.02261	20.047
.92	5.02608	6.20693	19.025	6.50026	22.680
.93	5.25610	6.73381	21.945	7.08104	25.774
.94	5.50818	7.38956	25.460	7.80692	29.446
.95	5.78565	8.23614	29.753	8.74822	33.866
.96	6.09257	9.38702	35.096	10.03397	39.282
.97	6.43387	11.07971	41.931	11.93479	46.092
.98	6.81568	13.93042	51.073	15.15385	55.025
.99	7.24566	20.39301	64.470	22.49814	67.795
1.00	7.73355	$\infty$	100.000	$\infty$	100.000

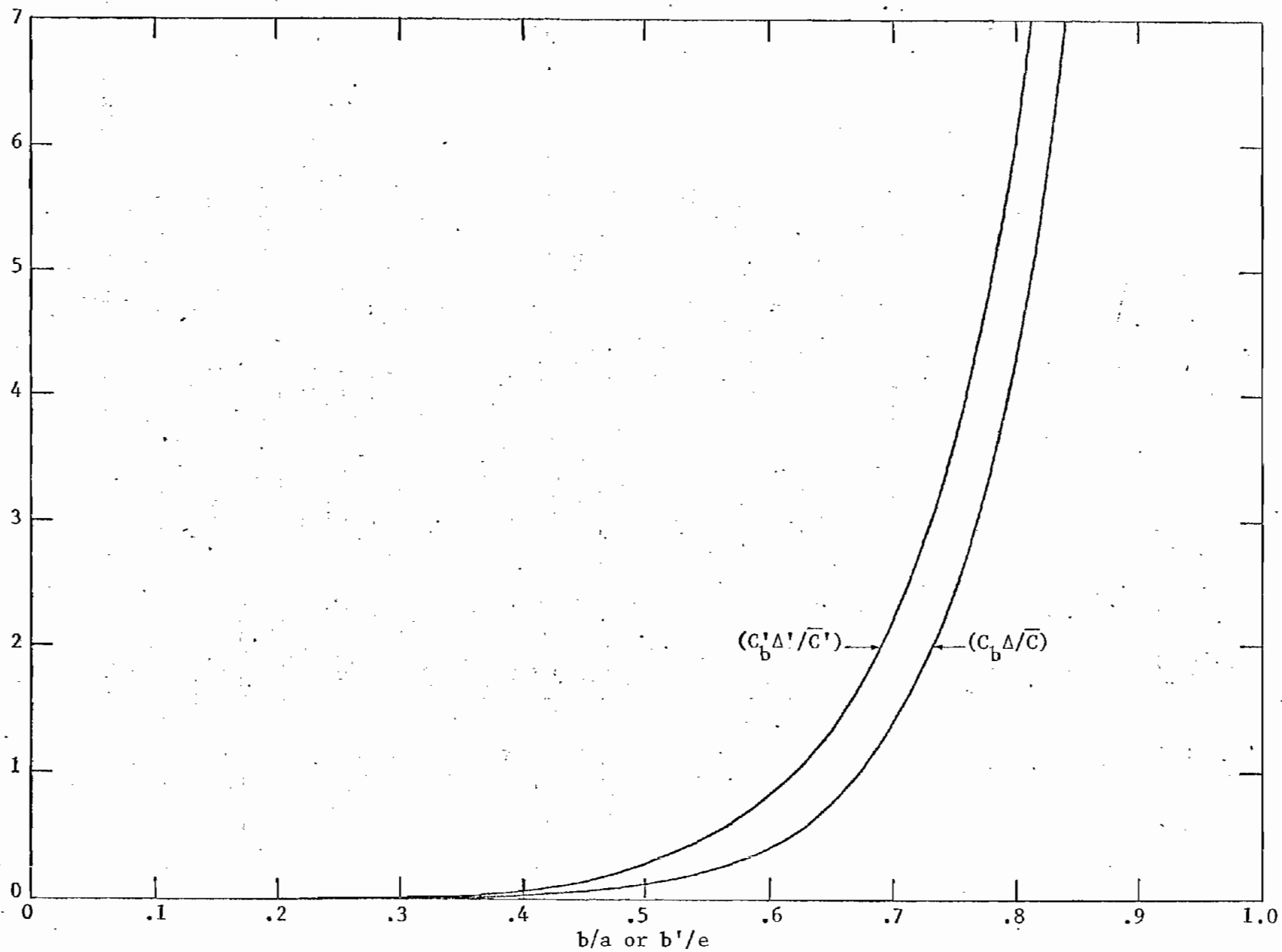
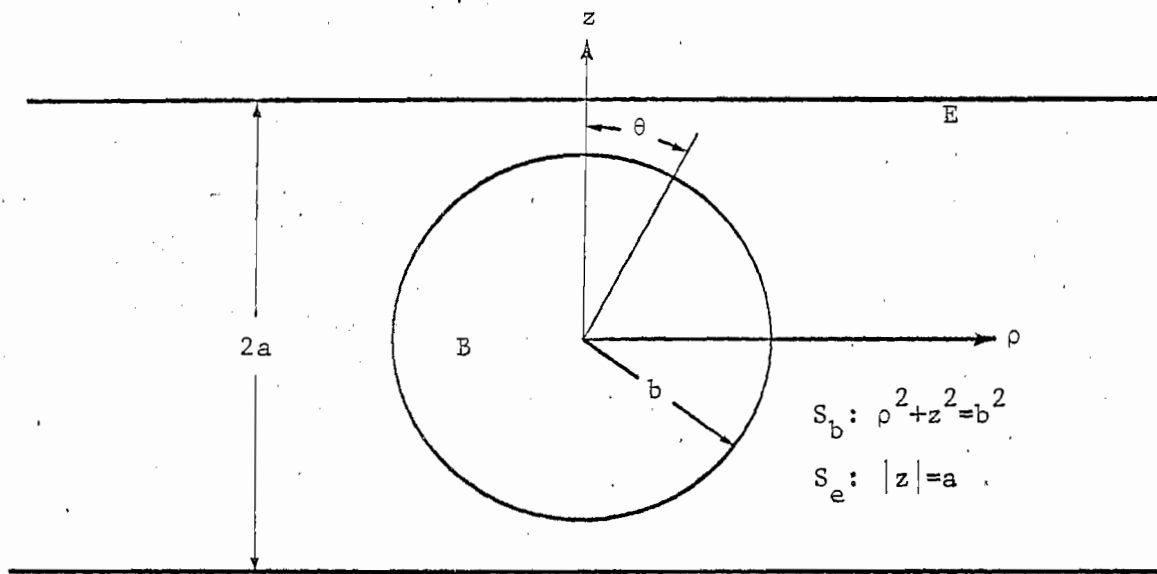
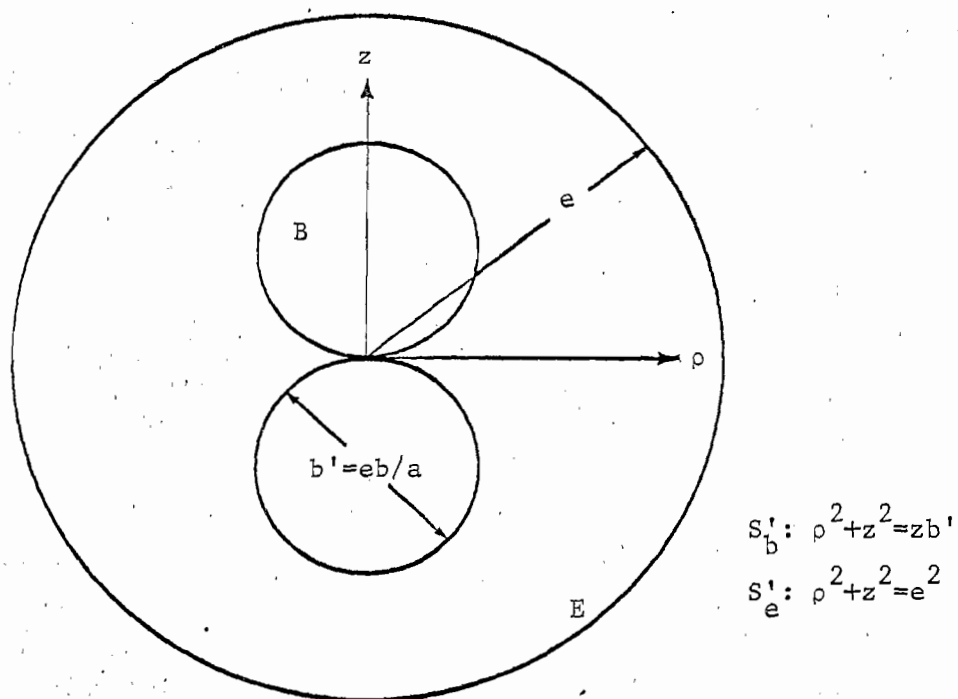
error  
in  
percent

Figure 4. Error of the approximation for the case of a sphere in an infinite cylinder.



5a. original geometry



5b. geometry after inversion

Figure 5. A sphere between parallel plates.

Thus the  $r_1'$  of two osculating spheres of diameter  $b'$  is just  $b' \ln 2$  (in agreement with [7]).

That equation (4.18) gives the correct value of  $\alpha$  follows from the fact that the Green's function for the parallel-plate region, with the source point at the origin, may be represented by the image series

$$G_e(\rho, z; 00) = \frac{1}{4\pi\sqrt{\rho^2+z^2}} + \frac{1}{2\pi} \sum_{n=1}^{\infty} \frac{(-)^n}{\sqrt{\rho^2+(z-2nd)^2}}, \quad (4.19)$$

and so, from equations (3.6) and (4.19),

$$\frac{1}{r_2} = - \sum_{n=1}^{\infty} \frac{(-)^n}{nd}$$

which, together with the definition  $r_2 \equiv \alpha a$ , results in equation (4.18).

As in the previous subsection, we will concentrate on calculating the capacitance when B is the sphere, and only return to the geometry of figure 5b when we tabulate the results.

The problem of figure 5a has actually been treated in a previous note in this series [18], although no numerical results were calculated at that time. Therefore, let us assume that that note is available to anyone reading the present note, and just briefly discuss the method of solution and then state the equations to be used for the numerical work.

The method of solution, as in the previous subsection, is to derive an infinite set of linear algebraic equations for the spherical harmonic expansion of the surface charge density on the sphere. Again this can be accomplished by considering linear combinations of the successive  $z$ -derivatives of  $G_e(\rho, z; 00)$ , and enforcing the condition that the potential be unity over the whole sphere. This calculational program leads to a set of equations for the normalized charge density coefficients  $x_{2n}$ , defined by

$$\sigma(\theta) = \sum_{n=0}^{\infty} x_{2n} \frac{(4n+1)}{b} \epsilon_0 P_{2n}(\cos \theta). \quad (4.20)$$

The set of equations to be solved is

$$\sum_{m=0}^{\infty} M_{nm} x_{2m} = \delta_{no} \quad (4.21)$$

where

$$M_{00} = 1 - (b/a) \ln 2$$

$$M_{nm} = \delta_{nm}$$

$$- \frac{(2n+2m)!}{(2n)!(2m)!} (2^{-2(n+m)} - 2^{-4(n+m)}) \zeta(2n+2m+1) (b/a)^{2n+2m+1},$$

$$n \text{ or } m > 0, \quad (4.22)$$

and  $\zeta(z)$  is the Riemann-Zeta function ([19], Chap. 23).

Once the  $x_{2n}$ 's have been determined by truncating and solving the set (4.21), the capacitance is determined by the simple relation [18],

$$\bar{C}/C_b = x_0$$

Table 2 contains the numerical data on this problem. Again we have tabulated  $\bar{C}/C_b$ ,  $\bar{C}/C'_b$ ,  $\bar{C}'/C'_b$ , and the errors of the effective radii approximation for the two inversion-related geometries of figure 5. Figure 6 is similar to figure 4; it shows graphically how the error of the effective radii approximation varies with  $b/a$  (or  $b'/e$ ) in the two inversion-related problems.

To the best of the author's knowledge, there has been no previous numerical data published on this problem. In fact, reference 18 seems to be the only other place where this problem has been considered for a sphere of arbitrary size, but there may be some relevant publication that the author is unaware of.

#### IV.C. Disk in an Infinite Cylinder

The geometry of the problem is shown in figure 7. The radius of the cylinder is  $a$ , and the radius of the disk, whose axis of symmetry is the same as that of the cylinder, is  $b$ . From symmetry, it is clear that  $\underline{r}_{-bm} = \underline{r}_e$ , and this point can be chosen anywhere on the axis of symmetry of the system. We can thus denote the capacitance between B and E when  $\underline{r}_e = \underline{r}_b = 0$  by  $\bar{C}$ .

Table 2. Capacitance of a sphere between parallel plates

b/a or b'/e	$\bar{C}/C_b = \bar{C}'/C'_b$	$\bar{C}/C_b$	$(C_b \Delta / \bar{C})\%$	$\bar{C}'/C'_b$	$(C'_b \Delta' / \bar{C}')\%$
.01	1.00698	1.00698	.000	1.00698	.000
.02	1.01505	1.01505	.000	1.01505	.000
.03	1.02124	1.02124	.000	1.02124	.000
.04	1.02852	1.02852	.000	1.02852	.000
.05	1.03590	1.03590	.000	1.03590	.000
.06	1.04339	1.04339	.000	1.04339	.000
.07	1.05099	1.05099	.000	1.05099	.000
.08	1.05871	1.05871	.000	1.05871	.000
.09	1.06653	1.06653	.000	1.06653	.000
.10	1.07448	1.07448	.000	1.07448	.000
.11	1.08254	1.08254	.000	1.08254	.000
.12	1.09072	1.09072	.000	1.09072	.000
.13	1.09903	1.09903	.000	1.09903	.000
.14	1.10747	1.10747	.000	1.10747	.000
.15	1.11604	1.11604	.000	1.11604	.001
.16	1.12474	1.12474	.000	1.12475	.001
.17	1.13358	1.13358	.000	1.13359	.001
.18	1.14255	1.14255	.000	1.14257	.002
.19	1.15167	1.15168	.000	1.15170	.002
.20	1.16094	1.16095	.000	1.16097	.003
.21	1.17036	1.17036	.001	1.17040	.003
.22	1.17993	1.17994	.001	1.17998	.004
.23	1.18966	1.18967	.001	1.18973	.006
.24	1.19955	1.19957	.001	1.19964	.007
.25	1.20961	1.20963	.002	1.20971	.009
.26	1.21984	1.21986	.002	1.21997	.011
.27	1.23024	1.23027	.002	1.23040	.013
.28	1.24082	1.24086	.003	1.24101	.016
.29	1.25158	1.25163	.004	1.25182	.019
.30	1.26254	1.26260	.005	1.26282	.023
.31	1.27368	1.27376	.006	1.27402	.027
.32	1.28503	1.28512	.007	1.28544	.032
.33	1.29658	1.29669	.009	1.29706	.037
.34	1.30834	1.30847	.010	1.30891	.044
.35	1.32031	1.32047	.012	1.32098	.051
.36	1.33250	1.33270	.015	1.33329	.059
.37	1.34493	1.34516	.018	1.34585	.069
.38	1.35758	1.35787	.021	1.35866	.079
.39	1.37048	1.37082	.025	1.37173	.091
.40	1.38362	1.38402	.029	1.38507	.104
.41	1.39702	1.39749	.034	1.39869	.119
.42	1.41068	1.41124	.040	1.41260	.136
.43	1.42461	1.42527	.046	1.42816	.149
.44	1.43882	1.43959	.054	1.44134	.175
.45	1.45331	1.45421	.062	1.45620	.198
.46	1.46810	1.46915	.071	1.47139	.224
.47	1.48319	1.48441	.082	1.48694	.252
.48	1.49860	1.50002	.094	1.50285	.283
.49	1.51433	1.51597	.108	1.51985	.317
.50	1.53039	1.53229	.123	1.53585	.355

Table 2 (Continued)

b/a or b'/e	$\bar{c}/c_b = \bar{c}'/c'_b$	$\bar{c}/c_b$	$(c_b \Delta / \bar{c})\%$	$\bar{c}'/c'_b$	$(c'_b \Delta' / \bar{c}')\%$
.51	1.54680	1.54898	.141	1.55297	.397
.52	1.56357	1.56607	.160	1.57052	.443
.53	1.58070	1.58358	.182	1.58854	.493
.54	1.59821	1.60151	.206	1.60703	.549
.55	1.61611	1.61989	.233	1.62602	.609
.56	1.63442	1.63874	.263	1.64554	.676
.57	1.65315	1.65807	.297	1.66561	.748
.58	1.67231	1.67792	.334	1.68627	.827
.59	1.69192	1.69831	.376	1.70753	.914
.60	1.71200	1.71926	.422	1.72945	1.009
.61	1.73256	1.74080	.473	1.75204	1.112
.62	1.75362	1.76296	.530	1.77536	1.224
.63	1.77520	1.78578	.593	1.79944	1.347
.64	1.79731	1.80930	.662	1.82433	1.481
.65	1.81999	1.83354	.739	1.85007	1.626
.66	1.84324	1.85856	.824	1.87674	1.785
.67	1.86710	1.88441	.919	1.90437	1.957
.68	1.89158	1.91112	1.023	1.93304	2.145
.69	1.91671	1.93876	1.138	1.96282	2.349
.70	1.94251	1.96739	1.265	1.99379	2.572
.71	1.96903	1.99708	1.405	2.02604	2.814
.72	1.99627	2.02790	1.560	2.05965	3.077
.73	2.02428	2.05994	1.731	2.09476	3.364
.74	2.05309	2.09329	1.920	2.13146	3.677
.75	2.08273	2.12805	2.130	2.16991	4.018
.76	2.11324	2.16434	2.361	2.21024	4.389
.77	2.14465	2.20229	2.617	2.25265	4.794
.78	2.17701	2.24205	2.901	2.29731	5.237
.79	2.21037	2.28380	3.215	2.34447	5.720
.80	2.24476	2.32772	3.564	2.39437	6.248
.81	2.28024	2.37405	3.952	2.44733	6.827
.82	2.31686	2.42305	4.382	2.50369	7.462
.83	2.35467	2.47502	4.862	2.56386	8.159
.84	2.39374	2.53034	5.398	2.62835	8.926
.85	2.43412	2.58944	5.998	2.69774	9.772
.86	2.47590	2.65285	6.671	2.77274	10.706
.87	2.51913	2.72122	7.426	2.85424	11.741
.88	2.56390	2.79535	8.280	2.94334	12.891
.89	2.61029	2.87625	9.247	3.04142	14.175
.90	2.65839	2.96525	10.348	3.15028	15.614
.91	2.70829	3.06405	11.611	3.27230	17.236
.92	2.76011	3.17500	13.067	3.41071	19.075
.93	2.81394	3.30138	14.765	3.57010	21.180
.94	2.86992	3.44802	16.766	3.75717	23.615
.95	2.92817	3.62238	19.164	3.98241	26.472
.96	2.98883	3.83702	22.105	4.26349	29.897
.97	3.05206	4.11548	25.840	4.63370	34.133
.98	3.11803	4.51075	30.876	5.16831	39.670
.99	3.18690	5.19213	38.620	6.10905	47.833
1.00	3.25889	$\infty$	100.00	$\infty$	100.00

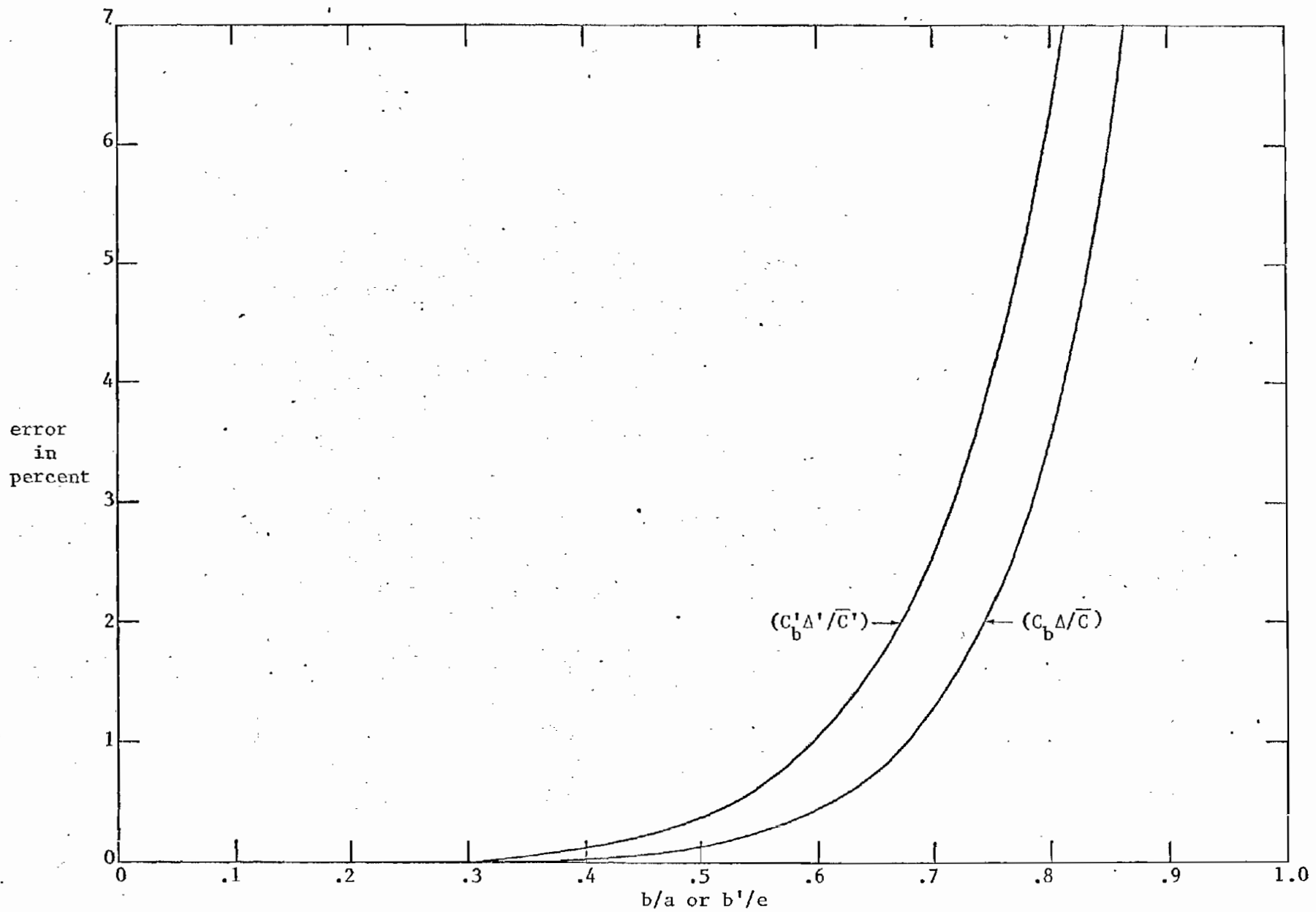


Figure 6. Error of the approximation for the case of a sphere between parallel plates.

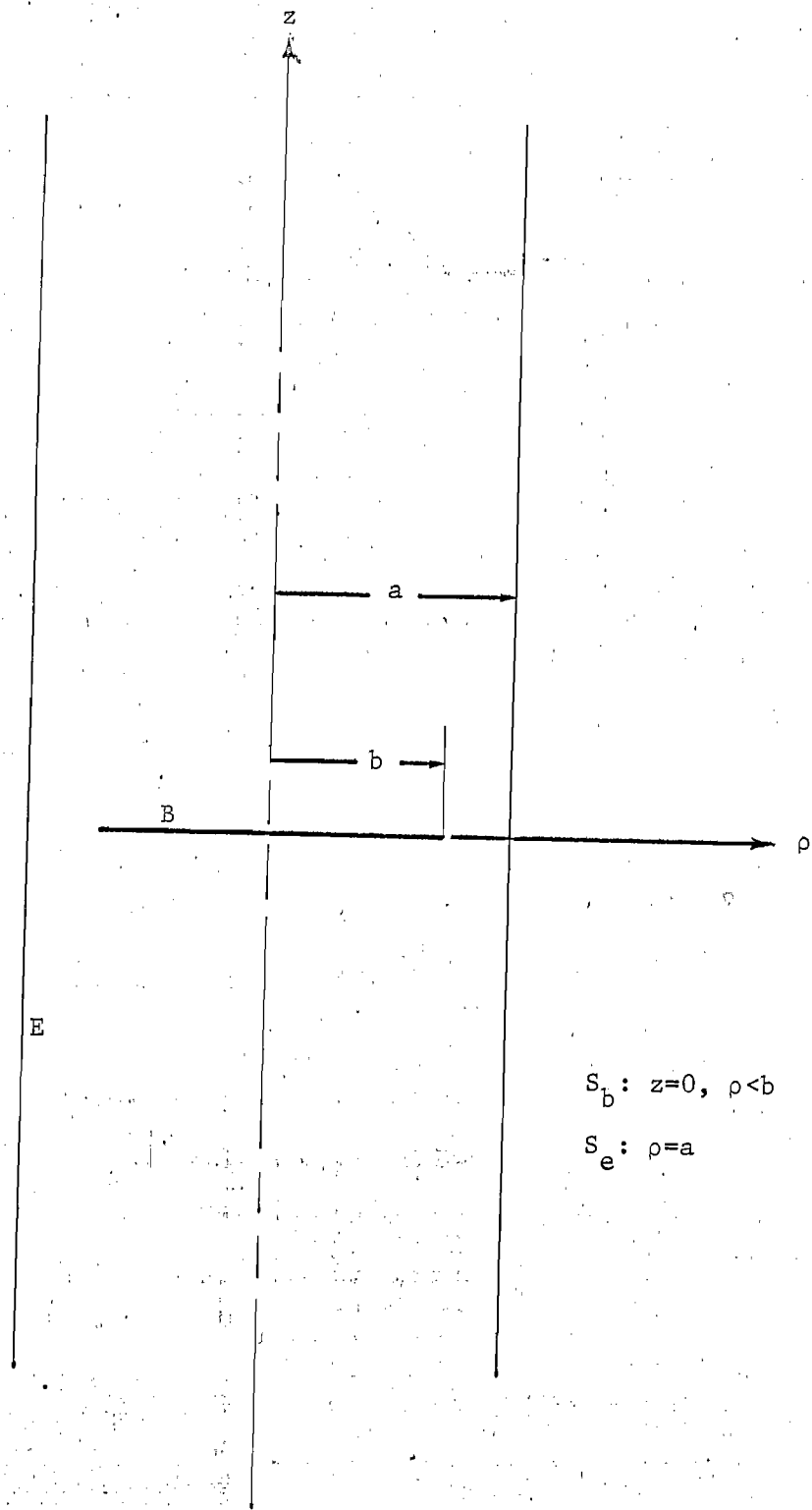


Figure 7. A disk in an infinite cylinder.

The equivalent radii of this B-E configuration are easily obtained. From the capacitance of an isolated disk ([47], §5.03),

$$r_1 = \frac{8\epsilon b}{4\pi\epsilon} = \frac{2}{\pi} b, \quad (4.23)$$

and from Section IV.A,

$$r_2 = 1.148515a.$$

Thus

$$\frac{\bar{C}}{C_b} = \frac{1}{1-\beta(b/a)}, \quad (4.24)$$

where

$$\beta = (2/\pi)(1.148515)^{-1} = .554298. \quad (4.25)$$

We must now determine  $\bar{C}$  in order to get our hoped for comparison between  $\bar{C}$  and  $C$ . Let us start by reviewing a little of the history of this problem. The first crack at it seems to have been by Smythe [20], in 1953. In a later paper [14], Smythe referred to his 1953 treatment as "crude", but this seems an overly harsh evaluation. He had done as much as could be expected, considering the state of the computational arts at that time. What he did was to assume the charge density on the disk to be the sum of the charge density on a disk in free space (i.e.,  $(1 - \rho^2/b^2)^{-1/2}$ ) and a uniform charge density. The constant multiplying the uniform charge density was adjusted so that the potential was as uniform as possible over the disk. By considering various of the equipotential surfaces of this system Smythe was able to derive a few bounds on  $\bar{C}$ . The cases he treated that are of interest to us are those with  $(b/a)$  values of .25, .5, and .75, for which he obtained:

$b/a$	$< \bar{C}/C_b <$	
.25	1.1627	1.1628
.50	1.4036	1.4089
.75	1.856	1.883

The next investigation of a problem somewhat like the present one is that of Kirkham [21] in 1957. He attacks the more general problem of concentric coaxial capped cylinders. A disk inside a cylinder is a special case of this. Kirkham also mentions the more specialized case of a disk inside an infinitely wide cylinder (i.e., between parallel plates), but his formulation does not allow him to consider the cylinder to become infinitely long. Therefore, there are no numbers of present interest to us in reference [21].

The next treatment of our problem was that of Cooke and Tranter [22] in 1959. Their approach, based on the use of dual Fourier-Bessel series, seems the most useful of all, for computational purposes, and it is quite possibly the most elegant as well. It is the method we will outline later in this subsection, and the one we used for our numerical work. Cooke and Tranter themselves made only two numbers:

b/a	$\bar{C}/C_b$
.25	1.1627+
.50	1.407

where the + indicates that the number is rounded from a number larger than 1.1627. The authors do give an interesting expansion for  $\bar{C}/C_b$  for small (b/a). It is equivalent to

$$\frac{\bar{C}}{C_b} = \frac{1}{1-F(b/a)} \quad (4.26)$$

where the small argument expansion of the function  $F(x)$  is

$$F(x) = \beta x + .08739x^3 + .03728x^5 \quad (4.27)$$

and  $\beta$  is given by equation (4.25). From equations (4.26) and (4.27), the third order error of the general effective radii approximation (Section III.A) is quite evident.

Collins [23] investigated the present problem in 1961. He derived a second kind integral equation for a function related to the charge density on the disk, but the kernel of this integral equation is a little complicated. It is possible, by subsequent transformations, to retrieve Cooke and Tranter's

equations from Collins' integral equation, but those equations can be obtained more directly. Collins made no numbers.

A generalized version of Collins' approach was given by Sneddon [25] in 1962. He was able to prescribe a non-axisymmetric potential over both the surface of the disk and the surface of the cylinder. He made no new numbers, but verified Cooke and Tranter's results. In his book ([24], p. 259), Sneddon presents some previously unpublished numerical results of Mathur. These, in our present notation, are:

a/b	b/a	$\bar{C}/C_b$
1.2	.833	2.178
1.3	.769	1.933
1.4	.714	1.780

(There is a misprint in Sneddon's table 7. The number for  $a/b = 1.2$  must be 2.178, not 2.718).

Smythe gave his second treatment of our problem in 1963 [14]. This time he considered it as a limiting case of a spheroid in a cylinder. By a generalization of the method described in Section IV.A, he obtained a matrix equation for the coefficients of the spheroidal harmonic expansion of the surface charge density on the spheroid; his matrix differs from Cooke and Tranter's matrix, but the two are equivalent. In this manner, Smythe was able to calculate the following values of capacitance.

b/a	$\bar{C}/C_b$
.1	1.05878
.2	1.12558
.3	1.20300
.4	1.29490
.5	1.40740
.6	1.55099
.7	1.74593
.8	2.03915
.9	2.58610
.95	3.17778

Smythe attributes only 3-figure accuracy to the last of these values and 5-figure accuracy to the second last.

Let us now outline the method of Cooke and Tranter, and use it to extend Smythe's table. For the sake of simplicity, we will not describe the method in its full generality, but just use it to solve the particular problem we are interested in (in [22] our problem was treated as an example of a more general approach).

A representation of the potential in the geometry of figure 7 is ([4] §§5.297, 5.298)

$$\phi(\rho, z) = \sum_{n=1}^{\infty} \frac{a_n}{\mu_n} e^{-\mu_n |z/a|} J_0(\mu_n \rho/a) \quad (4.28)$$

where the  $\mu_n$ 's are the roots of

$$J_0(\mu_n) = 0$$

Representation (4.28) satisfies Laplace's equation and is equal to zero on E. The constants,  $a_n$ , must be determined by enforcing the boundary conditions on the  $z = 0$  plane. These conditions can be written in the forms

$$\sum_{n=1}^{\infty} \frac{a_n}{\mu_n} J_0(\mu_n \rho/a) = 1 \quad 0 < \rho < b \quad (4.29)$$

$$\sum_{n=1}^{\infty} a_n J_0(\mu_n \rho/a) = 0 \quad b < \rho < a \quad (4.30)$$

Now, by making use of the identity (a special case of [24], equation 5.2.6)

$$\sum_{j=1}^{\infty} \frac{J_{2n+1/2}(\mu_j b/a) J_0(\mu_j \rho/a)}{\mu_j^{1/2} J_1^2(\mu_j)} = 0, \quad b < \rho < a, \quad n \text{ an integer } \geq 0 \quad (4.31)$$

it is easy to show, by an interchange in the order of summations, that if we set

$$a_n = \frac{1}{\mu_n^{1/2} J_1^2(\mu_n)} \sum_{m=0}^{\infty} b_m J_{2m+1/2}(\mu_n b/a), \quad (4.32)$$

then equation (4.30) will be satisfied identically for any values of  $b_m$ . Substituting equation (4.32) in equation (4.29), we obtain

$$\sum_{m=0}^{\infty} b_m \sum_{n=0}^{\infty} \frac{J_{2m+\frac{1}{2}}(\mu_n b/a) J_0(\mu_n b/a)}{\mu_n^{3/2} J_1^2(\mu_n)} = 1 \quad 0 < \rho < b. \quad (4.33)$$

Multiply both sides of this equation by

$$2^{\frac{1}{2}} \frac{\Gamma(s+1)}{\Gamma(s+\frac{1}{2})} \rho (b^2 - \rho^2)^{-\frac{1}{2}} P_{2s}(\sqrt{1 - (\rho/b)^2}),$$

where  $P_{2s}$  is a Legendre polynomial and  $s$  is an arbitrary integer, then integrate over  $\rho$  from 0 to  $b$  by using the identity (a special case of [24], equation 5.2.9)

$$\frac{2^{\frac{1}{2}}}{b} \frac{\Gamma(s+1)}{\Gamma(s+\frac{1}{2})} \int_0^b \frac{\rho}{\sqrt{b^2 - \rho^2}} P_{2s}(\sqrt{1 - (\rho/b)^2}) J_0(x\rho/a) d\rho = \frac{J_{2s+\frac{1}{2}}(xb/a)}{(xb/a)^{\frac{1}{2}}}.$$

The result is

$$\sum_{m=0}^{\infty} b_m \sum_{n=1}^{\infty} \frac{J_{2m+\frac{1}{2}}(\mu_n b/a) J_{2s+\frac{1}{2}}(\mu_n b/a)}{\mu_n^2 (b/a)^{\frac{1}{2}} J_1^2(\mu_n)} = \left(\frac{2}{\pi}\right)^{\frac{1}{2}} \delta_{s,0} \quad (4.34)$$

But ([24], equation 5.2.13)

$$2 \sum_{n=1}^{\infty} \frac{J_{2m+\frac{1}{2}}(\mu_n b/a) J_{2s+\frac{1}{2}}(\mu_n b/a)}{\mu_n^2 J_1^2(\mu_n)} = \frac{\delta_{m,s}}{4s+1} - (-)^{m+s} \frac{2}{\pi} \int_0^{\infty} \frac{K_0(t)}{t I_0(t)} I_{2m+\frac{1}{2}}(bt/a) I_{2s+\frac{1}{2}}(bt/a) dt, \quad (4.35)$$

and thus, relabing indices,

$$\frac{b_n}{4n+1} - \sum_{m=0}^n M_{nm} b_m = 2 \left(\frac{2b}{\pi a}\right)^{\frac{1}{2}} \delta_{n,0} \quad (4.36)$$

where

$$M_{nm} = (-)^{n+m} \frac{2}{\pi} \int_0^{\infty} \frac{K_0(t)}{t I_0(t)} I_{2m+\frac{1}{2}}(bt/a) I_{2n+\frac{1}{2}}(bt/a) dt \quad (4.37)$$

The capacitance we wish to calculate is equal to the total charge on the disk. Thus

$$\begin{aligned}
\frac{\bar{C}}{C_b} &= -\frac{1}{8b} \int_0^b 2 \frac{\partial \phi(\rho, 0)}{\partial z} \cdot 2\pi\rho d\rho \\
&= \frac{\pi}{2} \sum_{n=1}^{\infty} a_n \frac{J_1(\mu_n b/a)}{\mu_n} \\
&= \frac{\pi}{2} \sum_{m=0}^{\infty} b_m \sum_{n=1}^{\infty} \frac{J_{2m+1/2}(\mu_n b/a) J_1(\mu_n b/a)}{\mu_n^{3/2} J_1^2(\mu_n)}.
\end{aligned}$$

But, from reference [22], the inner sum in the above equation is just  $(2/\pi)^{1/2} \delta_{m,0}$ , and so

$$\frac{\bar{C}}{C_b} = \left(\frac{\pi a}{2b}\right)^{1/2} \frac{b_0}{2}. \quad (4.38)$$

Let us simplify our equations a little by defining

$$x_n \equiv 2 \left(\frac{2b}{\pi a}\right)^{1/2} b_n.$$

From equations (4.36) and (4.38), we can therefore say that

$$\frac{\bar{C}}{C_b} = x_0 \quad (4.39)$$

where

$$\frac{x_n}{4n+1} - \sum_{m=0}^{\infty} M_{nm} x_m = \delta_{n,0}, \quad (4.40)$$

and  $M_{nm}$  is given by equation (4.37). By expanding the product of half-integer Bessel functions in the integrand of equation (4.37) in a power series in  $(bt/a)$  ([26], §5.4), and then inverting the order of summation and integration, we can obtain the following algorithm for computing the  $M_{nm}$  in terms of the  $I(2n,1)$  integrals defined in Section IV.A:

$$M_{nm} = \left(\frac{2}{\pi}\right)^2 (-)^{n+m} \left(\frac{b}{2a}\right)^{2n+2m+1} \sum_{j=0}^{\infty} (b/a)^{2j} I(2n+2m+2j,1) T_j(n,m) \quad (4.41)$$

where

$$T_j(n,m) = \frac{(n+m+j)^3 (n+m+j-\frac{1}{2})}{j(2n+2m+j+1)(2n+j+\frac{1}{2})(2m+j+\frac{1}{2})} T_{j-1}(n,m) \quad (4.42)$$

with

$$T_0(n,m) = 2^{4n+4m+1} \frac{(2n)!}{(4n+1)!} \cdot \frac{(2m)!}{(4m+1)!} \frac{[(n+m)!]^2}{2n+2m+1} \quad (4.43)$$

Equations (4.39) through (4.43) were the ones used for the numerical work. The results of this numerical work are given in table 3 and figure 8. This table and curve exhibit a slightly larger error for  $\tilde{C}/C_b$  than was calculated in the first two examples. The reason for this is simply that the present example is of the more general type, discussed in Section III.A, having a third order error term for small  $b/a$ . The previous two examples, where either B or E was a sphere, had a fifth or sixth order error term. We see, nevertheless, that the error in  $\tilde{C}/C_b$  is still not very large. It doesn't exceed 5% until  $b/a$  is greater than 2/3.

#### IV.D. Disk in a Circular Aperture

The geometry of the problem is shown in figure 9. The radius of the circular aperture is  $a$ ; the radius of the disk, whose axis of symmetry is the same as that of the aperture, is  $b$ . Strictly speaking, this geometry is not the type for which the equivalent radii approximation was designed, since the real  $r_{bm}$  is at an infinite distance from the plane with the aperture ( $C$  decreases as the disk moves away from the plane, until it reaches its minimum value,  $C_b$ , at infinity). Nevertheless, we should still expect a third order error in the numbers obtained from a formal application of the  $\tilde{C}$  equation, because  $C$  is a maximum with respect to the disk's motion perpendicular to the plane and a minimum with respect to the disk's motion in the plane. A review of Section III.A should convince one that these conditions are sufficient to assure a third order error for  $\tilde{C}$  if we set  $r_b = r_e = 0$ . Again we will denote the capacitance for this  $r_b$  and  $r_e$  by  $\tilde{C}$ .

The effective radii approximation for this problem is easy to write down. From the previous subsection we have

Table 3. Capacitance of a disk in an infinite cylinder

b/a	$\tilde{C}/C_b$	$\bar{C}/C_b$	$(\Delta C_b/\bar{C})\%$	b/a	$\tilde{C}/C_b$	$\bar{C}/C_b$	$(\Delta C_b/\bar{C})\%$
.01	1.00557	1.00557	.000	.51	1.39410	1.42013	1.833
.02	1.01121	1.01121	.000	.52	1.40496	1.43317	1.968
.03	1.01691	1.01691	.000	.53	1.41599	1.44655	2.113
.04	1.02267	1.02268	.001	.54	1.42719	1.46028	2.266
.05	1.02850	1.02852	.001	.55	1.43857	1.47437	2.428
.06	1.03440	1.03442	.002	.56	1.45013	1.48885	2.601
.07	1.04037	1.04040	.003	.57	1.46188	1.50373	2.783
.08	1.04640	1.04645	.005	.58	1.47382	1.51903	2.976
.09	1.05251	1.05258	.007	.59	1.48596	1.53477	3.180
.10	1.05868	1.05878	.010	.60	1.49830	1.55099	3.397
.11	1.06493	1.06506	.012	.61	1.51085	1.56770	3.626
.12	1.07126	1.07143	.016	.62	1.52361	1.58494	3.869
.13	1.07765	1.07788	.021	.63	1.53659	1.60273	4.127
.14	1.08413	1.08441	.026	.64	1.54979	1.62110	4.399
.15	1.09068	1.09104	.033	.65	1.56322	1.64010	4.688
.16	1.09732	1.09775	.039	.66	1.57688	1.65976	4.993
.17	1.10403	1.10456	.048	.67	1.59079	1.68012	5.317
.18	1.11083	1.11147	.057	.68	1.60494	1.70124	5.661
.19	1.11771	1.11848	.068	.69	1.61934	1.72315	6.024
.20	1.12468	1.12558	.080	.70	1.63401	1.74593	6.410
.21	1.13174	1.13279	.093	.71	1.64895	1.76963	6.820
.22	1.13888	1.14016	.112	.72	1.66416	1.79432	7.254
.23	1.14612	1.14755	.125	.73	1.67965	1.82008	7.716
.24	1.15344	1.15510	.143	.74	1.69543	1.84700	8.206
.25	1.16087	1.16276	.163	.75	1.71152	1.87516	8.727
.26	1.16838	1.17055	.185	.76	1.72791	1.90469	9.281
.27	1.17600	1.17846	.209	.77	1.74462	1.93570	9.871
.28	1.18372	1.18651	.235	.78	1.76166	1.96834	10.500
.29	1.19154	1.19468	.263	.79	1.77903	2.00277	11.172
.30	1.19946	1.20300	.295	.80	1.79675	2.03916	11.888
.31	1.20749	1.21146	.328	.81	1.81482	2.07774	12.654
.32	1.21562	1.22007	.365	.82	1.83326	2.11875	13.474
.33	1.22387	1.22883	.404	.83	1.85208	2.16249	14.354
.34	1.23223	1.23775	.446	.84	1.87129	2.20931	15.300
.35	1.24070	1.24683	.492	.85	1.89091	2.25962	16.317
.36	1.24929	1.25608	.540	.86	1.91094	2.31393	17.416
.37	1.25800	1.26551	.593	.87	1.93140	2.37286	18.605
.38	1.26684	1.27511	.649	.88	1.95230	2.43718	19.895
.39	1.27580	1.28491	.709	.89	1.97365	2.50787	21.302
.40	1.28488	1.29490	.774	.90	1.99548	2.58620	22.841
.41	1.29410	1.30510	.843	.91	2.01780	2.67383	24.535
.42	1.30345	1.31550	.916	.92	2.04063	2.77305	26.412
.43	1.31294	1.32612	.994	.93	2.06397	2.88704	28.509
.44	1.32256	1.33697	1.078	.94	2.08786	3.02052	30.877
.45	1.33233	1.34806	1.167	.95	2.11231	3.18083	33.593
.46	1.34224	1.35939	1.262	.96	2.16295	3.38028	36.771
.47	1.35230	1.37098	1.362	.97	2.18920	3.64211	40.613
.48	1.36252	1.38284	1.470	.98	2.21609	4.01869	45.525
.49	1.37288	1.39497	1.583	.99	2.24365	4.67795	52.627
.50	1.38341	1.40740	1.704	1.00	2.27191	$\infty$	100.00

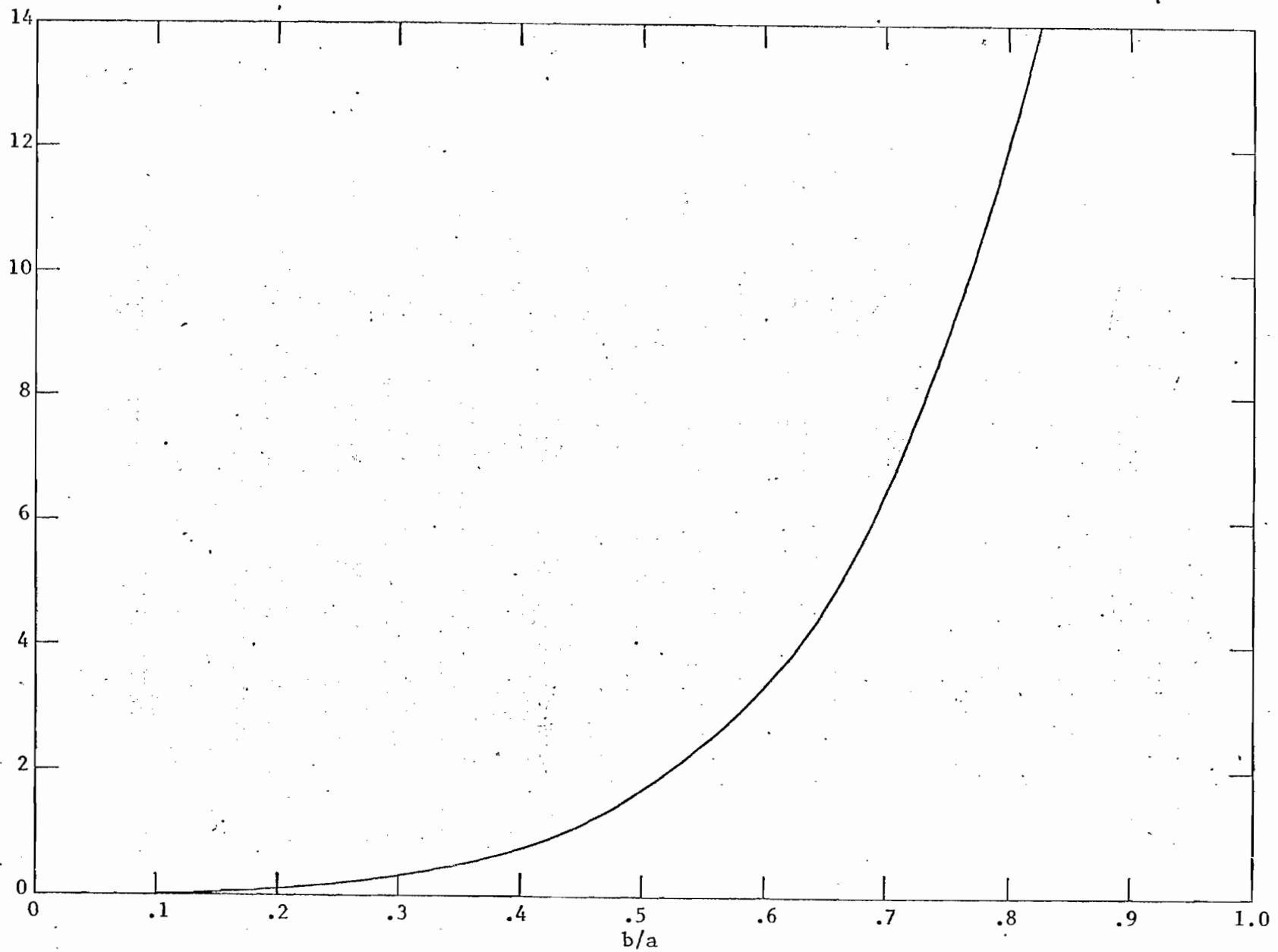
error  
in  
percent

Figure 8. Error of the approximation for the case of a disk in an infinite cylinder.

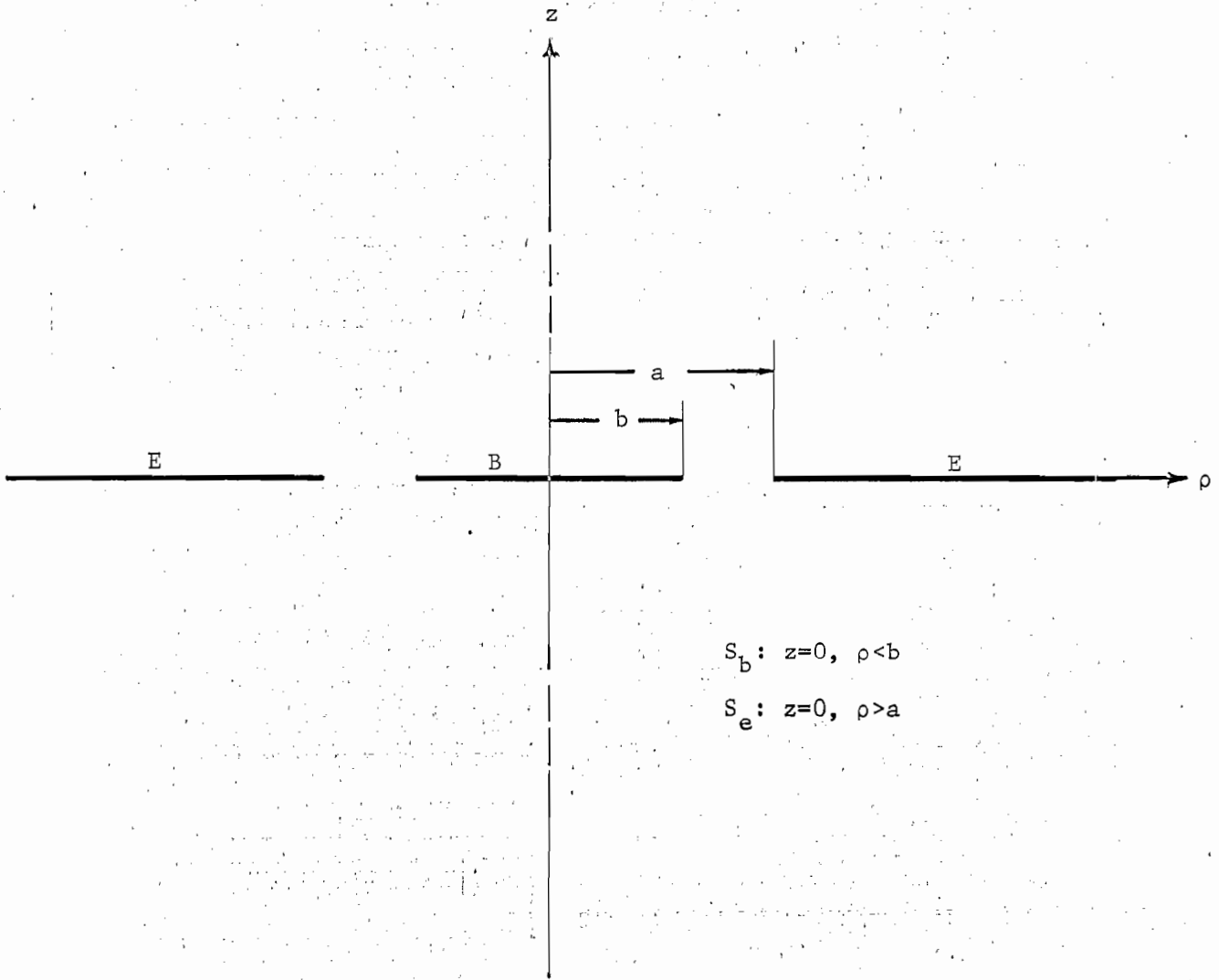


Figure 9. A disk in a circular aperture (cross-section).

$$r_1 = \frac{8\epsilon b}{4\pi\epsilon} = \frac{2}{\pi} b, \quad (4.44)$$

while from equation (3.21), using an inversion sphere of radius  $a$ , we have

$$r_2 = \frac{a^2}{r_1} = a^2 \frac{4\pi\epsilon}{8\epsilon a} = \frac{\pi}{2} a \quad (4.45)$$

Thus

$$\frac{\bar{C}}{C_b} = \frac{1}{1 - (2/\pi)^2 (a/b)} \quad (4.46)$$

The calculation of  $\bar{C}$  has been given in detail in a previous note in this series [27]. In fact, we will not need to make any other numbers than those given in that note. We will assume that the previous note is available to anyone reading the present one. Thus we will merely present the equations that had to be solved numerically, and arrange the numerical data in a format that is suitable for evaluating the accuracy of the effective radii approximation.

Before doing this, however, we would be remiss if we did not mention the only other paper that is known to the author (besides [27]) on the exact solution of the present problem. The paper by Spence [28] came out almost simultaneously with reference [27], and was unknown to the authors of [27] until quite recently. The two investigations upon which these two papers were based were completely independent, but, inevitably, much of the development is similar. One difference is that Spence concentrates largely on the case where  $(1 - b/a)$  is small, while in [27] a great deal of time was devoted to developing a variational expression for  $\bar{C}$  that is quite accurate when  $b/a$  is small. Another difference is that in [28] only a dozen  $(b/a)$  cases were treated numerically, while a hundred  $(b/a)$  cases were treated in [27]. It is interesting that both papers give equation (4.46) as an approximation for  $\bar{C}$ . Spence attributes this form of the approximation to J. C. Cooke, who apparently was one of the reviewers of Spence's paper. Of course, neither reference [27] nor reference [28] give any indication of the general applicability of the effective radii approximation.

Now let us state the equations for computing  $\bar{C}/C_b$ . These are [27]

$$\frac{\bar{C}}{C_b} = \int_0^{\pi/2} P_1(\theta) \sin \theta d\theta, \quad (4.47)$$

where  $P_1(\theta)$  is determined from the numerical solution of the coupled pair of integral equations

$$P_1(\theta) + \frac{b}{a} \int_0^{\pi/2} G(\theta, \theta') P_2(\theta') d\theta' = 1 \quad 0 < \theta < \pi/2 \quad (4.48)$$

$$P_2(\theta) + \int_0^{\pi/2} G(\theta, \theta') P_1(\theta') d\theta' = 0 \quad (4.49)$$

and

$$G(\theta, \theta') = \frac{2}{\pi} \frac{\sin \theta' [1 - (b/a)^2 \sin^2 \theta']^{-1/2}}{1 - (b/a)^2 \sin^2 \theta \sin^2 \theta'} \quad (4.50)$$

The results of this calculation are presented in table 4 and figure 10. As with the previous problem, the error in  $\tilde{C}$  exhibits a third order dependence on  $(b/a)$ .

This completes our treatment of exemplary problems. We have had examples of each of the three types of error (third, fifth, and sixth orders) discussed in Section III. In all cases, the effective radii approximation has turned out to be surprisingly accurate as long as condition (4.0) is fulfilled. Therefore, until some future work proves the contrary, the author will believe that condition (4.0) is sufficient for the effective radii approximation to give an accurate value (to within, say, a percent or two) for  $\tilde{C}/C_b$  in any B-E problem.

Therefore, let us now turn our attention to another part of the B-E capacitance problem -- the calculation of  $r_2$ . This subject will occupy us for the next three sections.

Table 4. Capacitance of a disk in a circular aperture

b/a	$\bar{c}/c_b$	$\bar{c}/c_b$	$(c_b/\bar{c})\%$	b/a	$\bar{c}/c_b$	$\bar{c}/c_b$	$(c_b/\bar{c})\%$
.01	1.00407	1.00407	.000	.51	1.26055	1.28267	1.725
.02	1.00817	1.00817	.000	.52	1.26702	1.29089	1.849
.03	1.01231	1.01231	.000	.53	1.27356	1.29929	1.980
.04	1.01648	1.01648	.000	.54	1.28017	1.30789	2.119
.05	1.02068	1.02070	.001	.55	1.28685	1.31668	2.266
.06	1.02492	1.02494	.002	.56	1.29359	1.32569	2.421
.07	1.02920	1.02923	.003	.57	1.30041	1.33491	2.584
.08	1.03351	1.03356	.005	.58	1.30730	1.34437	2.757
.09	1.03786	1.03793	.007	.59	1.31426	1.35408	2.940
.10	1.04224	1.04234	.010	.60	1.32130	1.36404	3.133
.11	1.04666	1.04679	.013	.61	1.32842	1.37427	3.337
.12	1.05112	1.05129	.016	.62	1.33561	1.38479	3.552
.13	1.05562	1.05584	.021	.63	1.34288	1.39562	3.779
.14	1.06015	1.06043	.026	.64	1.35022	1.40676	4.019
.15	1.06473	1.06508	.033	.65	1.35765	1.41824	4.272
.16	1.06934	1.06977	.040	.66	1.36517	1.43009	4.540
.17	1.07400	1.07451	.048	.67	1.37276	1.44231	4.822
.18	1.07869	1.07931	.057	.68	1.38044	1.45495	5.121
.19	1.08343	1.08417	.068	.69	1.38821	1.46802	5.437
.20	1.08821	1.08908	.080	.70	1.39606	1.48155	5.770
.21	1.09303	1.09405	.093	.71	1.40401	1.49558	6.123
.22	1.09789	1.09907	.107	.72	1.41204	1.51015	6.497
.23	1.10280	1.10417	.124	.73	1.42017	1.52529	6.892
.24	1.10775	1.10932	.142	.74	1.42839	1.54106	7.311
.25	1.11274	1.11454	.161	.75	1.43671	1.55749	7.755
.26	1.11779	1.11983	.183	.76	1.44512	1.57465	8.226
.27	1.12287	1.12519	.206	.77	1.45363	1.59261	8.726
.28	1.12801	1.13062	.231	.78	1.46225	1.61144	9.258
.29	1.13319	1.13613	.259	.79	1.47097	1.63121	9.824
.30	1.13841	1.14172	.290	.80	1.47979	1.65203	10.426
.31	1.14369	1.14738	.323	.81	1.48872	1.67401	11.069
.32	1.14902	1.15313	.357	.82	1.49775	1.69728	11.756
.33	1.15439	1.15896	.394	.83	1.50690	1.72199	12.491
.34	1.15982	1.16488	.434	.84	1.51616	1.74832	13.279
.35	1.16530	1.17089	.478	.85	1.52553	1.77649	14.126
.36	1.17083	1.17700	.525	.86	1.53503	1.80675	15.039
.37	1.17641	1.18320	.574	.87	1.54463	1.83942	16.026
.38	1.18204	1.18951	.628	.88	1.55437	1.87492	17.097
.39	1.18773	1.19592	.684	.89	1.56422	1.91372	18.263
.40	1.19348	1.20244	.745	.90	1.57420	1.95649	19.540
.41	1.19928	1.20907	.810	.91	1.58431	2.00408	20.946
.42	1.20514	1.21582	.879	.92	1.59455	2.05764	22.506
.43	1.21105	1.22269	.952	.93	1.60492	2.11882	24.254
.44	1.21703	1.22969	1.030	.94	1.61542	2.18999	26.236
.45	1.22306	1.23682	1.113	.95	1.62607	2.27488	28.521
.46	1.22915	1.24408	1.200	.96	1.63686	2.37973	31.217
.47	1.23531	1.25149	1.293	.97	1.64779	2.51627	34.515
.48	1.24152	1.25905	1.392	.98	1.65887	2.71092	38.808
.49	1.24780	1.26676	1.497	.99	1.67010	3.04810	45.209
.50	1.25414	1.27463	1.607	1.00	1.68148	$\infty$	100.00

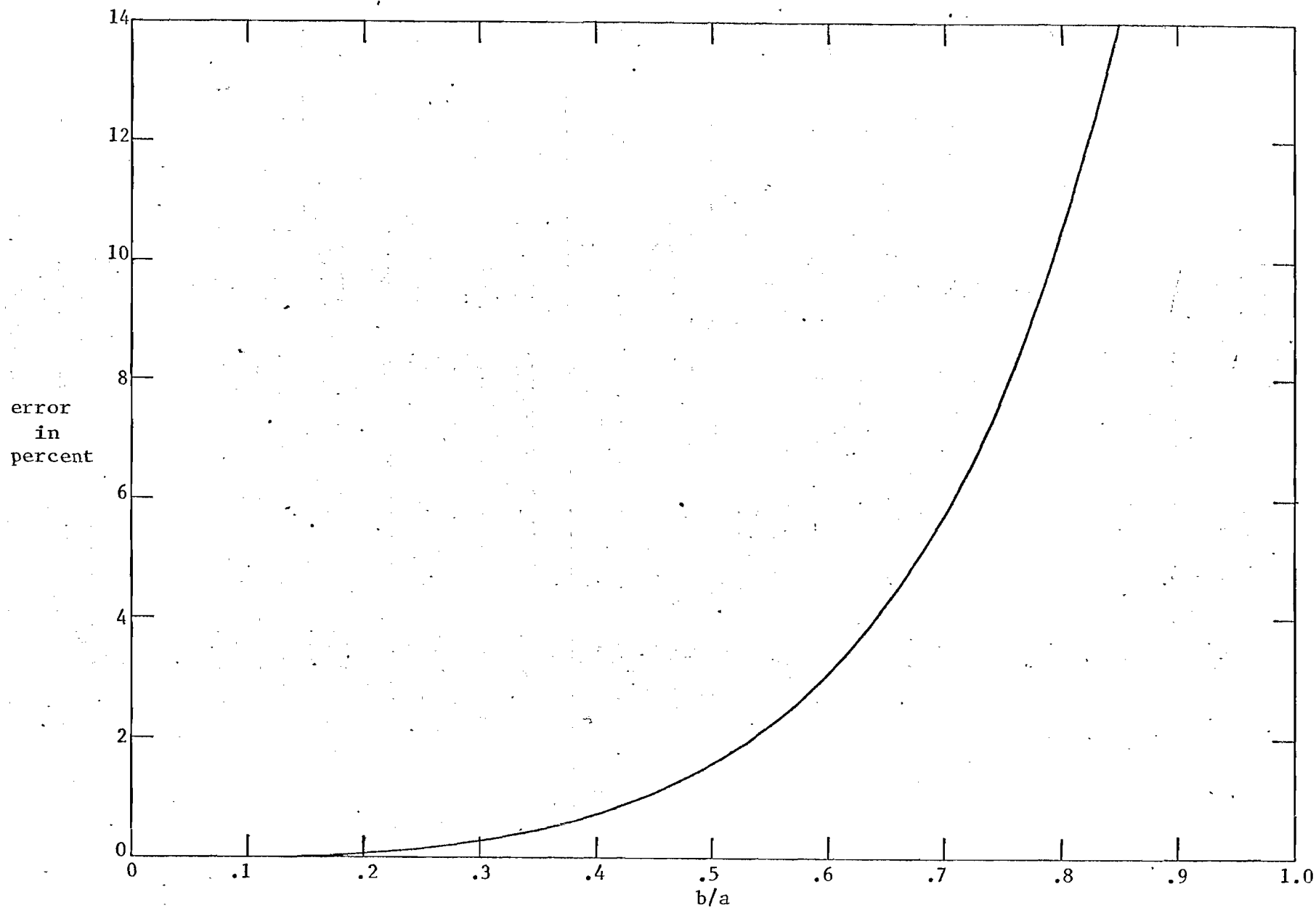


Figure 110. Error of the approximation for the case of a disk in a circular aperture.

## V. Enclosure Radius Calculations -- Available Methods

Now that we have gained some confidence in the accuracy of the effective radii approximation, we have to press on and develop ways of calculating the two parameters appearing in the approximation,  $r_1$  and  $r_2$ .

The problem of calculating  $r_1$  will not be treated here. It is equivalent, according to equation (2.10), to the well studied problem of determining the capacitance of a single isolated body. A few references to the extensive literature on this subject will be given in Section IX. At this time we will mention only reference [3], where the problem is treated by finding two ellipsoids related to B, one ellipsoid being the smallest within which B can be contained and the other ellipsoid being the largest contained in B (the measure for determining "smallest" and "largest" is capacitance). The readily computed capacitances of these two ellipsoids bound the capacitance of B. The arithmetic mean of the two bounding capacitances is not too bad an estimate of the capacitance of B in the cases examined so far.

In this section, we will give a brief outline of four of the methods available for calculating  $r_2$ , with a few comments on each. Of course, by equation (3.21), this general problem is the same as the general problem of calculating  $r_1$ . Nevertheless, there are enough differences between the detailed treatments of the interior and exterior boundary-value problems that a quick review of some basic methods seems useful. We will mention integral equation methods, the method of nets, the method of inversion, and the method of separation of variables.

### V.A. Integral Equation Methods

Integral equations give us a general approach to the calculation of  $r_2$ , applicable to enclosures of arbitrary shape.

Consider the problem represented in figure 11, where  $\underline{r}_0$  is the location of a point source within the enclosure E. The surface of the small sphere centered on  $\underline{r}_0$  is  $S_e$ , and the surface of E is, as usual,  $S_e$ . From Green's theorem ([6], Chap. VIII, eq. III)

$$G_e(\underline{r}, \underline{r}_0) = \int_{S_e + S_e} \left\{ G_e(\underline{r}', \underline{r}_0) \frac{\partial G_o(\underline{r}, \underline{r}')}{\partial n'} - G_o(\underline{r}, \underline{r}') \frac{\partial G_e(\underline{r}', \underline{r}_0)}{\partial n'} \right\} dS' \quad (5.1)$$

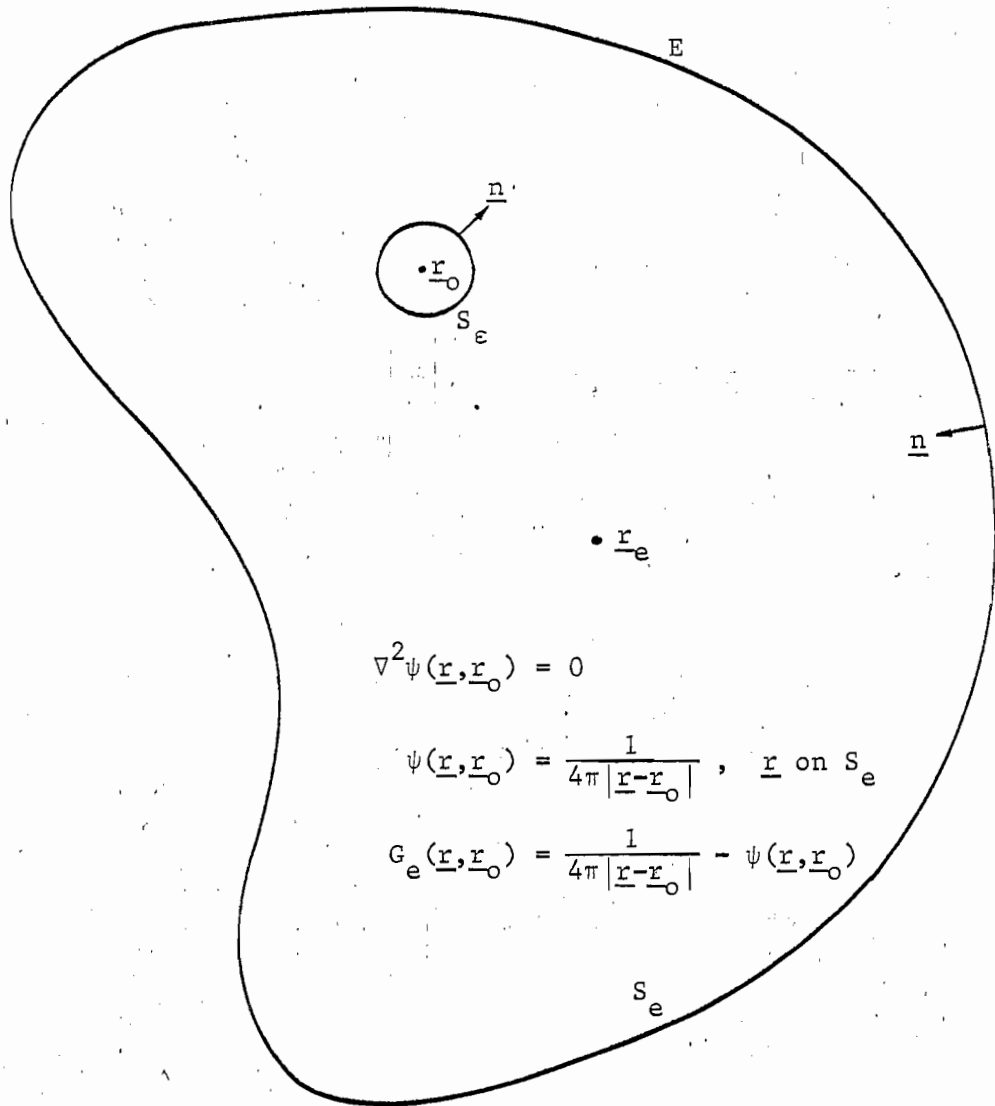


Figure 11. A general enclosure shape.

where  $G_e(\underline{r}, \underline{r}_0)$  is the interior Green's function of  $E$  whose source point is at  $\underline{r}_0$  and whose value on  $S_e$  is zero. The directions of the normals are indicated on the figure, and

$$G_o(\underline{r}, \underline{r}') = \frac{1}{4\pi |\underline{r} - \underline{r}'|}. \quad (5.2)$$

Performing the  $S$  integral of equation (5.1) in the limit of small spheres, and using the fact that on  $S_e$  we have  $G_e(\underline{r}, \underline{r}_0) = 0$ , it follows that

$$G_e(\underline{r}, \underline{r}_0) = \frac{1}{4\pi |\underline{r} - \underline{r}_0|} - \frac{1}{4\pi} \int_{S_e} \frac{\partial G_e(\underline{r}', \underline{r}_0)}{\partial n'} \cdot \frac{1}{|\underline{r} - \underline{r}'|} dS' \quad (5.3)$$

Now allow  $\underline{r}$  to approach  $S_e$ ; the result is a surface integral equation over  $S_e$  for

$$\tau(\underline{r}, \underline{r}_0) \equiv \frac{\partial G_e(\underline{r}, \underline{r}_0)}{\partial n'}, \quad \underline{r} \text{ on } S_e,$$

in the form

$$\frac{1}{|\underline{r} - \underline{r}_0|} = \int_{S_e} \frac{\tau(\underline{r}', \underline{r}_0)}{|\underline{r} - \underline{r}'|} dS', \quad \underline{r} \text{ on } S_e \quad (5.4)$$

Once this equation has been solved for  $\tau(\underline{r}, \underline{r}_0)$ , we can use equations (3.4) and (5.3) to say that

$$\psi(\underline{r}_0, \underline{r}_0) = \frac{1}{4\pi} \int_{S_e} \frac{\tau(\underline{r}, \underline{r}_0)}{|\underline{r}_0 - \underline{r}|} dS, \quad (5.5)$$

and thus, from equation (3.6),

$$\frac{1}{r_2} = \min_{\underline{r}_0 \text{ in } E} \int \frac{\tau(\underline{r}, \underline{r}_0)}{|\underline{r}_0 - \underline{r}|} dS \quad (5.6)$$

If  $E$  possesses enough symmetry, it may be possible to pick out  $\underline{r}_e$  by inspection and set  $\underline{r}_0 = \underline{r}_e$ . Thus it would only be necessary to solve equation (5.4) once. In some other cases, it might be possible to use symmetry to restrict  $\underline{r}_e$  to a line or a surface. Any such restriction would lead to a great reduction in the complexity of the numerical search for  $\underline{r}_e$ , through equations (5.4) and (5.6), that will be necessary if  $E$  has a completely arbitrary shape.

Up to now, we have tacitly assumed that the solution of equation (5.4)

could really be obtained, by some means or other. There are several quite similar numerical methods that are suitable for this purpose. The kernel of the equation is the same as the kernel of an equation that has often been used to calculate the surface charge density on an isolated conducting body at potential  $V_0$ , i.e. ([29], eq. (4.1)),

$$\int_{S_b} \frac{\sigma(\underline{r}')}{|\underline{r}-\underline{r}'|} dS' = 4\pi\epsilon_0 V_0.$$

Any numerical method that can be used to solve this equation can be used to solve equation (5.4). One such method has been called the "method of subareas" [30], [31]. It has recently become popular among electrical engineers to call such methods "moment methods," probably because of reference [32]. An elegant discussion of such methods has been given by Kantorovich and Krylov ([33], Chap. II), who remind us that the method of moments is equivalent to replacing the kernel of the original integral equation by a degenerate kernel.

Numerical solutions will result in more accurate values of  $\psi(\underline{r}_0, \underline{r}_0)$  if used in conjunction with a variational representation of that quantity [34]. Such an expression is the following

$$\psi(\underline{r}_0, \underline{r}_0) = \left\{ \int_{S_e} \frac{\tau(\underline{r}, \underline{r}_0)}{|\underline{r}_0 - \underline{r}|} dS \right\}^2 \left\{ \int_{S_e} \int_{S_e} \frac{\tau(\underline{r}', \underline{r}_0) \tau(\underline{r}, \underline{r}_0)}{|\underline{r}' - \underline{r}|} dS dS' \right\}^{-1}. \quad (5.7)$$

Before concluding this subsection, we should at least make note of an alternative integral equation formulation that is available. The integral equation we mean is the one on which existence theorems on the solution of the interior Dirichlet problem are based, i.e., since  $\psi(\underline{r}, \underline{r}_0) = G_0(\underline{r}, \underline{r}_0)$  on  $S_e$ , and  $\psi(\underline{r}, \underline{r}_0)$  has no singularities within  $E$ , we can write ([6], Chap. XI, §2)

$$\psi(\underline{r}_0, \underline{r}_0) = \int_{S_e} \mu(\underline{r}', \underline{r}_0) \frac{\partial G_0(\underline{r}_0, \underline{r}')}{\partial n'} dS' \quad (5.8)$$

where  $\mu(\underline{r})$  is the solution of the integral equation

$$G_0(\underline{r}, \underline{r}_0) = \frac{\mu_0(\underline{r}, \underline{r}_0)}{2} + \int_{S_e} \mu(\underline{r}', \underline{r}_0) \frac{\partial G_0(\underline{r}, \underline{r}')}{\partial n'} dS' \quad (5.9)$$

Although the kernel of this equation looks a little messier than that of

equation (5.4), the numerical solution of equation (5.9) could often lead to more accurate values of  $\psi(\underline{r}, \underline{r}_0)$  than the numerical solution of equation (5.4), using the same number of subareas on  $S_e$  in each case. If  $\tau(\underline{r}, \underline{r}_0)$  is used with an expression line (5.7), this comment is less relevant, since no comparable expression can be obtained for use with  $\mu(\underline{r}, \underline{r}_0)$ .

#### V.B. Method of Nets

This method is a natural for the solution of interior potential problems; it's a strain to use it for exterior problems. Therefore, because the calculation of  $r_2$  is essentially an internal potential problem, the method of nets is more useful for calculating  $r_2$  than  $r_1$ . This fact has led some investigators who like the method of nets to turn  $r_1$ -calculations into  $r_2$ -calculations by invoking equation (3.21) [8]. We will look at the reverse of this procedure in the next subsection.

The method of nets ([33], Chap. III) is quite easy to understand in its simplest form. One simply defines a three-dimensional lattice of points within  $E$ , and approximates Laplace's equation by some finite difference formula involving the values of the potential at the points of the lattice. If the lattice is cubic, and we choose the simplest possible finite difference approximation to  $\nabla^2\psi(\underline{r}; \underline{r}_0)$ , the equation for  $\Psi(i, j, k)$ , the finite difference approximation to  $\psi(x_i, y_j, z_k; \underline{r}_0)$ , is just

$$\begin{aligned} \Psi(i, j, k) = \frac{1}{6} \{ & \Psi(i + 1, j, k) + \Psi(i, j + 1, k) + \Psi(i, j, k + 1) \\ & + \Psi(i - 1, j, k) + \Psi(i, j - 1, k) + \Psi(i, j, k - 1) \} \end{aligned} \quad (5.10)$$

The values of  $\Psi$  at the boundary points of the lattice can be determined by finding the value of  $\psi$  at the closest point on  $S_e$  to each lattice boundary point. At least, that is the most natural way of choosing boundary values. It may be easier in practice to choose the boundary  $\Psi$ 's according to some rule such as saying they are the same as the  $\psi$ 's at the closest points on  $S_e$  in a given direction, the x-direction, say. Of course, the boundary values of  $\psi$  are just  $G_0(\underline{r}, \underline{r}_0)$ .

Fans of the method of nets use it in the hope that, since solutions of

Laplace's equation are fairly well behaved when the boundary values are well behaved, one may not need a very fine net for equations like (5.10) to be quite accurate.

The solution of equations (5.10) could be obtained by any sparse matrix inversion routine or, perhaps more readily, by an iteration process. The straightforward and obvious iteration process applied to equations (5.10) is guaranteed to converge eventually ([33], p. 229), but it might not converge very fast.

It would be handy if  $\underline{r}_0$  could be chosen as one point of the net, but this is not necessary. Interpolation formulas involving the  $\Psi$ 's at nearby net points are readily available.

There are two ways in which a symmetry of  $E$  is useful in connection with a net-calculation of  $r_2$ . As with the integral equation methods, anything one can do toward picking out  $\underline{r}_e$  greatly reduces the amount of calculation. In addition, though, with the method of nets it is a little easier than with integral equation methods to make use of the symmetry of  $E$  to reduce the size of the matrix we have to consider. Of course, similar reductions are possible when one is using an integral equation method, but it is a little easier to build such reductions into a general computer code when one uses the method of nets.

We are not going to get into any extended discussion here on the relative merits of the integral equation methods and the method of nets. One's choice depends partly on taste and partly on ignorance. The integral equation methods lead to much smaller matrices, while the method of nets results in a large sparse matrix that is easier to invert for a given matrix size.

It's always nice to throw in an example. Let's consider a cubical  $E$ , whose edges are two units long, centered at the origin of a Cartesian coordinate system. It is clear, from symmetry, that  $\underline{r}_e = 0$ . Equation (5.10), applied to a one-point net, using boundary  $\Psi$ 's equal to the values of  $\psi$  at the same points, gives

$$\Psi(0,0,0) = \frac{1}{6} \left\{ \frac{6}{4\pi} \right\}$$

and thus

$$r_2^{(1)} = \frac{1}{4\pi\psi(0,0,0)} = 1.$$

where the superscript on  $r_2$  indicates the number of net points. Using a 27-point cubic lattice (net spacing =  $\frac{1}{2}$ ), the origin being one of the net points, it is not hard, if one makes use of all the symmetries of the cube, to show that

$$r_2^{(27)} = \frac{3.4}{1 + 8(1.5)^{-\frac{1}{2}} + 1.6(1.25)^{-\frac{1}{2}}} = 1.102.$$

Similarly, for a net spacing of  $\frac{1}{3}$  (this one is easier to do strictly numerically),

$$r_2^{(125)} = 1.135$$

A more precise value, obtained in Section VI by other means, is

$$r_2^{(\infty)} = 1.144.$$

In this subsection, we have done no more than to remind the reader of the existence of the method of nets; it seems to have been going out of style lately. To really learn about it, one will have to read a book or two (see, besides [33], perhaps [35] and [36]).

#### V.C. Method of Inversion

We have seen in Section III (equation (3.21)) that the  $r_2$  of any E and the  $r_1'$  of the B obtained from E by inverting in a sphere of radius R, centered at  $\underline{r}_e$ , are related by

$$r_1' r_2 = R^2.$$

This gives us a useful means of calculating  $r_2$  or, speaking more accurately, a way of determining E shapes that have a given  $r_2$ . Any B whose capacitance to infinity is known, by some means or other, will give us an E with a known  $r_2$  by inversion. The center of the inversion sphere must be at the center of charge of B; this condition is necessary because of the following argument.

The position of  $\underline{r}_e$  is determined from a minimization of  $\psi(\underline{r}_0, \underline{r}_0)$  and,

according to equation (3.10), this means the induced electric field at the point of the test charge is zero when  $\underline{r}_0 = \underline{r}_e$ . A zero electric field at  $\underline{r}_e$  corresponds to a zero dipole term in the far field of the inverted domain. With a finite charge on the body in the inverted domain, the only way to avoid a dipole term in the far field is to choose the origin (i.e., the center of inversion) to be at the center of charge.

Therefore, one can obtain only one E shape for a given B shape and a given  $r_2$ . Nevertheless, there are a large number of B shapes whose electrostatic properties are well known; each one will lead us to a new  $(r_2, E)$  pair by inversion. For example, this is the method we used to obtain the  $r_2$  of a circular aperture in Section IV.D. Several other inversion-related shapes are discussed in reference [8]. Spheroids, whose  $r_1$ 's are tabulated in reference [3], assume a wide variety of shapes on inversion. A lens, defined as the body within two intersecting spherical surface segments, will lead to another lens on inversion; a detailed study of lenses has been made by Herriot [37]. We will now examine a specific example of inversion. The B and E of the following example are actually degenerate forms of the lens, but we will make no use of Herriot's general lens formulas.

Consider the calculation of the  $r_2$  of a spherical shell of radius  $a$ , in which there is a circular hole whose diameter subtends an angle  $2\epsilon$  at the center of the sphere. The results of this calculation will give an upper bound on the  $r_2$  of a spherical enclosure with a circular "get lost" hole. The "get lost" region [2] must be finite in any real simulator, while in the model we will study it is infinite. These facts can be used to demonstrate the bounding property of the  $r_2$  we will calculate; the proof (which is easy, using the methods of Section VII) will be left to the reader.

So let us consider figure 12, where we have drawn two inversion-related spherical bowls,  $S$  and  $S'$ , where we want to identify  $S$  with our enclosure. The center of inversion is the center of charge of  $S'$  when the charge on that surface assumes its natural distribution (i.e., the distribution that gives a constant potential over  $S'$ ). The necessity of this position of the center of inversion has been explained above. From the solution of the potential problem for the  $S'$  surface (see, for example [24], §8.7), it is not difficult to show, in the notation of figure 12, that

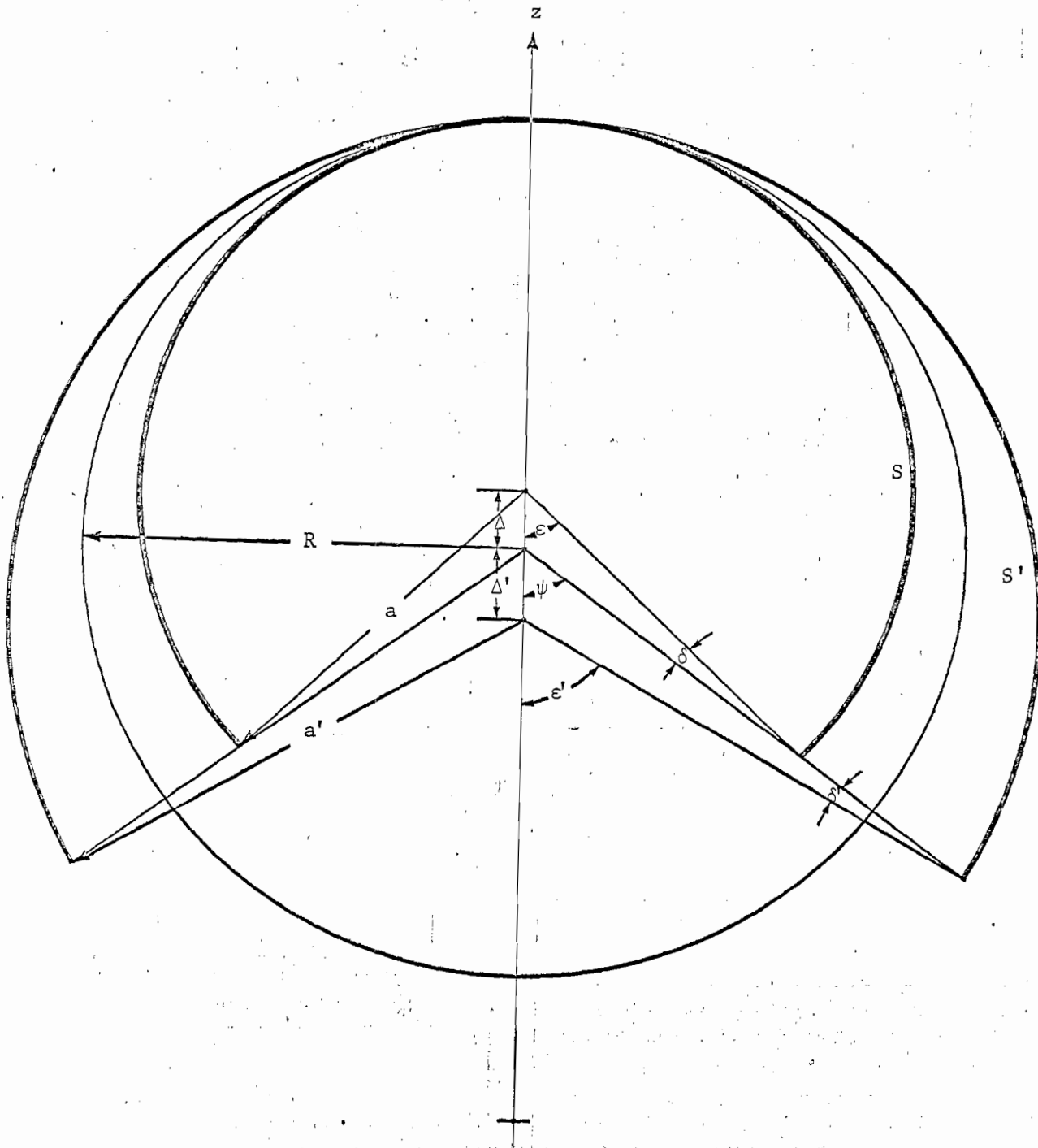


Figure 12. A spherical enclosure with a circular hole.

$$\frac{r_1'}{a'} = 1 + \frac{\sin \epsilon' - \epsilon'}{\pi} \quad (5.11)$$

and that

$$\frac{\Delta'}{a'} = \frac{\sin \epsilon' (1 - \cos \epsilon')}{\sin \epsilon' - \epsilon' + \pi} \quad (5.12)$$

Note that  $\Delta'$  is the distance from the center of  $S'$  to the center of inversion, and that the center of inversion is more remote from the hole than center of the sphere is. If  $S$  and  $S'$  osculate at the point opposite the center of the hole, the radius of inversion is clearly given by

$$R = a' - \Delta' \quad (5.13)$$

It then follows, after some simple manipulations, that

$$\frac{a}{a'} = \frac{1 - (\Delta'/a')}{1 + (\Delta'/a')} \quad (5.14)$$

and

$$\frac{\Delta}{a} = - \frac{\Delta'}{a} \quad (5.15)$$

where  $\Delta$  is the distance from the center of  $S$  to  $\underline{r}_e$  (the negative sign indicates that  $\underline{r}_e$  is on the hole side of the center of  $S$ ). Now equation (3.21) may be called upon, together with equations (5.11) through (5.16), to write

$$\frac{r_2}{a} = \frac{a'^2 (1 - \Delta'/a')^2}{r_1' a} = \frac{(1 - (\Delta/a))^2 \pi}{\sin \epsilon' - \epsilon' + \pi} \quad (5.16)$$

The remaining job is to relate  $(\Delta/a)$  and  $\epsilon'$  to  $\epsilon$ . To this end, observe from the diagram that

$$\frac{\sin \delta}{|\Delta|} = \frac{\sin \psi}{a} \quad \text{and} \quad \frac{\sin \delta'}{\Delta'} = \frac{\sin \psi}{a'}$$

and thus

$$\frac{\sin \delta'}{\sin \psi} = \frac{\Delta'}{a'} = \frac{|\Delta|}{a} = \frac{\sin \delta}{\sin \psi},$$

giving

$$\delta = \delta'.$$

Hence, since

$$\epsilon = \psi - \delta$$

$$\epsilon' = \psi + \delta',$$

we have

$$\sin\left(\frac{\epsilon' - \epsilon}{2}\right) = \sin \delta = \frac{|\Delta|}{a} \sin \psi = \frac{|\Delta|}{a} \sin \frac{\epsilon + \epsilon'}{2}.$$

By manipulating this equation, it follows that

$$\epsilon' = 2 \tan^{-1} \frac{1 + |\Delta|/a}{1 - |\Delta|/a} \cdot \tan\left(\frac{\epsilon}{2}\right) \quad (5.17)$$

When this equation is substituted into equation (5.12), and use is made of equation (5.15), we obtain an equation for  $(|\Delta|/a)$  as an implicit function of  $\epsilon$ . To get an explicit table of values we can solve the implicit equation by iteration. Once  $(|\Delta|/a)$  is found, equations (5.17) and (5.16) can be used to calculate  $r_2/a$ . Table 5 contains the information thus obtained. Also included in table 5 is a column giving the fraction of the surface area of the sphere that is cut out by the hole ( $= \sin^2(\epsilon/2)$ ). From the table, we see that there is very little change in either  $r_2$  or  $\underline{r}_e$  for  $\epsilon < 30^\circ$ .

It should be pointed out that as  $\epsilon$  becomes larger we eventually reach the point where there is no minimum in  $\psi(\underline{r}_0, \underline{r}_0)$  for finite  $\underline{r}_0$ , and thus  $r_2$  becomes undefined. This phenomenon manifests itself in the nonconvergence of the iterative solution for  $(|\Delta|/a)$  as a function of  $\epsilon$ . The maximum  $\epsilon$  for which  $r_2$  is defined is  $48.918^\circ$ .

Table 5. Effective radius of a spherical enclosure with a hole

$\epsilon^{\circ}$	$100 \sin^2(\epsilon/2)$	$ \Delta /a$	$( \Delta /a)(2\pi/\epsilon^3)$	$r_2/a$
1	.008	.00000	.99993	1.00000
2	.030	.00001	.99974	1.00000
3	.069	.00002	.99946	1.00001
4	.122	.00005	.99912	1.00002
5	.190	.00011	.99876	1.00004
6	.274	.00018	.99841	1.00007
7	.373	.00029	.99810	1.00010
8	.487	.00043	.99785	1.00014
9	.616	.00062	.99770	1.00021
10	.760	.00084	.99768	1.00028
11	.919	.00112	.99782	1.00038
12	1.093	.00146	.99814	1.00049
13	1.281	.00186	.99869	1.00062
14	1.485	.00232	.99948	1.00078
15	1.704	.00286	1.00055	1.00096
16	1.937	.00347	1.00194	1.00116
17	2.185	.00417	1.00366	1.00140
18	2.447	.00496	1.00577	1.00166
19	2.724	.00585	1.00828	1.00196
20	3.015	.00685	1.01124	1.00229
21	3.321	.00795	1.01470	1.00266
22	3.641	.00918	1.01868	1.00307
23	3.975	.01053	1.02323	1.00352
24	4.323	.01202	1.02842	1.00401
25	4.685	.01367	1.03427	1.00456
26	5.060	.01548	1.04088	1.00515
27	5.450	.01746	1.04828	1.00580
28	5.857	.01962	1.05658	1.00650
29	6.269	.02200	1.06583	1.00727
30	6.669	.02459	1.07617	1.00810
31	7.142	.02742	1.08767	1.00900
32	7.598	.03051	1.10049	1.00998
33	8.066	.03390	1.11478	1.01103
34	8.548	.03760	1.13072	1.01217
35	9.042	.04167	1.14852	1.01341
36	9.549	.04613	1.16846	1.01475
37	10.068	.05104	1.19086	1.01619
38	10.599	.05647	1.21612	1.01776
39	11.143	.06248	1.24477	1.01946
40	11.698	.06918	1.27747	1.02130
41	12.265	.07670	1.31511	1.02330
42	12.843	.08519	1.35892	1.02548
43	13.432	.09490	1.41061	1.02786
44	14.033	.10616	1.47281	1.03048
45	14.645	.11949	1.54965	1.03338
46	15.267	.13578	1.64852	1.03660
47	15.900	.15678	1.78458	1.04024
48	16.543	.18721	2.00052	1.04446
48.9	17.131	.25481	2.57538	1.04910

## V.D. Separation of Variables Method

This method is so well known that we need do no more than mention it, and make a few comments. The two special cases treated in Section VI are examples of the application of this method.

The number of distinct enclosure shapes that can be treated by this method is quite limited. In addition to the examples of Section VI, one can imagine applying this method to the calculation of the  $r_2$  of ellipsoids, finite elliptical cylinders, and certain "quasi-enclosures," such as the circular aperture of Section IV.D, a system of two spheres or an anchor ring. This almost exhausts the list of reasonably shaped "enclosures" to which the method can be applied straightforwardly. All these shapes have enough symmetry for one to be able to pick out  $r_e$  by inspection; this is probably true for any shape for which the separation of variables method is applicable.

Probably no real simulator enclosure will take exactly a shape for which the separation of variables method can be applied, but  $r_2$  calculations for such shapes are important for two reasons:

Firstly, small perturbations in the boundary-surface shape will have an insignificant effect on the  $r_2$  of an enclosure. We have seen an example of this already in Section V.C, where even a hole cut in the boundary surface had very little effect until the hole's area was a significant fraction of the original surface area of the enclosure. A detailed study of the effect of boundary perturbations on  $r_2$  might be an interesting topic for a future note.

Secondly, the  $r_2$ 's of simple shapes can be used to bound the  $r_2$ 's of more complex shapes. This is because the  $r_2$  of any E is less than  $r_2'$ , the  $r_2$  of any E' that can contain E, and greater than  $r_2''$ , the  $r_2$  of any E'' that E can contain. This will be proven in Section VII. We mention it here because it is the real motivation for the calculations of Section VI. An application of this bounding property, making use of the results of Section VI, may be found in Section VII.

## VI. Enclosure Radius Calculations -- Two Simple Shapes

In this section, we will make use of the separation of variables method, together with a judicious application of image theory, to calculate the  $r_2$  of two simple enclosure shapes -- finite circular cylinders and rectangular parallelepipeds. There are various alternative representations of the  $r_2$ 's of these two simple shapes. Our aim here will be to derive those representations that are most suited to numerical evaluation.

The numerical results of the calculations of this section can be used to bound the  $r_2$ 's of enclosures having more complicated shapes. This will be elaborated upon in Section VII.

### VI.A. Finite Circular Cylinders

Consider a finite circular cylindrical enclosure such as that shown in figure 13. From symmetry it is clear that, with the coordinate system shown in the figure,  $r_e = 0$ .

We will calculate the  $\psi(0,0)$  of a finite cylinder by making use of the Green's function of an infinite circular cylindrical enclosure with the source point on the axis. The finite cylinder Green's function will be found by assuming an infinite row of source points spaced uniformly (spacing =  $h$ ) along the axis of the infinite cylinder, the sources being of alternating sign. There are, of course, alternative methods of deriving the Green's function for a finite cylinder, but the one used here is perhaps the simplest for which it is easy to isolate the  $\psi(\underline{r}, \underline{r}_0)$  contribution to  $G_e(\underline{r}, \underline{r}_0)$ .

The Green's function for an infinite cylinder of radius  $a$  has already been given as equation (4.7); we repeat it here for convenience:

$$G_e^\infty(\rho, z; 0, z') = \frac{1}{4\pi\sqrt{\rho^2 + (z-z')^2}} - \frac{1}{2\pi^2} \int_0^\infty \frac{K_0(\lambda a)}{I_0(\lambda a)} I_0(\lambda \rho) \cos \lambda(z - z') d\lambda. \quad (6.1)$$

As we saw in Section IV.A, the  $G_e^\infty$  of equation (6.1) has all the properties required of a Green's function. A detailed derivation of equation (6.1), making use of the separation of variables method, has been given by Weber [38]. A detailed study of the properties of this  $G_e$  has been given by Boukamp and De Bruijn [39]. We are interested in the case where  $\rho$  is zero, and so we write

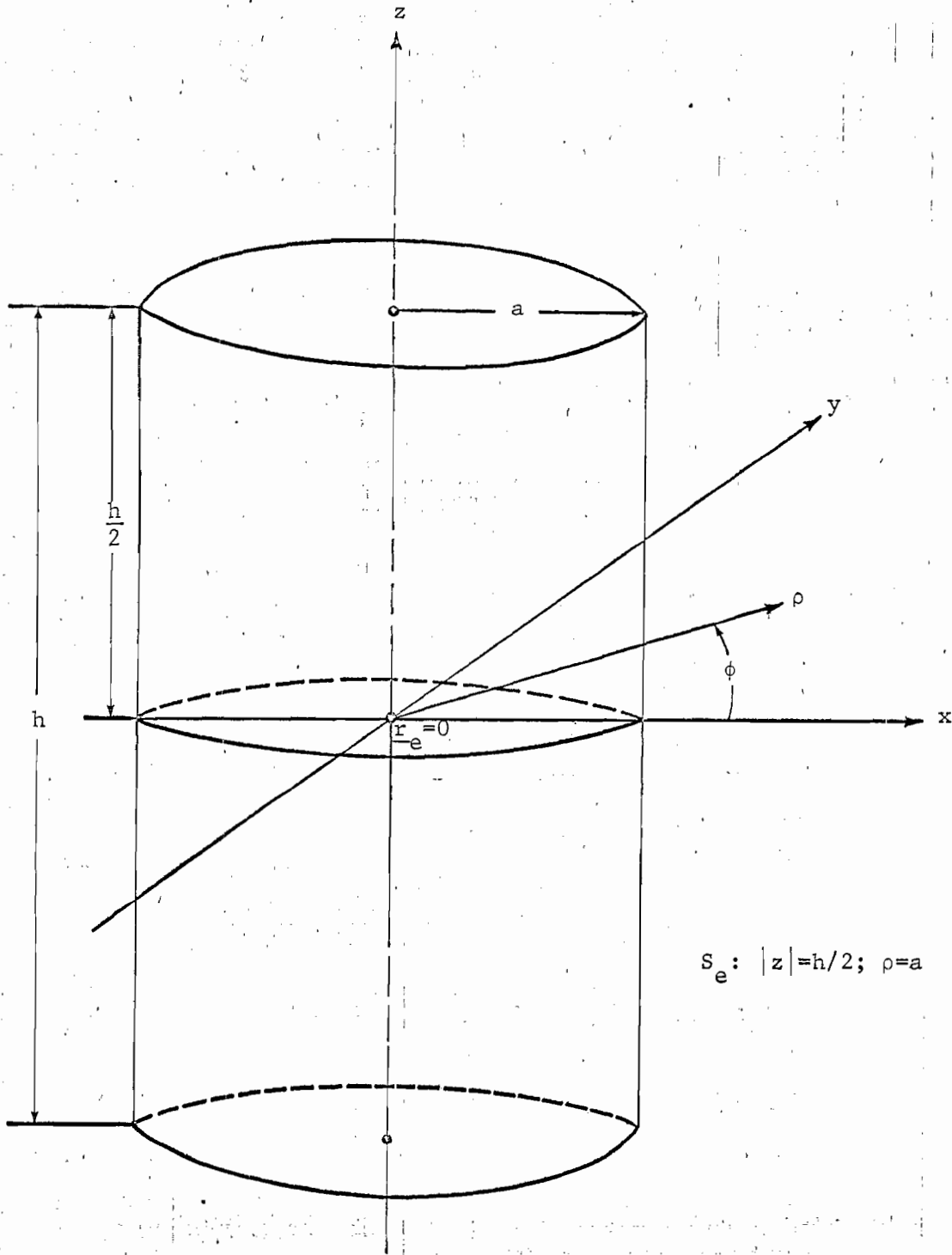


Figure 13. A right circular cylindrical enclosure.

$$G_e^\infty(0, z; 0, z') = \frac{1}{4\pi|z-z'|} - \frac{1}{2\pi^2} \int_0^\infty \frac{K_0(\lambda a)}{I_0(\lambda a)} \cos \lambda(z-z') d\lambda \quad (6.2)$$

It has been shown by Boukamp and De Bruijn ([39], equation (27)) that an alternative representation of  $G_e^\infty(0, z; 0, z')$  is

$$G_e^\infty(0, z; 0, z') = \frac{1}{2\pi a} \sum_{n=1}^{\infty} \frac{e^{-\mu_n |z-z'|/a}}{\mu_n J_1^2(\mu_n)} \quad (6.3)$$

where the  $\mu_n$ 's are the roots of

$$J_0(\mu_n) = 0.$$

Now, adding up a string of sources of alternating sign spaced uniformly along the z-axis with spacing h, using equation (6.2) for the source nearest the origin and equation (6.3) for all the other sources, we obtain the Green's function for the finite cylinder in the form

$$G_e(0, z; 0, z') = \frac{1}{4\pi|z-z'|} - \frac{1}{2\pi^2} \int_0^\infty \frac{K_0(\lambda a)}{I_0(\lambda a)} \cos \lambda(z-z') d\lambda + \frac{1}{2\pi a} \sum_{m=1}^{\infty} (-)^m \sum_{n=1}^{\infty} \frac{e^{-\mu_n |z-mh|/a} + e^{-\mu_n |z+mh|/a}}{\mu_n J_1^2(\mu_n)}, \quad (6.4)$$

from which we can identify  $\psi(0,0)$  as

$$\psi(0,0) = \frac{1}{2\pi^2} \int_0^\infty \frac{K_0(\lambda a)}{I_0(\lambda a)} d\lambda - \frac{1}{\pi a} \sum_{m=1}^{\infty} (-)^m \sum_{n=1}^{\infty} \frac{e^{-\mu_n mh/a}}{\mu_n J_1^2(\mu_n)} \quad (6.5)$$

Interchanging order of summation in the double sum, performing the new inner sum, and changing the integration variable to  $\lambda a$ , we obtain

$$4\pi a \psi(0,0) = \frac{2}{\pi} \int_0^\infty \frac{K_0(x)}{I_0(x)} dx + 4 \sum_{n=1}^{\infty} \frac{1}{(e^{\mu_n h/a} + 1) \mu_n J_1^2(\mu_n)}. \quad (6.6)$$

We can integrate the integral by parts and call upon equation (3.6) to write the equation for  $r_2$  in the form

$$\frac{r_2}{a} = \left\{ \frac{2}{\pi} \int_0^\infty \frac{dx}{I_0^2(x)} + 4 \sum_{n=1}^{\infty} \frac{1}{(e^{2\mu_n H} + 1) \mu_n J_1^2(\mu_n)} \right\}^{-1} \quad (6.7)$$

where

$$H \equiv (h/2a)$$

As  $H$  becomes large, the sum in equation (6.7) becomes negligible, and we revert to the  $r_2/a$  of an infinite cylinder given by equation (4.3). In the general case, we already know the value of the integral from Section IV.A, and so we may write

$$\frac{r_2}{a} = \left\{ .8706898 + 4 \sum_{n=1}^{\infty} \frac{1}{(e^{2\mu_n H} + 1) \mu_n J_1^2(\mu_n)} \right\}^{-1} \quad (6.8)$$

The values of  $\mu_n$  and  $J_1(\mu_n)$  have been tabulated ([19], p. 409), and so it is a straightforward matter, by using even a desk-top computer, to evaluate expression (6.8) for various values of  $H$ . This is the manner in which we obtained the data exhibited in table 6 and figure 14, except that for the smaller values of  $H$  we summed the asymptotic form of the terms of the series to say that

$$\frac{r_2}{a} \approx .8706898 + \sum_{n=1}^N \frac{4}{(e^{2\mu_n H} + 1) \mu_n J_1^2(\mu_n)} + \frac{2\pi e^{-(2N+3/2)\pi H}}{1 - e^{-2\pi H}}. \quad (6.9)$$

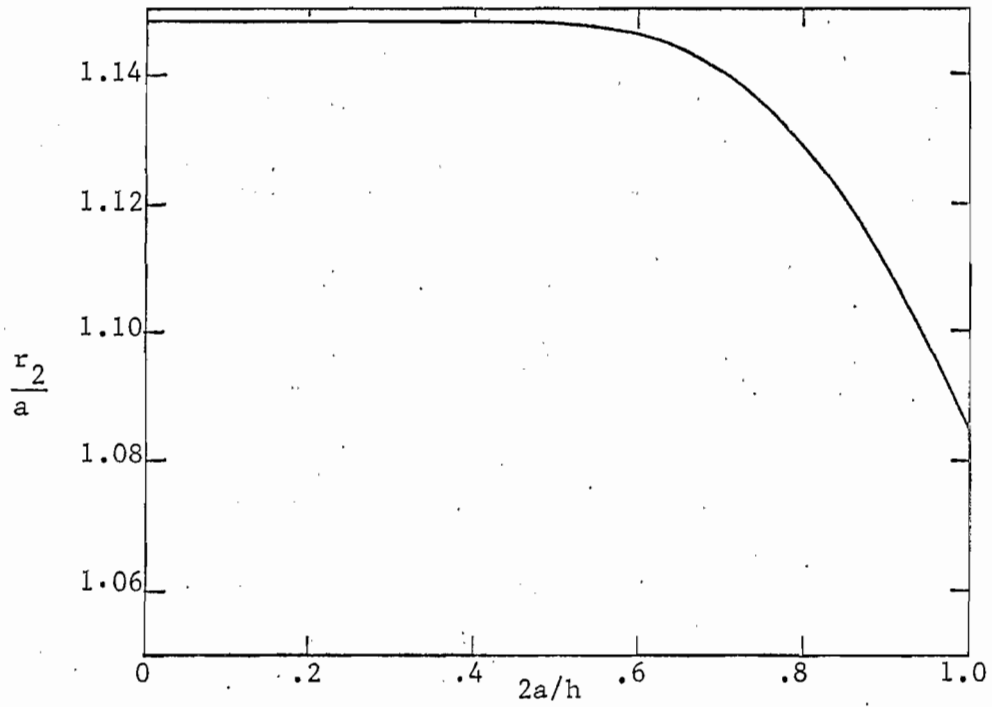
Using equation (6.9), an  $N$  of 20 gives the accuracy indicated by table 6. We note that the correct small  $H$  limit is obtained, to the number of significant figures given, since for small  $H$  we have essentially a parallel-plate region for which, from Section IV.B (equation 4.18),

$$\frac{2r_2}{h} = \frac{1}{\ln 2} = 1.442695+.$$

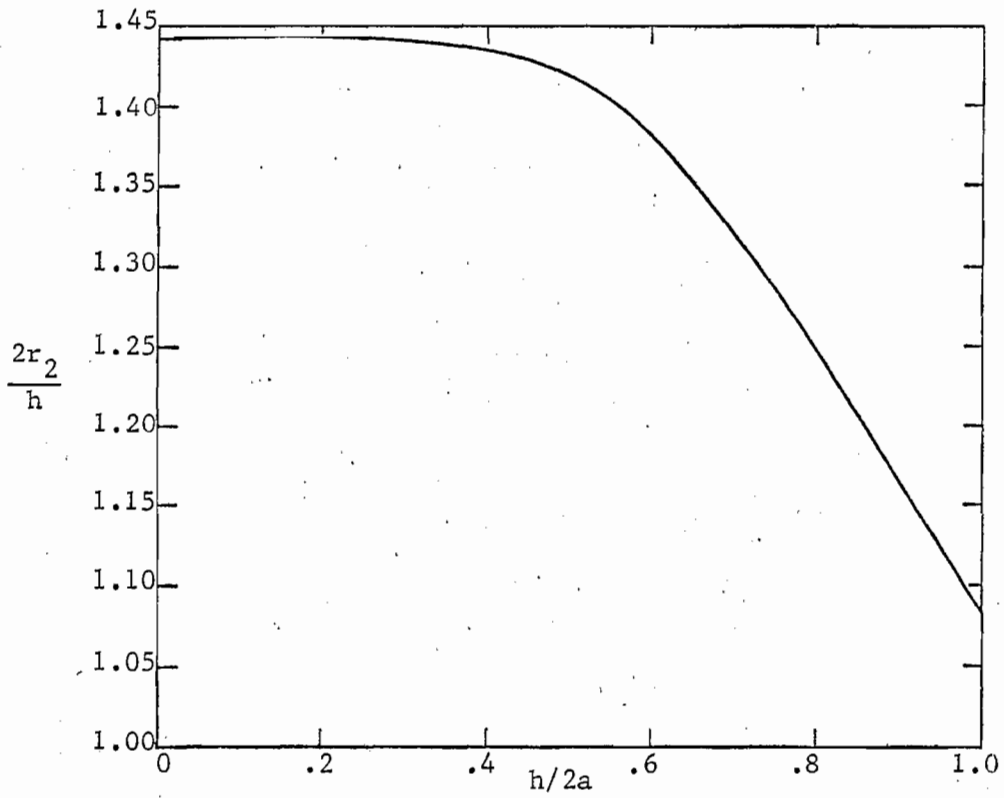
An interesting thing about the results is that the magnitude of  $r_2$  is primarily determined by the minimum distance from  $r_e$  to the surface of the enclosure; it is a little larger than this minimum distance.

Table 6: Effective radii of right circular cylindrical enclosures

long thin cylinders				short fat cylinders			
2a/h	$r_2/a$	2a/h	$r_2/a$	h/2a	$2r_2/h$	h/2a	$2r_2/h$
.01	1.14851	.51	1.14786	.01	1.44270	.51	1.41782
.02	1.14851	.52	1.14773	.02	1.44270	.52	1.41480
.03	1.14851	.53	1.14758	.03	1.44270	.53	1.41157
.04	1.14851	.54	1.14741	.04	1.44270	.54	1.40811
.05	1.14851	.55	1.14722	.05	1.44270	.55	1.40442
.06	1.14851	.56	1.14700	.06	1.44270	.56	1.40052
.07	1.14851	.57	1.14676	.07	1.44270	.57	1.39638
.08	1.14851	.58	1.14648	.08	1.44270	.58	1.39202
.09	1.14851	.59	1.14617	.09	1.44270	.59	1.38744
.10	1.14851	.60	1.14583	.10	1.44270	.60	1.38264
.11	1.14851	.61	1.14546	.11	1.44270	.61	1.37763
.12	1.14851	.62	1.14505	.12	1.44270	.62	1.37240
.13	1.14851	.63	1.14459	.13	1.44270	.63	1.36696
.14	1.14851	.64	1.14410	.14	1.44270	.64	1.36133
.15	1.14851	.65	1.14356	.15	1.44270	.65	1.35549
.16	1.14851	.66	1.14298	.16	1.44269	.66	1.34947
.17	1.14851	.67	1.14234	.17	1.44269	.67	1.34326
.18	1.14851	.68	1.14166	.18	1.44269	.68	1.33687
.19	1.14851	.69	1.14093	.19	1.44269	.69	1.33032
.20	1.14851	.70	1.14014	.20	1.44269	.70	1.32360
.21	1.14851	.71	1.13929	.21	1.44269	.71	1.31673
.22	1.14851	.72	1.13839	.22	1.44269	.72	1.30972
.23	1.14851	.73	1.13743	.23	1.44268	.73	1.30257
.24	1.14851	.74	1.13641	.24	1.44267	.74	1.29529
.25	1.14851	.75	1.13533	.25	1.44265	.75	1.28789
.26	1.14851	.76	1.13419	.26	1.44262	.76	1.28038
.27	1.14851	.77	1.13298	.27	1.44258	.77	1.27277
.28	1.14851	.78	1.13171	.28	1.44253	.78	1.26506
.29	1.14851	.79	1.13036	.29	1.44245	.79	1.25726
.30	1.14851	.80	1.12896	.30	1.44234	.80	1.24939
.31	1.14851	.81	1.12748	.31	1.44220	.81	1.24144
.32	1.14851	.82	1.12594	.32	1.44202	.82	1.23344
.33	1.14851	.83	1.12432	.33	1.44178	.83	1.22537
.34	1.14851	.84	1.12264	.34	1.44150	.84	1.21726
.35	1.14851	.85	1.12088	.35	1.44114	.85	1.20911
.36	1.14850	.86	1.11905	.36	1.44070	.86	1.20093
.37	1.14850	.87	1.11716	.37	1.44017	.87	1.19272
.38	1.14849	.88	1.11519	.38	1.43955	.88	1.18448
.39	1.14848	.89	1.11315	.39	1.43882	.89	1.17624
.40	1.14847	.90	1.11104	.40	1.43796	.90	1.16799
.41	1.14845	.91	1.10886	.41	1.43698	.91	1.15973
.42	1.14843	.92	1.10661	.42	1.43585	.92	1.15148
.43	1.14840	.93	1.10429	.43	1.43457	.93	1.14323
.44	1.14837	.94	1.10190	.44	1.43313	.94	1.13500
.45	1.14833	.95	1.09944	.45	1.43152	.95	1.12679
.46	1.14828	.96	1.09691	.46	1.42973	.96	1.11860
.47	1.14822	.97	1.09432	.47	1.42775	.97	1.11044
.48	1.14815	.98	1.09166	.48	1.42558	.98	1.10230
.49	1.14807	.99	1.08894	.49	1.42320	.99	1.09421
.50	1.14797	1.00	1.08615	.50	1.42061	1.00	1.08615



14a. long thin cylinders.



14b. short fat cylinders.

Figure 14. Effective radii of right circular cylindrical enclosures.

We will use the data of table 6 in our discussion of bounds in Section VII.

### VI.B. Rectangular Parallelepipeds

Consider a rectangular parallelepiped enclosure such as the one shown in figure 15. We have chosen a coordinate system whose origin is at the center of the enclosure, and the edges of the enclosure parallel to the x, y, and z axes are of length 2a, 2b, and 2c, respectively. We will assume that we have oriented the enclosure so that  $a \geq b \geq c$ . From symmetry it is clear that  $r_e = 0$ .

We will calculate  $\psi(0;0)$  by making use of the Green's function for the infinite parallel-plate region,  $|z| \leq c$ . The Green's function for the actual enclosure can be thought of as being the superposition of a doubly infinite sum of parallel-plate Green's functions. More precisely, it is clear from image theory that if the parallel-plate Green's function is given by  $G_e^\infty(x,y,z;x',y',z')$ , then the parallelepiped Green's function is just

$$\begin{aligned}
 G_e(x,y,z;x',y',z') = & \sum_{n=-\infty}^{\infty} \sum_{m=-\infty}^{\infty} \{G_e^\infty(x,y,z;x' + 4an,y' + 4bm,z') \\
 & + G_e^\infty(x,y,z;2a - x' + 4an,2b - y' + 4bn,z') \\
 & - G_e^\infty(x,y,z;2a - x' + 4an,y' + 4bn,z') \\
 & - G_e^\infty(x,y,z;x' + 4an,2b - y' + 4bn,z')\}. \quad (6.10)
 \end{aligned}$$

For the source point at the origin this reduces to

$$G_e(x,y,z;0) = \sum_{n=-\infty}^{\infty} \sum_{m=-\infty}^{\infty} (-)^{n+m} G_e^\infty(x,y,z;2an,2bm,0), \quad (6.11)$$

which we will write as

$$\begin{aligned}
 G_e(x,y,z;0) = & G_e^\infty(x,y,z;0) + 2 \sum_{n=1}^{\infty} (-)^n [G_e^\infty(x,y,z;2an,0,0) + G_e^\infty(x,y,z;0,2bn,0)] \\
 & + 4 \sum_{n=1}^{\infty} \sum_{m=1}^{\infty} (-)^{n+m} G_e^\infty(x,y,z;2an,2bm,0). \quad (6.12)
 \end{aligned}$$

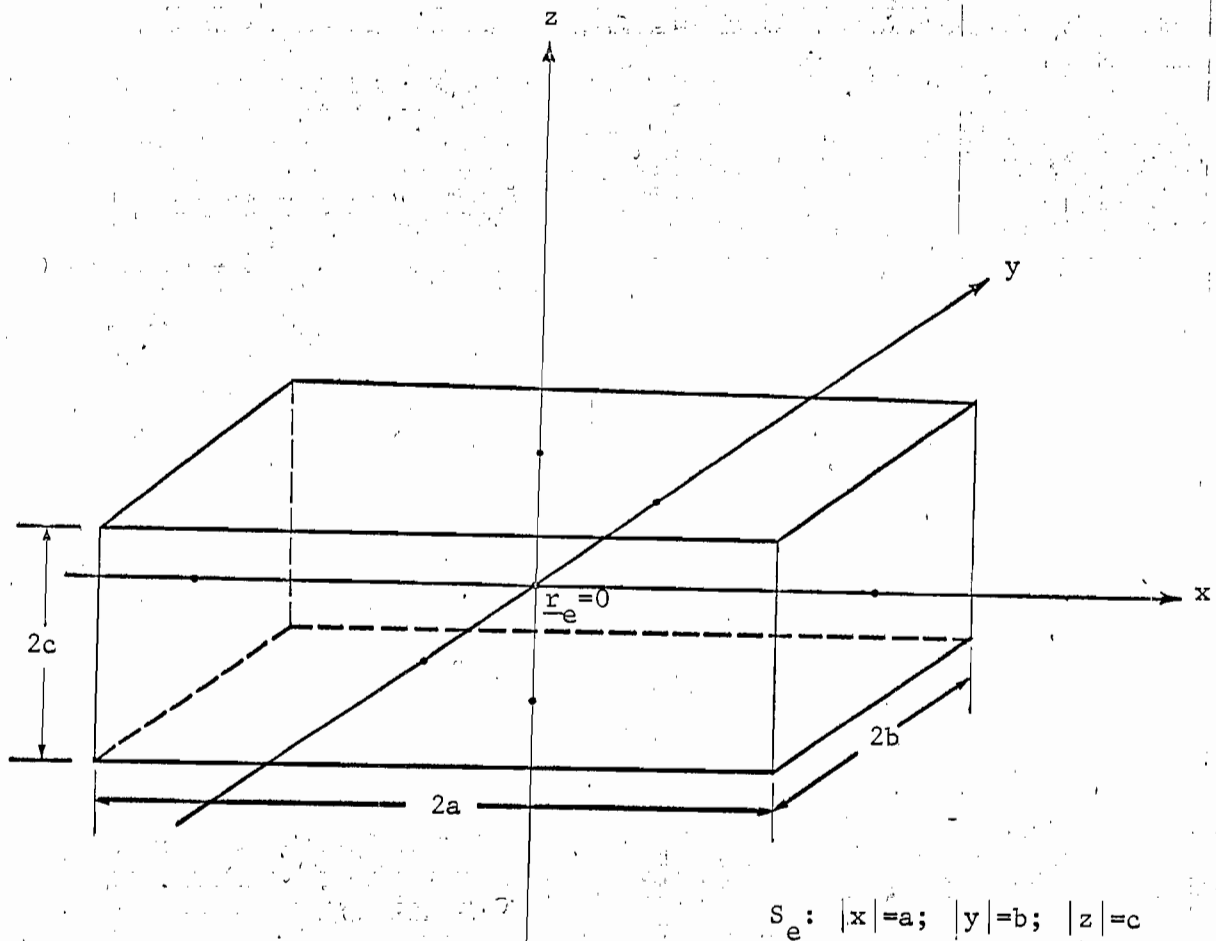


Figure 15. A rectangular parallelepiped enclosure.

The singularity as the field point approaches the origin is due solely to the term  $G_e^\infty(x,y,z;0)$ , which we can write as

$$\begin{aligned}
 G_e^\infty(x,y,z;0) &= \frac{1}{4\pi} \sum_{n=-\infty}^{\infty} \frac{(-)^n}{\sqrt{x^2+y^2+(z-2nc)^2}} \\
 &= \frac{1}{4\pi\sqrt{x^2+y^2+z^2}} \\
 &\quad + \frac{1}{4\pi} \sum_{n=1}^{\infty} (-)^n \frac{1}{[x^2+y^2+(z-2nc)^2]^{\frac{1}{2}}} + \frac{1}{[x^2+y^2+(z+2nc)^2]^{\frac{1}{2}}} \quad (6.13)
 \end{aligned}$$

We can therefore subtract the appropriate singularity from this term and use equation (6.12) to write

$$\begin{aligned}
 \psi(\underline{0};\underline{0}) &= \psi^\infty(\underline{0};\underline{0}) - 2 \sum_{n=1}^{\infty} (-)^n [G_e^\infty(\underline{0};2an,0,0) + G_e^\infty(\underline{0};0,2bn,0)] \\
 &\quad - 4 \sum_{n=1}^{\infty} \sum_{m=1}^{\infty} (-)^{n+m} G_e^\infty(\underline{0};2an,3bm,0), \quad (6.14)
 \end{aligned}$$

where

$$\psi^\infty(\underline{0};\underline{0}) = \frac{1}{2\pi} \sum_{n=1}^{\infty} \frac{(-)^{n+1}}{2nc} = \frac{1}{4\pi c} \ln 2, \quad (6.15)$$

as we have already seen in Section IV.B.

From equations (6.14) and (6.15), and the definition of  $r_2$  (equation (3.6)), we can see that

$$\begin{aligned}
 \frac{c}{r_2} &= \ln 2 - 4\pi c \left\{ 2 \sum_{n=1}^{\infty} (-)^n [G_e^\infty(\underline{0};2an,0,0) + G_e^\infty(\underline{0};0,2bn,0)] \right. \\
 &\quad \left. - 4 \sum_{n=1}^{\infty} \sum_{m=1}^{\infty} (-)^{n+m} G_e^\infty(\underline{0};2an,2bm,0) \right\}. \quad (6.16)
 \end{aligned}$$

We still have to determine an appropriate representation of  $G_e^\infty(\underline{0};2an,2bm,0)$ .

From the symmetry of Green's functions this can also be written as  $G_e^\infty(2an, 2bm, 0; \underline{0})$  and so, in principle, one could use equation (6.13), but that representation of  $G_e^\infty$  is useless for numerical work because of its slow convergence. An alternative representation which is well adapted for numerical evaluation may be found by using circular cylindrical coordinates to calculate the potential of a point charge between two infinite parallel plates. If the point charge is at the origin we obtain, by a simple separation of variables calculation,

$$G_e^\infty(2an, 2bm, 0; \underline{0}) = \frac{1}{2\pi c} \sum_{k=0}^{\infty} K_0 \left\{ (2k+1)\pi \frac{\sqrt{a^2 n^2 + b^2 m^2}}{c} \right\} \quad (6.17)$$

where  $K_0$  is a modified Bessel function.

Alternatively, the above representation may be obtained by the following rather formal manipulations of equation (6.13).

$$\begin{aligned} G_e^\infty(x, y, 0; \underline{0}) &= \frac{1}{4\pi} \sum_{n=-\infty}^{\infty} \frac{(-)^n}{\sqrt{x^2 + y^2 + (2nc)^2}} \\ &= \frac{1}{4\pi} \sum_{n=-\infty}^{\infty} (-)^n \frac{2}{\pi} \int_0^{\infty} K_0(\sqrt{x^2 + y^2} \omega) \cos(2nc\omega) d\omega. \end{aligned}$$

This equation results from a use of a Fourier transform given in reference [17], p. 412. Continuing with  $\rho \equiv (x^2 + y^2)^{\frac{1}{2}}$ ,

$$\begin{aligned} G_e^\infty(x, y, 0; \underline{0}) &= \frac{1}{4\pi^2} \sum_{n=-\infty}^{\infty} \int_{-\infty}^{\infty} K_0(\rho|\omega|) e^{in(2\omega c + \pi)} d\omega \\ &= \frac{1}{4\pi^2} \int_{-\infty}^{\infty} K_0(\rho|\omega|) \sum_{k=-\infty}^{\infty} \frac{\delta(\omega + (\pi/c)(\frac{1}{2} - k))}{c/\pi} d\omega \\ &= \frac{1}{2\pi c} \sum_{k=0}^{\infty} K_0\left(\frac{\pi\rho}{c} \cdot \frac{2k+1}{2}\right) \end{aligned}$$

which, with the substitution  $\rho = 2(n^2 a^2 + m^2 b^2)^{\frac{1}{2}}$ , returns us to equation (6.17).

We can now define the function

$$F(x) \equiv \sum_{k=0}^{\infty} K_0\{(2k+1)\pi x\}, \quad (6.18)$$

and rearrange the double sum in equation (6.16) to write

$$\frac{r_2}{c} = \left\{ \ln 2 - 4 \sum_{n=1}^{\infty} (-)^n [F(n/\alpha) + F(n/\alpha\beta)] - 8 \sum_{n=2}^{\infty} (-)^n \sum_{m=1}^{n-1} F\left(\sqrt{\frac{m^2}{\alpha^2} + \frac{(n-m)^2}{\alpha^2\beta^2}}\right) \right\}^{-1} \quad (6.19)$$

where

$$\alpha \equiv c/b$$

and

$$\beta \equiv b/a$$

Equation (6.19) was evaluated numerically for  $\alpha = 0(.1)1$  and  $\beta = 0(.1)1$ . All sums converged quite rapidly. The results of the numerical work are displayed in table 7 and in figures 16 and 17.

From these data displays we see again, as in the case of the finite circular cylinder, that the magnitude of  $r_2$  depends primarily on the minimum distance from  $\underline{r}_e$  to the wall of the enclosure;  $r_2$  is a little larger than this distance.

Table 7. Effective radii of rectangular parallelepipeds

$$a \geq b \geq c$$

c/b = .2		c/b = .3		c/b = .4	
b/a	r <sub>2</sub> /c	b/a	r <sub>2</sub> /c	b/a	r <sub>2</sub> /c
0	1.44269	0	1.44260	0	1.44127
.1	1.44269	.1	1.44260	.1	1.44127
.2	1.44269	.2	1.44260	.2	1.44127
.3	1.44269	.3	1.44260	.3	1.44127
.4	1.44269	.4	1.44260	.4	1.44127
.5	1.44269	.5	1.44260	.5	1.44127
.6	1.44269	.6	1.44260	.6	1.44127
.7	1.44269	.7	1.44260	.7	1.44124
.8	1.44269	.8	1.44260	.8	1.44111
.9	1.44269	.9	1.44258	.9	1.44076
1.0	1.44269	1.0	1.44252	1.0	1.43995

c/b = .5		c/b = .6		c/b = .7	
b/a	r <sub>2</sub> /c	b/a	r <sub>2</sub> /c	b/a	r <sub>2</sub> /c
0	1.43511	0	1.41943	0	1.39104
.1	1.43511	.1	1.41943	.1	1.39104
.2	1.43511	.2	1.41943	.2	1.39104
.3	1.43511	.3	1.41943	.3	1.39104
.4	1.43511	.4	1.41942	.4	1.39103
.5	1.43511	.5	1.41939	.5	1.39089
.6	1.43505	.6	1.41911	.6	1.39008
.7	1.43479	.7	1.41808	.7	1.38751
.8	1.43398	.8	1.41542	.8	1.38168
.9	1.43210	.9	1.41009	.9	1.37116
1.0	1.42854	1.0	1.40112	1.0	1.35495

c/b = .8		c/b = .9		c/b = 1.0	
b/a	r <sub>2</sub> /c	b/a	r <sub>2</sub> /c	b/a	r <sub>2</sub> /c
0	1.34966	0	1.29747	0	1.23797
.1	1.34966	.1	1.29747	.1	1.23797
.2	1.34966	.2	1.29747	.2	1.23797
.3	1.34966	.3	1.29747	.3	1.23797
.4	1.34963	.4	1.29740	.4	1.23784
.5	1.34927	.5	1.29672	.5	1.23678
.6	1.34758	.6	1.29389	.6	1.23273
.7	1.34280	.7	1.28658	.7	1.22299
.8	1.33294	.8	1.27258	.8	1.20537
.9	1.31649	.9	1.25060	.9	1.17900
1.0	1.29278	1.0	1.22055	1.0	1.14445

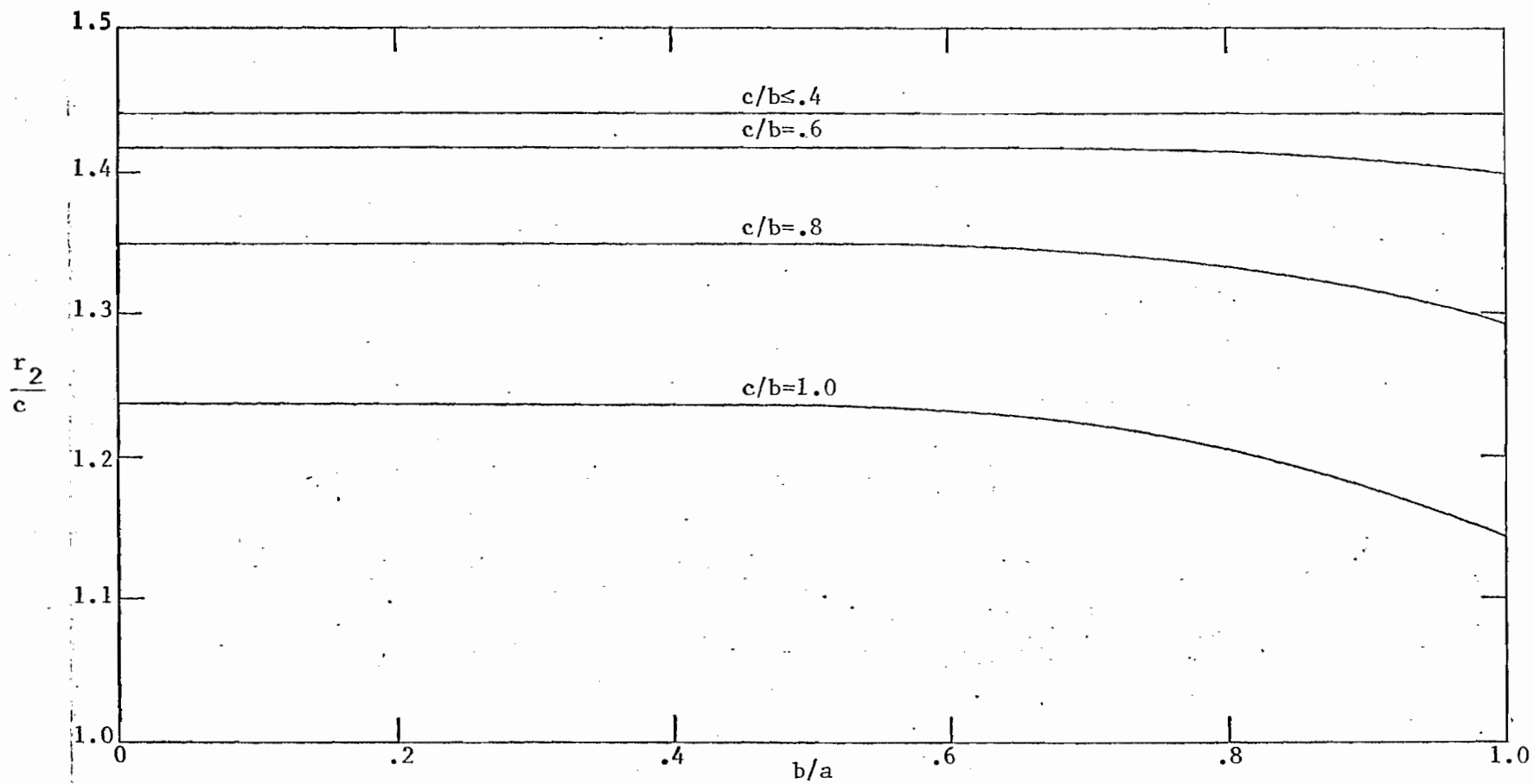


Figure 16. Effective radii of rectangular parallelepipeds --  $(c/b)$  a parameter.

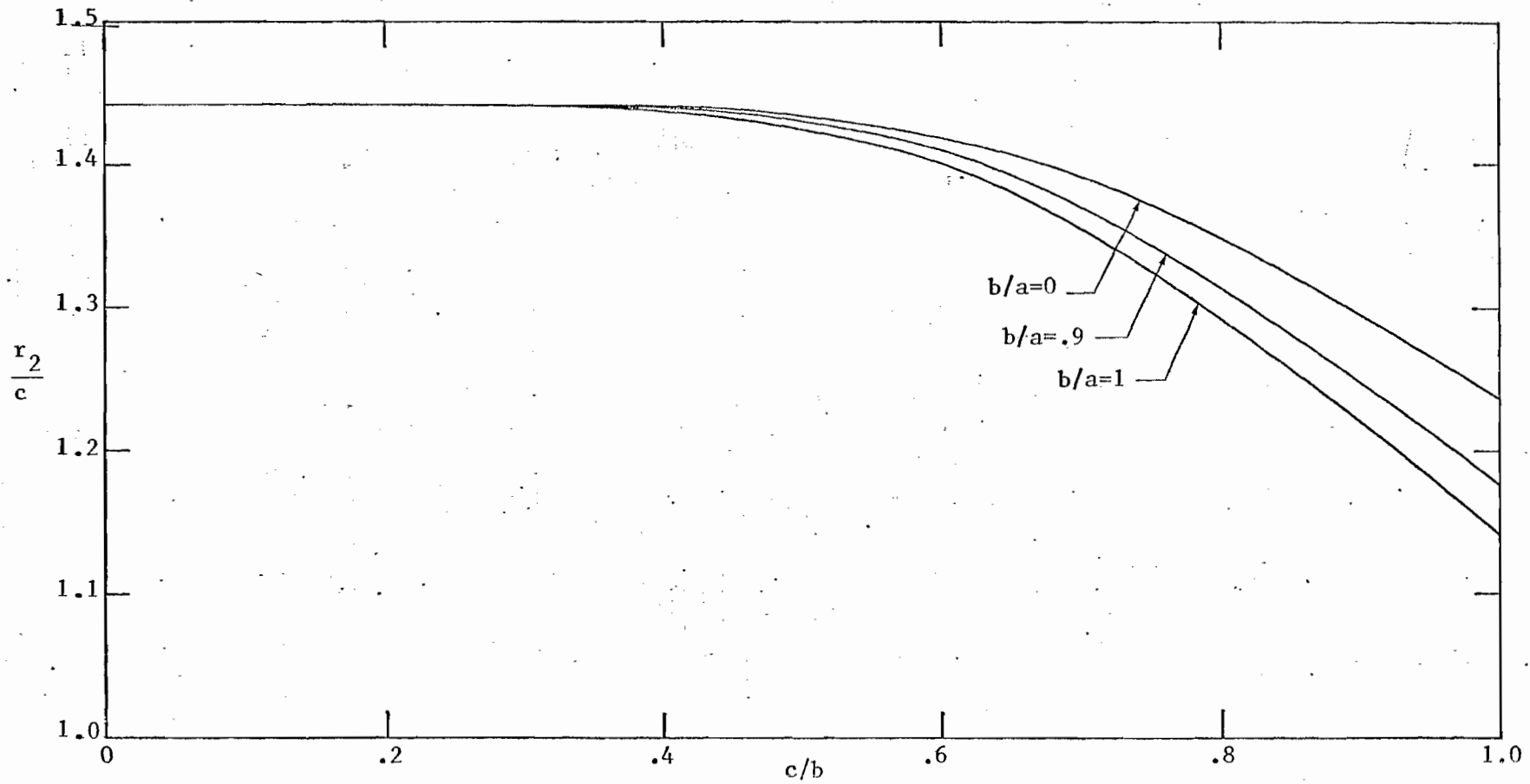


Figure 17. Effective radii of rectangular parallelepipeds --  $(b/a)$  a parameter.

## VII. Enclosure Radius Calculations -- Bounds

In this section, we will give a brief description, together with a few examples, of some of the kinds of bounds one can put on the  $r_2$  of an enclosure. The literature on the bounds one can put on the capacitance of an isolated body, or  $r_1$ , is rather extensive (references [40] through [47] are just a sampling of this literature). The setting of bounds seems to be the way mathematicians have liked to attack the capacitance problem. It would therefore seem prudent to once again invoke the inversion relation between  $r_1$  and  $r_1'$  (equation (3.21)) in order to transform the many available results on  $r_1$  bounds into equivalent statements about  $r_2$ . That is what we will do here. We will not make an exhaustive study of bounds; that can await a future note. We will content ourselves with just a couple of statements of upper bounds and a couple of statements of lower bounds. The upper bounds, which are simpler, will be treated first.

### VII.A. Upper Bounds

Reconsider equation (3.21), which we will repeat here, for convenience, in the form

$$r_2 = \frac{R^2}{r_1'} \quad (7.1)$$

From this equation it is obvious that, if we can make any lower bound statement about  $r_1'$ , say in the form

$$r_1' \geq (r_1')_b, \quad (7.2)$$

then we can make an equivalent statement about  $r_2$  in the form

$$r_2 \leq \frac{R^2}{(r_1')_b} \quad (7.3)$$

Of course, equation (7.3) will be more useful if we can write  $(r_1')_b$  in terms of the parameters of the uninverted geometry. Let us make this a little clearer by looking at a particular example of an  $(r_1')_b$  -- the "volume radius" lower bound. It is shown in reference [40] that

$$r_1' \geq \left(\frac{3V'}{4\pi}\right)^{1/3} \equiv (r_1')_{V'} \quad (7.4)$$

where  $V'$  is the volume of the body inverse to the  $E$  in question. Note, as a matter of interest, that  $(r_1')_{V'}$  is the radius of the sphere whose volume is  $V'$ . From equations (7.3) and (7.4) we can see that

$$r_2 \leq R^2 \left(\frac{4\pi}{3V'}\right)^{1/3}, \quad (7.5)$$

but we need to write  $V'$  in terms of unprimed variables in order to make this inequality easy to use. This can be accomplished as follows (we denote the solid angle subtended at the center of inversion by  $\Omega$ )

$$\begin{aligned} V' &= \int_{E'} r'^2 dr' d\Omega' \\ &= \int_{4\pi} \frac{r'^3(S')}{3} d\Omega' \\ &= \frac{R^6}{3} \int_{4\pi} \frac{d\Omega}{r^3(S)} \\ &= \frac{R^6}{3} \int_{S_e} \frac{\underline{n} \cdot \underline{r}}{r^6} dS \end{aligned} \quad (7.6)$$

where  $\underline{n}$  is now the outward normal from  $E$ . Taken together, equations (7.5) and (7.6) give

$$r_2 \leq \left\{ \frac{1}{4\pi} \int_{S_e} \frac{\underline{n} \cdot \underline{r}}{r^6} dS \right\}^{-1/3}. \quad (7.7)$$

Thus we have an upper bound on  $r_2$ , which we will denote by  $(r_2)_{V'}$ , in memory of where it came from, given by

$$(r_2)_{V'} \equiv \left\{ \frac{1}{4\pi} \int_{S_e} \frac{\underline{n} \cdot \underline{r}}{r^6} dS \right\}^{-1/3} \quad (7.8)$$

where the origin of coordinates is  $\underline{r}_e$ .

Let's calculate  $(r_2)_{V'}$  for a couple of simple shapes. The finite cylinder of figure 13 is a nice example for which we already have the numbers to check on the closeness of the  $(r_2)_{V'}$  bound. The working is simple:

$$\begin{aligned}
 \int_{S_e} \frac{\cdot r}{r^6} dS &= 4\pi a^2 \int_0^{h/2} \frac{dz}{(a^2+z^2)^3} + 2\pi h \int_0^a \frac{\rho d\rho}{(\rho^2+(h/2)^2)^3} \\
 &= \frac{4\pi}{a^3} \int_0^{\tan^{-1}H} \cos^4\theta d\theta + \frac{1}{H^3} \int_0^{1/H} \frac{xdx}{(Hx^2)^3} \\
 &= \frac{4\pi}{a^3} \left\{ \frac{3}{8} \left[ \frac{H}{1+H^2} + \tan^{-1}H \right] + \frac{1}{4H^3} \right\} \tag{7.9}
 \end{aligned}$$

where  $H \equiv (2h/a)$ . From equations (7.8) and (7.9) it follows that, for a finite cylinder,

$$(r_2)_{V'} = \left\{ \frac{3}{8} \left[ \frac{H}{1+H^2} + \tan^{-1}H \right] + \frac{1}{4H^3} \right\}^{-1/3} \tag{7.10}$$

We have chosen to exhibit the closeness of the  $(r_2)_{V'}$  bound in the finite cylinder case by plotting the ratio of  $r_2$  (using the numerical values computed in Section VI.A) to  $(r_2)_{V'}$ , versus  $H^{-1}$ . This plot is given as figure 18. From the plot, we can see that  $(r_2)_{V'}$  never exceeds  $r_2$  by more than about 10%, and for  $H$  around unity the difference is only about 2%. It would seem that one could expect this kind of behavior in general -- the more the enclosure looks like a sphere, the better the  $(r_2)_{V'}$  bound will be.

We could go on to calculate the  $(r_2)_{V'}$  of a rectangular parallelepiped. The required integrals can be performed analytically, and the result can be written in terms of elementary functions. But it is a little messy. We will not inflict this nugatory algebra on the reader. We will merely make note of the fact that, for a cube,  $(r_2)_{V'}$  exceeds  $r_2$  by only about 3.6%.

Let us instead look at the enclosure shown in figure 19, a hemispherically-capped circular cylinder of radius one and overall length four. We will come back to this enclosure a couple of more times in this section. It is a fairly simple shape for which no analytical representation of  $r_2$  exists, and yet it is not too unlikely a candidate for a practical enclosure shape. It will serve as

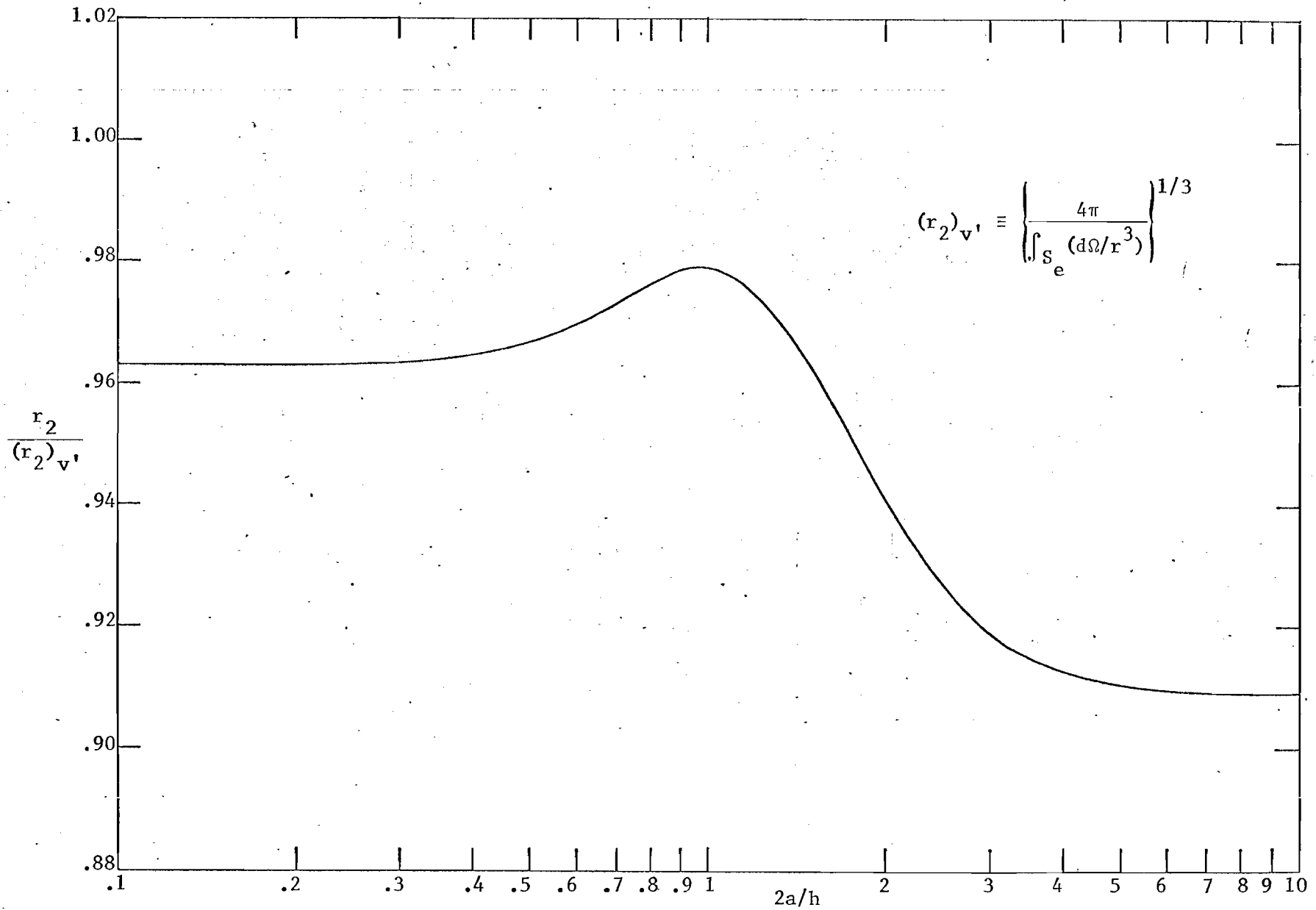
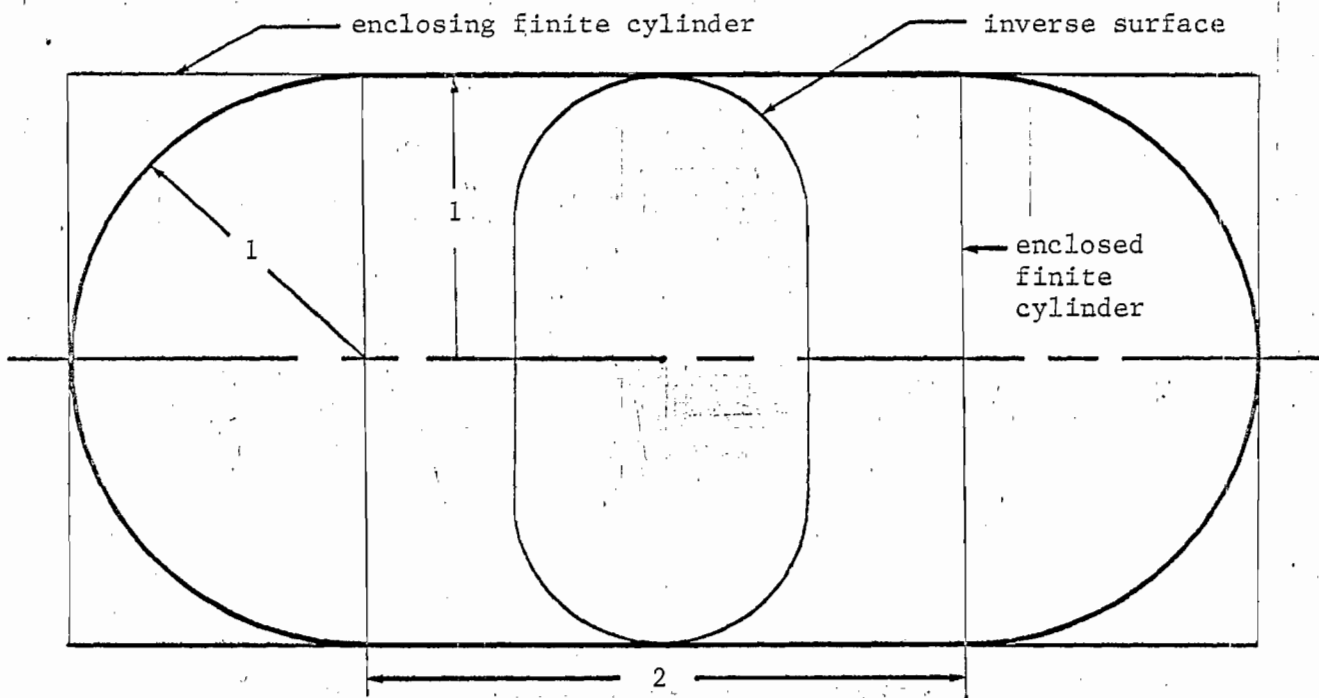


Figure 18. Accuracy of the volume upper bound for right circular cylinders.



$$r_2 \leq 1.1810 \quad (\text{inverse volume upper bound})$$

$$r_2 \leq 1.1480 \quad (\text{enclosing finite cylinder})$$

$$r_2 \geq 1.0861 \quad (\text{enclosed finite cylinder})$$

$$r_2 \geq 1.1342 \quad (\text{Pólya-Szegő bound})$$

$$r_2 \geq 1.1438 \quad (\text{best linear Parr bound})$$

Figure 19. A hemispherically-capped circular cylinder.

a convenient example with which to demonstrate the closeness of the various bounds. The only bound we have mentioned so far,  $(r_2)_{V'}$ , can be calculated most easily, for this particular enclosure, by calculating  $V'$  in the inverted domain. The inverse surface, for a radius of inversion equal to unity, is indicated on the figure. The volume within it is just

$$\begin{aligned} V' &= 2 \int_0^{1/2} \pi \left[ \frac{1}{2} + \sqrt{\left(\frac{1}{2}\right)^2 - x^2} \right] dx \\ &= \frac{\pi}{24} (10 + 3\pi) \end{aligned}$$

Thus, from equation (7.5)

$$\begin{aligned} (r_2)_{V'} &= \left( \frac{32}{10+3\pi} \right)^{1/3} \\ &= 1.1810 \end{aligned} \tag{7.11}$$

Let us now discuss briefly a slightly different kind of upper bound on  $r_2$ . A well known property of the capacitance of a body is that it is increased by the addition of any conducting material. In other words, the capacitance of a body is greater than that of any body it could contain and less than that of any body that could contain it. A proof of a statement equivalent to this is given in Smythe's book, for example ([4], §3.11). Smythe proves that, if conductor is added to a system without adding charge, the total energy of the system decreases. Since this energy is equal to  $\frac{1}{2}Q^2/C$ , we see that the capacitance must have increased. This property of capacitance, together with equation (7.3), makes it quite obvious that the  $r_2$  of any enclosure is less than the  $r_2$  of any enclosure containing it and greater than the  $r_2$  of any other enclosure that it can contain. Thus we can have many bounds on  $r_2$  to choose from if we can calculate the  $r_2$  of many simple shapes. As we mentioned previously, this was the real motivation for the calculations of Section VI.

Now we will make use of the numbers of Section VI to put an upper bound on the  $r_2$  of our hemispherically-capped circular cylinder. The capped circular

cylinder can be contained within a right circular cylinder of length four and radius one. Thus, from table 6,

$$r_2 \leq 1.1480 \quad (7.12)$$

This is an improvement on the  $(r_2)_V$  bound of equation (7.11). In fact, we will see in the following subsection that equation (7.12) gives a bound that can differ from the true  $r_2$  by no more than about a third of a percent. Of course, this won't always be true; some enclosure shapes will undoubtedly have an  $(r_2)_V$  bound that is less than any upper bound we could find in the tables.

#### VII.B. Lower Bounds

We will first mention a simple lower bound on  $r_2$  that applies to enclosures of arbitrary shape, the trouble being that the bound may not be very close. We will then briefly discuss a couple of closer lower bounds that apply to enclosure shapes that fulfill certain special requirements.

The simple lower bound is the one that arose during the discussion of the final upper bound of the previous subsection. A lower bound on the  $r_2$  of  $E$  is the  $r_2$  of any  $E'$  that fits inside  $E$ . The proof of this statement has already been given in Section VII.A. We may therefore use the tables of Section VI to give us a lower bound on  $r_2$  by finding the largest right circular cylinder, or rectangular parallelepiped that fits inside  $E$ .

For example, the largest right circular cylinder that fits inside a cube whose edges are two units long is one with  $2a = h = 1$ . This tells us, from table 6, that the  $r_2$  of such a cube is greater than 1.08615. The actual  $r_2$ , from table 7, is 1.14445, so we have not obtained a very close bound in this case. But it isn't too bad (5% low). The same cylinder ( $2a = h = 1$ ) is also the largest one that will fit inside the hemispherically-capped cylinder of figure 19, so that, for that enclosure as well, we can say that  $r_2$  is greater than 1.08615. Better lower bounds on the  $r_2$  of that enclosure will be obtained below.

We should also mention explicitly some very simple upper and lower bounds on the  $r_2$  of an enclosure, also based on the enclosed and enclosing enclosure  $r_2$ 's. The sphere itself can serve as the enclosed or enclosing enclosure, and

the  $r_2$  of a sphere is just its radius. The spherical enclosure bounds will often be quite a bit rougher than those obtained from canonical enclosures for which we have one or more parameters to play with in trying to fill up as much of  $E$  as possible (in the case of a lower bound calculation). For example, the spherical enclosure bounds on the  $r_2$  of a cube whose edges are two units long are:

$$1 < r_2 < 1.73205,$$

while the cylindrical enclosure bounds for the same cube are

$$1.08615 < r_2 < 1.32360.$$

Nevertheless, the spherical enclosure bounds are quite simple, and, if the enclosure under study is almost spherical, the spherical enclosure bounds could be closer than the bounds given by the best of the canonical enclosures treated in Section VI.

Let us now look at another type of lower bound, one that only applies to enclosures inverse to a convex body. It has been shown by Polya and Szegö [40] that an upper bound on the  $r_1'$  of a convex body,  $B'$ , is

$$(r_1')_M = \frac{M'}{4\pi} \frac{2\varepsilon'}{\ln[(1+\varepsilon')/(1-\varepsilon')]} \quad (7.13)$$

where  $M'$ , the surface integral of mean curvature over  $S_b'$  (known as the Minkowski number, hence the  $M'$ ), is given by

$$M' \equiv \int_{S_b'} \frac{1}{2} \left\{ \frac{1}{r_u'(S)} + \frac{1}{r_v'(S)} \right\} dS, \quad (7.14)$$

$r_u'(S)$  and  $r_v'(S)$  being the two principal radii of curvature at the point  $S$  on  $S_b'$ . In equation (7.13),  $\varepsilon'$  is given by

$$\varepsilon' = \sqrt{1 - \frac{4\pi A_b'}{M'^2}} \quad (7.15)$$

where  $A_b'$  is the surface area of  $S_b'$ . From equations (3.21) and (7.13), it follows

that, if  $S'_b$  is convex

$$r_2 \geq (r_2)_{M'} \equiv \frac{4\pi R^2}{M'} \frac{\ln[(1+\epsilon')/(1-\epsilon')]}{2\epsilon'} \quad (7.16)$$

In order to facilitate the use of this formula, there are two more things that should be done. We should develop formulas for  $M'$  and  $\epsilon'$  (i.e.,  $M'$  and  $A'_b$ ) in terms of the unprimed variables, and we should find some means (in the unprimed variable system) of determining if  $B'$  is convex. Both these topics are dealt with in books on differential geometry (see, for example, [48], pp. 162-164). The results are

$$\frac{M'}{R^2} = \frac{1}{2} \int_{S_e} \left\{ \frac{4\mathbf{n} \cdot \mathbf{r}}{r^2} - \frac{1}{r_u(S)} - \frac{1}{r_v(S)} \right\} \frac{dS}{r^2} \quad (7.17)$$

$$A'_b = R^4 \int_{S_e} \frac{dS}{r^4} \quad (7.18)$$

where  $\mathbf{n}$  is the outward normal from  $E$ . Also,  $B'$  is convex if

$$\frac{2\mathbf{n} \cdot \mathbf{r}}{r^2} \geq \frac{1}{r_u} \quad \text{over } S_e \quad (7.19)$$

where  $r_u(S)$  and  $r_v(S)$  are the two principal radii of curvature at the point  $S$  on  $S_e$ , and  $r_v \geq r_u$ .

We can relax the condition that  $B'$  be convex, if we are willing to put up with a little lower bound, by filling in  $B'$  until it is convex. For example, the surface inverse to an infinite cylindrical  $E$  is the torus without a hole shown as the  $B$  of figure 3b. By filling in this  $B$  until it is just barely convex we obtain the inverse surface of figure 19. Thus, as a lower bound on the  $r_2$  of an infinite circular cylindrical  $E$  of unit radius, we could calculate the  $(r_2)_{M'}$  of the hemispherically-capped cylinder of figure 19. Let's calculate this  $(r_2)_{M'}$ . Note that inequality (7.19) is just barely fulfilled, so we may proceed. From equation (7.18),

$$\begin{aligned}
A'_b &= 2 \int_0^1 \frac{2\pi dx}{(1+x^2)^2} + 2 \int_0^{\pi/2} \frac{2\pi \sin \theta}{(2+2 \cos \theta)^2} d\theta \\
&= \pi(1 + \frac{\pi}{2}) + \frac{\pi}{2} \\
&= \frac{\pi}{2} (3 + \pi)
\end{aligned} \tag{7.20}$$

where we have split the  $S_e$  integration into one integration over the cylindrical portion and another integration over the spherical caps. In a similar manner, from equation (7.17) we have

$$\begin{aligned}
\frac{M'}{R^2} &= \int_0^1 \left\{ \frac{4}{1+x^2} - 1 \right\} \frac{2\pi dx}{1+x^2} + \int_0^{\pi/2} (2 - 2) \frac{2\pi \sin \theta}{2+2 \cos \theta} d\theta \\
&= 2\pi(1 + \frac{\pi}{4}).
\end{aligned} \tag{7.21}$$

Thus, from equations (7.15), (7.20), and (7.21), and a little algebra,

$$\epsilon' = \frac{\sqrt{\pi^2 - 8}}{\pi + 4} = .19146. \tag{7.22}$$

Then, from equations (7.16), (7.21), and (7.22),

$$\begin{aligned}
(r_2)_{M'} &= \frac{2}{1+\pi/4} \frac{\ln(1.19146/.80854)}{.38292} \\
&= 1.1342
\end{aligned} \tag{7.23}$$

This is a pretty good lower bound on  $r_2$ . Even for the infinite cylinder it is only 1¼% low. For the hemispherically-capped cylinder it has to be a little better, because the  $r_2$  of the capped cylinder is less than the  $r_2$  of the infinite cylinder.

We wish to bring the reader's attention to the generalization of the Polya-Szegö bound invented by Parr [41]. To apply Parr's bound we still require  $B'$

to be convex, but, by minimizing certain functionals of a function  $\dot{\theta}(x)$  (details may be found in Parr's paper), we can arrive at a better lower bound than the  $(r_2)_{M'}$  bound on  $r_2$ . If we restrict  $\dot{\theta}(x)$  to be a linear function a priori (this process won't give us the best bound that Parr's procedure is capable of, but it will still be better than  $(r_2)_{M'}$ ), we find from Parr's procedure that, for the hemispherically capped cylinder of figure 19,

$$r_2 \geq 1.1438. \quad (7.24)$$

The bound implied by this inequality differs by only a third of a percent from the upper bound of equation (7.12), and so we see that Parr's bound can be quite close indeed.

This concludes our discussion of  $r_2$  bounds. We have done no more than give a taste of the subject, in the hope of stimulating some interest and some future notes.

## VIII. Conclusions and Possible Extensions

We have presented a rather long examination of the effective radii approximation, with numerous examples. Our intention has been to demonstrate, and give reasons for, the accuracy of the approximation. It is hoped that enough particular cases have been examined to instill some confidence in the accuracy of the approximation in general. Of course, the order of error arguments of Section III apply to general bodies and enclosures, as long as the body is small compared to the enclosure. The examples of Section IV were presented to show that the error of the approximation can still be small, even though the body's size becomes comparable to the enclosure's.

It seems useful at this point to summarize, in a few statements, what we have learned so far, and then to list several directions in which the present work could be extended. Some of the extensions have been mentioned previously; we bring them all together here because we feel that knowing what hasn't been done is a good thing.

First, what we know:

- (1) The accuracy of the effective radii capacitance approximation for a body inside a spherical enclosure, or for a spherical body inside any enclosure, is very good indeed. The developments in Section III give good reasons for this accuracy if the body is small. The examples of Section IV show that the error of the approximation doesn't exceed 1% until the body size is about two-thirds the enclosure size (here "size" means a linear dimension), when either is a sphere.
- (2) The accuracy of the effective radii capacitance approximation for an arbitrarily-shaped body and enclosure is still good, better than one might expect until one has looked into the problem. Again, Section III contains reasons for this accuracy. The examples of Section IV show that the error of the approximation doesn't much exceed 1% until the body size is about half the enclosure size, where again "size" means a linear dimension.
- (3) The calculation of  $r_2$  can be reduced to the solution of an interior Dirichlet problem for the enclosure (or perhaps several solutions, if we can't pick out  $r_e$  from symmetry).

- (4) The two simple shapes for which  $r_2$  calculations were made in Section VI exhibit what is probably a general property of convex enclosures --  $r_2$  is determined primarily by the shortest distance between  $\underline{r}_e$  and the wall of the enclosure; it is just a little larger than this shortest distance.
- (5) It is possible to put rather good upper and lower bounds on the  $r_2$  of an enclosure by invoking the many types of bounds known for the  $r_1'$  of the body inverse to the enclosure. Unfortunately, up to now an easy calculation of these bounds requires a prior knowledge of  $\underline{r}_e$ , either from symmetry or by some other argument.

Now, what it would be nice to know:

- (1) What is the capacitance between an arbitrary B and E when the center of charge of B is a little off  $\underline{r}_e$ ? In other words, what is the generalization of equation (3.32) to arbitrarily shaped enclosures?
- (2) How do  $\bar{C}$  and  $\tilde{C}$  compare for some other examples than those treated in this note? Some cases that come to one's mind are a disk inside a sphere, a disk between two plates, and a sphere in a cube.
- (3) What is the best way to write a general computer code to calculate the  $r_2$  of an arbitrary enclosure? In other words, what is the most efficient formulation of the interior Dirichlet problem that will give us, say, less than 1% error in the numerical calculation of  $r_2$ .
- (4) What are the  $r_2$ 's of some other simple enclosure shapes besides those treated in Section VI? The  $r_2$ 's of ellipsoids and finite length elliptical cylinders would give us more possibilities to get good bounds on the  $r_2$ 's of more complicated enclosures.
- (5) What kind of simple bounds can one put on  $\bar{C}$ ? We have discussed a few simple bounds on  $r_2$  in Section VII. Can these bounds be generalized, in some simple way, to give bounds on  $\bar{C}$  itself?
- (6) Can one put a bound on the proportionality constant between  $(C_b \Delta / \bar{C})$  and  $(r_1/r_2)^3$  for any small B in any E?
- (7) Most of the bounds we talked about in Section VII required a prior knowledge of the position of  $\underline{r}_e$ . What kind of bounds can one put on  $r_2$  without knowing  $\underline{r}_e$ ?

- (8) For all the examples of Section IV,  $\tilde{C}$  was a lower bound on  $\bar{C}$ . Is there any general statement one can make about the kinds of bodies for which this is true? The example of a disk between two plates would show that it can't be true for an arbitrary B and E.
- (9) How do slight perturbations in a spherical E affect the order of error arguments of Section III.B?
- (10) How do perturbations of the boundary of a general E affect its  $r_2$ ?
- (11) What is the error in  $r_2$  incurred by replacing the actual electrostatic boundary of a simulator enclosure (probably a wire grid of some sort) by the smooth surface that facilitates analytical and numerical calculations?
- (12) How should one best calculate the effect of space charge on  $\bar{C}$ ?

IX. References and Other Relevant Publications

- [1] Carl E. Baum, "EMP Simulators for Various Types of Nuclear EMP Environments: An Interim Categorization," Sensor and Simulation Notes, Note 151, July, 1972.
- [2] Carl E. Baum, "A Technique for Simulating the System Generated Electromagnetic Pulse Resulting from an Exoatmospheric Nuclear Weapon Radiation Environment," Sensor and Simulation Notes, Note 156, September, 1972.
- [3] T. H. Shumpert, "Capacitance Calculations for Satellites, Part I: Isolated Capacitances of Ellipsoidal Shapes with Comparisons to Some Other Simple Bodies," Sensor and Simulation Notes, Note 157, September 1972.
- [4] William R. Smythe, Static and Dynamic Electricity, second edition, McGraw-Hill, New York, 1950.
- [5] G. Szego, "On the Capacity of a Condenser," Bulletin of the American Mathematical Society, vol. 51, (1945), pp. 325-350.
- [6] Oliver Dimon Kellogg, Foundations of Potential Theory, Dover edition, 1953.
- [7] C. J. Bouwkamp, "A Simple Method of Calculating Electrostatic Capacity," Physica, vol. 24, (1958), pp. 538-542.
- [8] Donald Greenspan, "Resolution of Classical Capacity Problems by Means of a Digital Computer," Canadian Journal of Physics, vol. 44, (1966), pp. 2605-2614.
- [9] R. E. Kleinman and T. B. A. Senior, "Rayleigh Scattering Cross Sections," Radio Science, vol. 7, no. 10, (1972), pp. 937-942.
- [10] R. C. Knight, "The potential of a Sphere Inside an Infinite Circular Cylinder," Quarterly Journal of Mathematics (Oxford Series), vol. 7, (1936), pp. 124-133.

- [11] G. N. Watson, F. R. S., "The Use of Series of Bessel Functions in Problems Connected with Cylindrical Wind-Tunnels," *Proceedings of the Royal Society*, vol. 130, (1930/31), pp. 29-37.
- [12] W. R. Smythe, "Charged Sphere in Cylinder," *Journal of Applied Physics*, vol. 31, no. 3, (1960), pp. 553-556.
- [13] W. R. Smythe, "Charged Spheroid in Cylinder," *Journal of Mathematical Physics*, vol. 4, no. 6, (1963), pp. 833-837.
- [14] I. C. Chang and I. Dee Chang, "Potential of a Charged Sphere Inside a Grounded Cylindrical Tube," *Journal of Mathematics and Physics*, vol. 47, (1968), pp. 366-370.
- [15] I. C. Chang and I. Dee Chang, "Potential of a Charged Axially Symmetric Conductor Inside a Cylindrical Tube," *Journal of Applied Physics*, vol. 41, no. 5, (1970), pp. 1967-1970.
- [16] M. Van Dyke, Perturbation Methods in Fluid Mechanics, Academic Press, New York, 1964.
- [17] W. Magnus, F. Oberhettinger, and R. P. Soni, Formulas and Theorems for the Special Functions of Mathematical Physics, Springer-Verlag, New York, 1966.
- [18] R. W. Latham, "Interaction Between a Cylindrical Test Body and a Parallel Plate Simulator," *Sensor and Simulation Notes*, Note 55, May, 1968.
- [19] Milton Abramowitz and Irene A. Stegun, editors, Handbook of Mathematical Functions, National Bureau of Standards, AMS-55, 1964.
- [20] W. R. Smythe, "Charged Disk in a Cylindrical Box," *Journal of Applied Physics*, vol. 24, (1953), pp. 773-775.
- [21] D. Kirkham, "Potential and Capacity of Concentric Coaxial Capped Cylinders,"

Journal of Applied Physics, vol. 28, no. 6, (1957), pp. 724-31.

- [22] J. C. Cooke and C. J. Tranter, "Dual Fourier-Bessel Series," Quarterly Journal of Mechanics and Applied Mathematics, vol. 12, (1959), pp. 379-386.
- [23] W. D. Collins, "Note on an Electrified Disk Situated Inside an Earthed Coaxial Infinite Hollow Cylinder," Proceedings of the Cambridge Philosophical Society, vol. 57, (1961), pp. 623-627.
- [24] Ian N. Sneddon, Mixed Boundary Value Problems in Potential Theory, John Wiley & Sons, Inc. (Interscience Publishers Division), New York, 1966.
- [25] I. N. Sneddon, "Note on an Electrified Circular Disk Situated Inside a Coaxial Infinite Hollow Cylinder," Proceedings of the Cambridge Philosophical Society, vol. 58, (1962), pp. 621-624.
- [26] G. N. Watson, A Treatise on the Theory of Bessel Functions, First paperback edition, University Press, Cambridge, 1966.
- [27] R. W. Latham and K. S. H. Lee, "Capacitance and Equivalent Area of a Disk in a Circular Aperture," Sensor and Simulation Notes, Note 106, May, 1970.
- [28] D. A. Spence, "A Wiener-Hopf Solution to the Triple Integral Equations for the Electrified Disc in a Coplanar Gap," Proceedings of the Cambridge Philosophical Society, vol. 68, (1970), pp. 529-545.
- [29] J. Van Bladel, Electromagnetic Fields, McGraw-Hill, New York, 1964.
- [30] D. K. Reitan and T. J. Higgins, "Calculation of the Electrical Capacitance of a Cube," Journal of Applied Physics, vol. 22, no. 2, (1951), pp. 223-226.
- [31] Daniel Kinseth Reitan, "Accurate Determination of the Capacitance of Rectangular Parallel-plate Capacitors," Journal of Applied Physics, vol. 30, no. 2, (1959), pp. 172-176.

- [32] R. F. Harrington, Field Computation by Moment Methods, Macmillan, New York, 1968.
- [33] L. V. Kantorovich and V. I. Krylov, Approximate Methods of Higher Analysis, John Wiley & Sons, Inc., New York, 1964.
- [34] J. Van Bladel and K. Mei, "On the Capacitance of a Cube," *Applied Scientific Research, Section B*, vol. 9, (1961), pp. 267-270.
- [35] David M. Young, Jr., "The Numerical Solution of Elliptic and Parabolic Partial Differential Equations," Chapter 11 of Survey of Numerical Analysis, John Todd, editor, McGraw-Hill, New York, 1962.
- [36] Donald Greenspan, Introductory Numerical Analysis of Elliptic Boundary Value Problems, Harper and Row, New York, 1965.
- [37] J. G. Herriot, "Inequalities for the Capacity of a Lens," *Duke Mathematical Journal*, vol. 15, (1948), pp. 743-753.
- [38] Ernst Weber, "The Electrostatic Field Produced by a Point Charge in the Axis of a Cylinder," *Journal of Applied Physics*, vol. 10, no. 9, (1939), pp. 663-666.
- [39] C. J. Boukamp and N. G. De Bruijn, "The Electrostatic Field of a Point Charge Inside a Cylinder, in Connection with Wave Guide Theory," *Journal of Applied Physics*, vol. 18, no. 6, (1947), pp. 562-577.
- [40] G. Polya and G. Szegö, Isoperimetric Inequalities in Mathematical Physics, *Annals of Mathematical Studies*, Number 27, Princeton University Press, 1951.
- [41] Wallace E. Parr, "Upper and Lower Bounds for the Capacitance of the Regular Solids," *Journal of the Society of Industrial and Applied Mathematics*, vol. 9, no. 3, (1961), pp. 334-386.

- [42] G. Polya and G. Szegő, "Inequalities for the Capacity of a Condenser," American Journal of Mathematics, vol. 67, (1945), pp. 1-32.
- [43] J. Conlan, J. B. Diaz, and W. E. Parr, "On the Capacity of the Icosahedron," Journal of Mathematical Physics, vol. 2, (1961), pp. 259-261.
- [44] J. B. Diaz and A. Weinstein, "Schwartz' Inequality and the Methods of Rayleigh-Ritz and Trefftz," Journal of Mathematics and Physics, vol. 26, (1947), pp. 133-136.
- [45] H. J. Greenberg, "The Determination of Upper and Lower Bounds for the Solution of the Dirichlet Problem," Journal of Mathematics and Physics, vol. 27, (1948), pp. 161-182.
- [46] L. E. Payne, "New Isoperimetric Inequalities for Eigenvalues and Other Physical Quantities," Communications on Pure and Applied Mathematics, vol. 9, (1956), pp. 531-542.
- [47] L. E. Payne, "Isoperimetric Inequalities and Their Applications," S.I.A.M. Review, vol. 9, (1967), pp. 453-488.
- [48] C. E. Weatherburn, Differential Geometry of Three Dimensions, Volume I, Cambridge University Press, 1961.
- [49] S. C. Loh, "The Calculation of the Electric Potential and the Capacity of a Tore by Means of Toroidal Functions," Canadian Journal of Physics, vol. 37, no. 6, (1959), pp. 698-702.
- [50] H. Poritsky, "Potential of a Charged Cylinder Between Two Grounded Plates," Journal of Mathematics and Physics, vol. 39, (1960), pp. 35-48.
- [51] L. A. Tseitlin, "The Determination of the Capacity of Conductors by the Mean Potential Method," Zh. Tekh. Fiz. (U.S.S.R.), vol. 41, no. 7, (1971), pp. 1340-1344. English translation in Soviet Physics-Technical Physics, (U.S.A.), pp. 1055-1058.

- [52] A. G. Ramm, "Approximate Equations for the Polarizability Tensor and the Capacitance of Bodies of Arbitrary Shape, and Some of Their Applications," Dok. Akad. Nauk. S.S.S.R. in Russian. English translation in Soviet Physics-Doklady, (U.S.A.), vol. 15, no. 12, (1971), pp. 1108-1111.
- [53] E. Pisler and T. Adhikari, "Numerical Calculation of Mutual Capacitance Between Two Equal Metal Spheres," Physica Scripta, vol. 2, (1970), pp. 81-83.